Modeling Transportation Emissions Using Radar-based Vehicle Detection Data

by

Lang Yu

A dissertation submitted in partial fulfillment of
the requirements for the degree of

Doctor of Philosophy
(Civil and Environmental Engineering)

at the

UNIVERSITY OF WISCONSIN-MADISON
2016

Date of final oral examination: 12/08/2016

The dissertation is approved by the following members of the Final Oral Committee:

David A. Noyce, Professor and Chair, Civil and Environmental Engineering
Bin Ran, Professor, Civil and Environmental Engineering
Soyoung Ahn, Associate Professor, Civil and Environmental Engineering
Richard (Zhixia) Li, Assistant Professor, Civil and Environmental Engineering, University of Louisville
Peter (Zhiguang) Qian, Professor, Department of Statistics

Abstract

This dissertation introduces a new and novel methodology for estimating vehicle emissions at signalized intersections. Radar based vehicle detection systems, when placed at intersection approaches, is able to track vehicle operational characteristics at very high frequency, thus provides an ideal data source for emission estimation. By combining radar based vehicle detection data and MOVES project level analysis operating mode distribution approach, a real-time emission estimation system for signalized intersections is proposed. The Emission Computation Tool for Radar Data is developed to facilitate the automatic and continuous computation of operating mode distribution and emissions. The emission rates computed can also be integrated with existing air dispersion models in order to be used for air quality conformity and hot spot analysis.

A case study is conducted to test the feasibility and validity of the proposed real-time emission estimation system. The results showed that the data collected should be used for computing a variety of parameters, including traffic volume, average speed, operating mode distribution, total emissions and emission rates for various pollutants. With emission rates, existing pollutant dispersion models such as AERMOD are applied, yielding pollutant concentrations at various locations, providing additional functionalities to the system. Evaluation results showed that the traffic volume and emission rates computed matches closely with AADT data and EPA's emission standards.

Finally, an operating mode based macroscopic emission model is developed by using both empirical data from the case study as well as incorporating existing traffic flow dynamics model. This predictive model is based on estimating total time spent in each operating mode directly from traffic demand and other variables. Total time idling is modeled using kinematic wave theory and queuing theory, while others are modeled using empirical data. The validation results showed that the model is able to achieve a high degree of accuracy, within approximately 10 percent of emission results computed using the radar data. In conclusion, both the proposed real-time emission estimation system at signalized intersections and the emission model developed showed to yield highly accurate and detailed results, and are applicable in real world intersection locations.

Acknowledgements

I would like to express my gratitude and appreciation to my academic advisor, Professor David A. Noyce for his support, patience, and encouragement throughout my graduate studies at the University of Wisconsin-Madison. All the insights, advices and words of encouragement he provided have given me the determinations and confidence for completing this dissertation.

My thanks also go to Professor Bin Ran, Professor Soyoung Ahn, Professor Zhixia (Richard) Li, and Professor Peter Qian for serving on my thesis committee and providing valuable feedback on this research.

I would also like to thank the staff and students of the Traffic Operations and Safety Laboratory (TOPS Lab) at the University of Wisconsin-Madison for their help and support throughout this research effort. Dr. Richard Li, Andrea Bill and Dr. Madhav Chitturi were essential sources of knowledge, experience, and guidance in many projects that I've worked on in the TOPS Lab. I would also like to thank Kelvin Santiago-Chapparo at the TOPS Lab for his support and providing the field collected radar data that is used in this dissertation.

Last but not the least, I would like to express my gratitude to my beloved wife, Xiao Li, for her unconditional support and encouragement throughout my work and life. My parents receive my deepest gratitude and love for their dedication and the many years of support during my graduate studies that provided the foundation for this work.

Table of Contents

List of Figures

List of Tables

1 Introduction

1.1 Background

Air pollution has become an important issue and concern during the past decades due to the industrialization of many developing countries and increasing consumption of fossil fuels worldwide *(1)*. It is becoming an increasingly serious hazard to human health especially in urban areas. According to World Health Organization (WHO), air pollution in 2012 caused the deaths of approximately 7 million people worldwide *(2)*. Among the different contributing sources of air pollution, transportation related emissions are a major factor. Statistics show that in 2002, transportation related emissions accounted for 82 percent of carbon monoxide (CO), 56 percent of nitrogen dioxide (NO_2) emissions, 45 percent of the volatile organic compounds (VOCs), 12 percent of lead (Pb) and 5 percent of sulfur dioxide (SO_2) emissions in the United States (U.S.) *(3)*. Transportation emissions also contribute to approximately 27 percent of all U.S. greenhouse gas (GHG) emissions in 2013 *(4)*. Among all transportation facilities, urban intersections have been identified as a major source for vehicle emissions, large traffic volume along with complex vehicle activities including stop-and-go, deceleration, idling, and acceleration lead to more pollutant emissions *(5)*. Therefore, emission monitoring and assessment at intersection level is highly needed and desired by transportation agencies and authorities as part of the overall performance measure of urban intersections.

Transportation researchers have continuously developed methods throughout the years to calculate or measure transportation emissions in order to obtain a more accurate estimation result. The most direct approach is to use air pollutant concentrations data via air quality monitoring stations across the country *(6)*. However, these values are only point-based values, which could not be used to infer the total amount of pollutant emitted. In addition, the air pollutant density measured may come from multiple sources, motor vehicle emissions cannot be separated from other sources, such as industrial, agriculture and electricity generation. Older methods developed emission inventories through annual average emissions estimates mainly derived from vehicle-miles-traveled (VMT) trends, which can provide a rough macroscopic level estimate of emissions. Emission estimate with an intermediate level of detail, usually at daily values were obtained through travel demand models, which is commonly used by Metropolitan Planning Organizations (MPOs) *(7)*. However, a major issue is that static planning models were not able to model individual vehicle activity, which includes passenger cars, trucks and buses. This inability to monitor individual vehicle activity leads to underestimation of pollutant emissions, as they do not account for link capacity and other variables. As a result, estimates of emissions based on static planning models suffer from significant biases in different traffic conditions *(8)*. During recent years, with the advent of more advanced tools such as EPA's MOVES, researchers have focused on getting more accurate emission estimates at the microscopic level through smaller time and distance ranges by splitting the road network into smaller links and utilizing second-by-second vehicle operations data to calculate emissions.

1.2 Problem Statement

MOVES is an acronym for "Motor Vehicle Emission Simulator", which is the U.S. Environmental Protection Agency's (EPA) state-of-the-art model for emission estimation. The latest version of the model is MOVES 2014a *(9)*. The purpose of MOVES is to provide an accurate estimate of emissions from passenger cars, trucks of all categories and non-highway mobile sources under a wide range of user-defined conditions. In the modeling process, the user specifies vehicle types, time periods, geographical areas, pollutants, vehicle operating characteristics, and road types to be modeled. The model then performs a series of calculations, and provide estimates of emission quantities or emission rates. Compared with other emissions estimation models such as Comprehensive Modal Emissions Model (CMEM) *(10)* and Emission Factors Model (EMFAC) *(11)*, MOVES is a national level model, and currently required to be used for transportation conformity purpose throughout the U.S. (except California, where EMFAC is used) *(12)*.

MOVES can be used both at the macroscopic and microscopic level. The microscopic level, which is also called project level, aims at analyzing specific roadway segments or intersections. To reach the highest level of accuracy, users need to input an operating mode distribution data. Although this method will yield the most accurate estimation result, this information cannot be obtained through direct measurements. Second-by-second vehicle operating data (i.e., speed, location at each timestamp) is commonly used as data source to convert to operating mode distributions.

Previous research used vehicle trajectory data obtained from microsimulation software as a surrogate method due to the difficulty of obtaining real-world vehicle trajectory data. Micro-simulation models, such as VISSIM *(13)* and PARAMICS *(14)* can represent traffic flow conditions to some extent if well calibrated, which requires extra time and input data. Micro-simulation modeling also relies on the validity of assumptions when changing model parameters *(15)*. Previous research studies have also used GPS probe vehicle data, which is, using a single or a few test vehicles operating within the traffic flow. Since probes are individual vehicles, method based on probes assumes that the probe vehicle can represent the characteristics of the entire traffic flow and often assumes that the driving behavior is the same for all vehicles *(16)*. This assumption may rarely be true as individual vehicles typically have different speed and acceleration characteristics even though they are in the same traffic platoon, and affected by sample bias *(17)*.

Radar-based vehicle detection technology, when placed at an intersection approach or along a roadway, is able to track approaching vehicles' trajectories for every per half second within an approximately 500 feet detection range. This detection range is large enough to cover most urban intersections functional area. Therefore, this technology provides sound technical feasibility to address the accuracy issue due to the limitations of GPS probe based method. Moreover, as radar detectors continuously track trajectories of all vehicles at an intersection in real time, it provides the possibility to develop a method for continuously monitoring intersection vehicle emissions.

With the combined availability of radar detection technology and project-level MOVES analysis, this research aims at developing, validating and testing a new and novel method, which is a real-time vehicle emission monitoring system for intersections using vehicle operations data from radar based vehicle detection system. With this new method, an exciting and novel framework of a real-time intersection emission monitoring system is established that transforms the ability to effectively consider emissions as one of Measures of Effectiveness (MOEs) in optimizing traffic signal operations. Specifically, the ability to continuously estimate emissions will greatly assist the monitoring of urban intersections from an environmental perspective, and the decision making of different countermeasures taken to reduce traffic congestion and air pollution such as signal re-timing and intersection reconfigurations. Furthermore, by linking emissions with air dispersion models, the pollutant concentration results can be used for air quality conformity and hot spot analysis, providing additional functionalities to the system.

Using detailed traffic data to compute through emission models such as MOVES could yield more accurate emission estimations. However, considering the cost of the implementation and the large amount of data, this system may not be feasible to implement at all locations. Based on this consideration, mathematical models can be developed as a surrogate method to predict emissions directly using parameters such as traffic volume and traffic signal variables. The main objective of this model is to provide a macroscopic predictive method to estimate vehicle emissions at intersection approaches while still providing details and resolutions in the computation process. It will serve as a surrogate method for predicting transportation emissions at signalized intersections at macroscopic level.

Previous researchers have developed few models that serve similar purpose. Specifically, none of the models are able to apply operating mode distribution as the basis for emission estimation. Another limitation is that the factors included in the developed model vary greatly, which may not consider the more important variables such as grade, percentage of heavy vehicles, and traffic signal variables. In this research, the proposed model will be able to directly estimate the total time spent in different operating modes and through incorporating emission factors, total emissions and emission rates can be directly computed. The model is based on both empirical data from radar based emission monitoring system, and existing traffic flow models such as kinematic wave theory (*18*). The effectiveness and accuracy of the model will be evaluated using the never-been-used part of radar-based vehicle emissions monitoring systems data.

The description above demonstrates the need for both capturing individual vehicle operations characteristics at microscopic level and developing transportation emission prediction models at macroscopic level. Developing such models could greatly enhance to the understanding of key transportation parameters to vehicular emissions in a stochastic-microscopic traffic environment.

1.3 Objectives and Scopes

Based on the problem statement described above, the specific objectives of this research are as follows:

- Develop an algorithm and tool to integrate radar based vehicle detection data and MOVES operating mode distribution approach to automatically and directly compute emissions for various pollutants.
- Establish a framework for real-time monitoring of intersection emissions based on radar-based vehicle detection data, and implement the system through a case study and evaluate its performance.
- Develop transportation emission model through total time spent in each operating mode based on traffic demand and signal variables and evaluate the developed model accuracy.

The scope of this research is restricted to the following constraints and assumptions:

- The proposed system for real-time estimation of vehicle emissions focuses on the application at microscopic level, at signalized intersections.
- The emissions computed in the proposed system are only from running exhaust as defined in MOVES. Other emission processes, such as tire wear and brake wear are not modeled.

1.4 Contributions

The contributions of this research are as follows:

- This research presents a new and novel methodology to implement radar-based vehicle detection data to estimate emissions at microscopic level. In addition, it is the first research effort to create a system for real-time emissions monitoring at intersections.
- Novel macroscopic emission models developed to estimate transportation emissions through estimating the total time spent in each operating mode using traffic volume and signal variables at signalized intersections can help better understand the key contributing parameters to transportation emissions.

1.5 Thesis Organization

This thesis is organized into six chapters. An overview of the research flow of this dissertation is presented in Figure 1.1. The contents of each chapter are introduced in the following paragraphs.

Chapter 1 includes background information on the research topic and presents the objectives and scopes along with expected contributions of this research.

Chapter 2 presents a comprehensive literature review of relevant topics. Current air quality measurement and standards are presented. State-of-the-art emission analysis models and air dispersion models are presented and compared. Previous research on real-time estimation and emission modeling are also summarized.

Chapter 3 presents the proposed methodology for this research. Project level emission analysis procedure is introduced along with the traffic and non-traffic data needed. The proposed system framework is introduced for achieving a real-time estimation of emissions based on Radar Based Vehicle Detection data, including the data collection process, data processing, and output of the system. The development and algorithm of the Emission Computation Tool for Radar-based Vehicle Detection data is also presented. The air dispersion modeling procedure is introduced and connections between emission analysis and dispersion analysis is highlighted.

Chapter 4 implements the proposed system through a case study at an urban signalized intersection. The data collection and reduction process, emission and air pollutant concentrations results are presented. Results are visualized through various graphs and tables.

Chapter 5 introduces the emission modeling efforts and results. The emission results are first compared with probe vehicle methods to show its advantages. The sensitivity and correlation between emission and several key contributing factors are explored. The model development procedure is presented and the model is evaluated using radar based emission monitoring system data.

Chapter 6 summarizes the major findings and contributions of this project and address possible short term and long term future work of on this research topic.

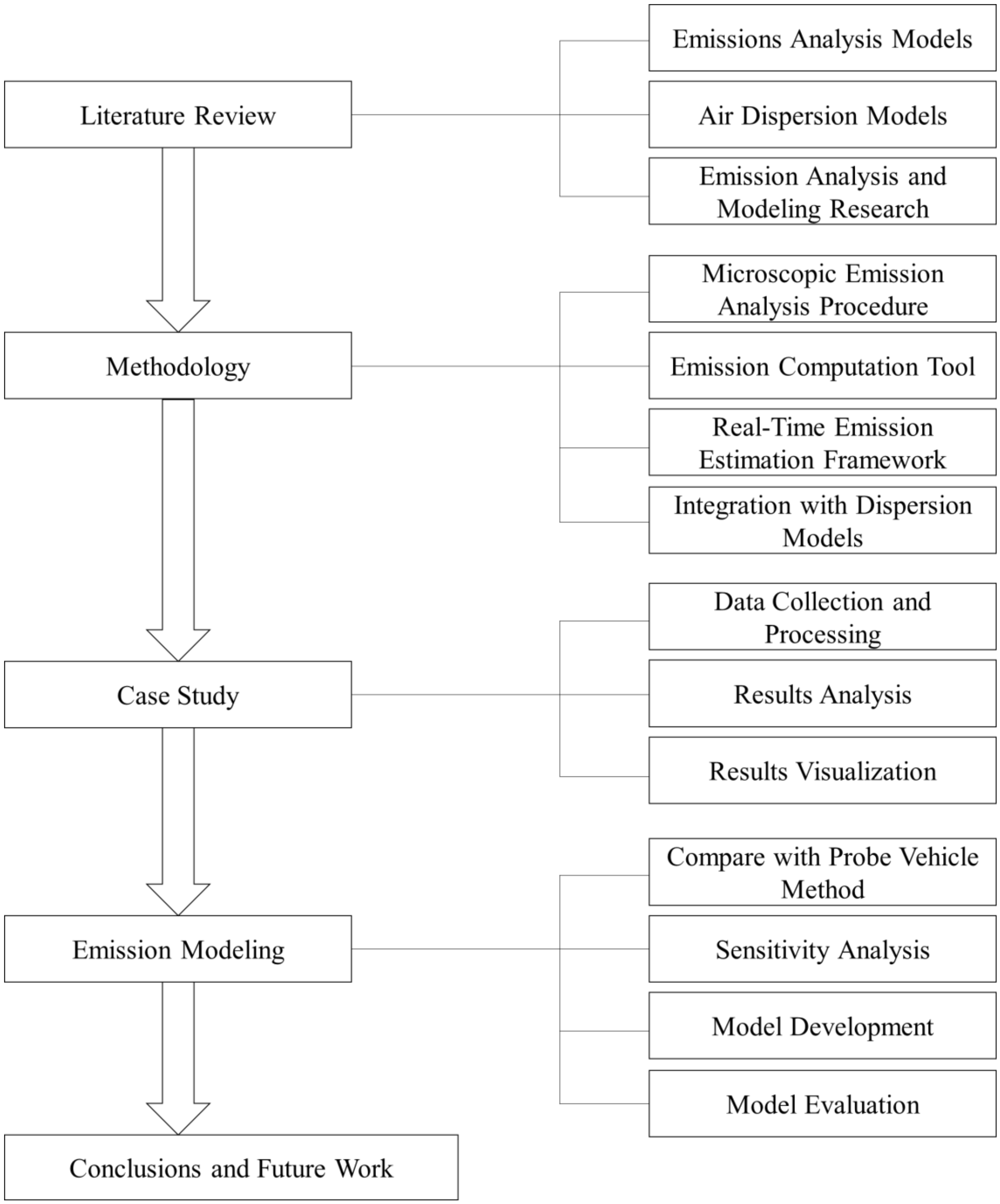

Figure 1.1 Dissertation Flowchart

2 Literature Review

2.1 Air Quality Measurement and Standards

2.1.1 Criteria Pollutants

Among all air pollutants, a few called “criteria air pollutants”, are common throughout the U.S. These pollutants can injure health, harm the environment and cause property damage. The current criteria pollutants are ozone, particulate matter (PM), carbon monoxide (CO), nitrogen oxides (NO_x), sulphur dioxide (SO_2) and lead (Pb). Significant portions of mobile source emissions are composed mainly of three of these criteria pollutants primarily CO, NO_x, PM and one other class of pollutants volatile organic compounds (VOCs) *(19)*. The following paragraphs summarize the causation and health impact for each criteria pollutant.

- Carbon Monoxide: CO is formed through vehicle’s incomplete combustion of fuels especially at low temperatures. Gasoline engines emit higher amounts of CO than diesel engines due to their lower combustion temperature compared to diesel. Carbon monoxide has the impact of decreasing the amount of oxygen in the blood, which may aggravate heart disease, resulting in chest pain and other symptoms *(19)*. The highest levels of CO usually occur during the colder months as mentioned earlier especially during nighttime due to temperature inversion where vehicle emissions are high and inversion conditions are more frequent. In 2010, motor vehicle emissions contribute to about half of all CO emissions nationwide *(19)*.
- Particulate Matter: Two common categories of PM are $PM_{2.5}$ which refers to the fine particles that are less than or equal to 2.5 μm in diameter and PM_{10} which

refers to all particles less than or equal to 10 μm in diameter. They can be both a primary or secondary pollutant. Primary particles come from several sources such as passenger cars, trucks, buses, factories and construction sites. Secondary particles are formed when gases from fuel combustion such as motor vehicles or power plants react with sunlight and water vapor. Diesel engines emit significantly more PM than gasoline engines. Fine particulate matter can be inhaled deeply in the lungs, which can aggravate symptoms in individuals suffering from respiratory or cardiovascular diseases *(19).*

- Nitrogen Oxides: NO_x is a group of gases that are formed during fuel combustion especially at high temperatures where engines burn a small amount of the nitrogen in the air along with nitrogen compounds from the vehicle fuels. Diesel engines generally produce greater amounts of NO_x than gasoline engines due to their higher combustion temperatures. NO_x aggravates lung diseases leading to respiratory symptoms *(19).* NO_x also are precursors of smog components such as Ozone (O_3).
- Sulphur Dioxide: SO_2 is emitted from the Sulphur combustion found in the fuel. Most of SO_2 come from diesel engines since they contain more Sulphur than gasoline engines. It aggravates asthma and increases respiratory symptoms *(19).*
- Other Pollutants: Vehicles also emit toxic air pollutants such as benzene, butadiene, soot, acrolein, and formaldehyde. Some components are VOCs, while others are in the form of particles. Freon or R12 used in older air conditioning systems are known as ozone depleting substances, which are emitted through leaks or during repairs. Newer vehicles refrigerant is still considered as GHG

pollutants although they are non-ozone depleting coolants. The storage and distribution of vehicle fuels also cause air pollution emissions such as the emission of hydrocarbon vapors during refueling of vehicles *(20).*

2.1.2 Air Quality Standards

The Clean Air Act, which was last amended in 1990, requires EPA to set National Ambient Air Quality Standards (NAAQS) for pollutants considered harmful to public health and the environment. The Clean Air Act identifies two types of national ambient air quality standards.

- Primary standards: provide public health protection, including protecting the health of "sensitive" populations such as asthmatics, children, and the elderly.
- Secondary standards: provide public welfare protection, including protection against decreased visibility and damage to animals, crops, vegetation, and buildings.

A district meeting a given standard is known as an "attainment area" for that standard and otherwise a "non-attainment area". The U.S. EPA has published guidance for performing "Project-Level" transportation conformity analysis of PM_{10}, $PM_{2.5}$, and CO "hot-spots", for areas where local pollution concentrations might exceed the NAAQS standards. Table 2.1 shows the detailed standard for each criteria pollutant according to NAAQS *(12).*

Table 2.1 NAAQS Standards *(21)*

Pollutant	Type	Averaging Time	Level	Form
CO	Primary	8-hour 1-hour	9 ppm 35 ppm	Not to be exceeded more than once per year
Pb	Primary and Secondary	Rolling 3-month average	0.15 μg/m^3	Not to be exceeded
NO_2	Primary	1-hour	100 ppb	98th percentile of 1-hour daily maximum concentrations, averaged over 3 years
	Primary and Secondary	Annual	53 ppb	Annual Mean
O_3	Primary and Secondary	8-hour	0.075 ppm	Annual fourth-highest daily maximum 8-hr concentration, averaged over 3 years
$PM_{2.5}$	Primary	Annual	12 μg/m^3	Annual mean, averaged over 3 years
	Secondary	Annual	15 μg/m^3	Annual mean, averaged over 3 years
	Primary and Secondary	24-hour	35 μg/m^3	98th percentile, averaged over 3 years
PM_{10}	Primary and Secondary	24-hour	150 μg/m^3	Not to be exceeded more than once per year on average over 3 years
SO_2	Primary	1-hour	75 ppb	99th percentile of 1-hour daily maximum concentrations, average over 3 years
	Secondary	3-hour	0.5 ppm	Not to be exceeded more than once per year

2.1.3 Air Quality Index

Air Quality Index (AQI) is an index for reporting daily air quality. It informs the general public about the cleanliness of air, and the associated health effects and concerns. The AQI focuses on health impacts that could be experienced within a few hours or days after breathing polluted air. EPA calculates the AQI for five major air pollutants regulated by the Clean Air Act: ground-level ozone (O_3), particle matter (PM), carbon monoxide (CO), sulfur dioxide (SO_2), and nitrogen dioxide (NO_2). For each of the pollutants, EPA has established national air quality standards to protect public health. Ground-level ozone and airborne particles are the two pollutants that pose the greatest threat to human health. Table 2.2 presents each air quality level along with its AQI range and potential impact. The air quality index is a piecewise linear function of the pollutant concentration. At the boundary between AQI categories, there is a discontinuous jump of one AQI unit. An AQI value of 100 generally corresponds to the level of the NAAQS for the pollutant *(6)*.

Table 2.2 US EPA Air Quality Index Categories *(6)*

Category	AQI	O_3 8-hr (ppm)	O_3 1-hr (ppm)	$PM_{2.5}$ (μg/m^3)	PM_{10} (μg/m^3)	CO (ppm)	SO_2 (ppm)	NO_2 (ppm)
Good	0-50	0-0.064		0-15.4	0-54	0-4.4	0-0.034	N/A
Moderate	51-100	0.065-0.084		15.5-40.4	55-154	4.5-9.4	0.035-0.144	N/A
Unhealthy, sensitive groups	101-150	0.085-0.104	0.125-0.164	40.5-65.4	155-254	9.5-12.4	0.145-0.224	N/A
Unhealthy	151-200	0.105-0.124	0.165-0.204	65.5-150.4	255-354	12.5-15.4	0.225-0.304	N/A
Very unhealthy	201-300	0.125-0.374	0.205-0.404	150.5-250.4	355-424	15.5-30.4	0.305-0.604	0.65-1.24
Hazardous	301-500	N/A	0.405-0.604	250.5-500.4	425-604	30.5-50.4	0.605-1.004	1.25-2.04

2.2 Factors Affecting Vehicle Emissions

As stated in an U.S. EPA fact sheet, emissions from an individual vehicle generally contribute to a small amount of air pollution *(22)*. However, as the number of vehicles adds up to a significantly large number, which is the case for major metropolitan areas, the amount of emissions can accumulate to a large number and lead to significant air pollution. Transportation emissions are often the biggest contributing source to air pollution in metropolitan areas.

The power to move a vehicle comes from burning fuel in an engine. Vehicle emissions come from by-products of this combustion process (exhaust) and from evaporation of the fuel itself. Ideally, the combustion process of the engine would convert all hydrogen in the fuel to water and all the carbon in the fuel to carbon dioxide. However, in reality, the combustion process cannot be perfect, and would thus emit several types of pollutants. The amount of pollutants emitted, though, will differ based on several factors. The major factors affecting vehicle emissions are listed in the following subsections. These factors can be classified into three categories: vehicle characteristics, vehicle operational characteristics and non-vehicle factors.

2.2.1 Vehicle Characteristics

Vehicle characteristics play an important role in affecting the amount of pollutants emitted. Specifically, the following characteristics are listed and explained below.

- Vehicle Type and Size:

Vehicle type is a fundamental classification method for motor vehicles. Typical motor vehicle types include passenger cars, trucks and buses. For the purpose of emission analysis, vehicle types are usually divided into categories that are more specific. For example, EPA MOVES listed 13 motor vehicles types, while FHWA has a slightly different classification *(23)*.

The emission rate for different vehicles varies significantly. Figure 2.1 shows the idling emissions factors for heavy-duty diesel vehicles with different GVW *(24)*. It illustrates that even within a single vehicle type, as the gross vehicle weight (GVW) increases, the amount of pollutants emitted also increases.

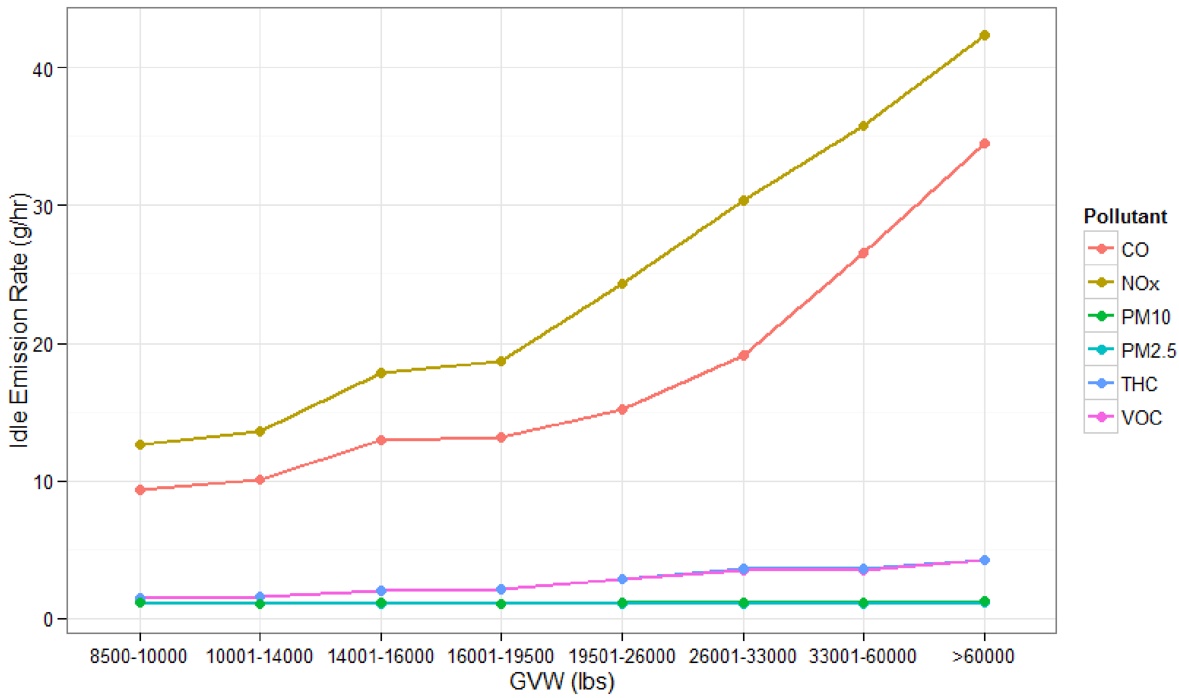

Figure 2.1 Idle Emission Factors for Heavy-Duty Diesel Vehicles by GVW

- Vehicle Age and Maintenance:

For a specific vehicle, as the vehicle age and mileage increases, the engine efficiency will decrease, leading to larger pollutant emissions. An EPA report stated that emissions do not appear to increase indefinitely with age, but rather tend to stabilize at some point between 12 and 15 years of age *(23)*. Figure 2.2 illustrates the relationship between CO emissions and vehicle age. Maintenance conditions also affect the amount of vehicle emissions. A well-maintained vehicle will emit fewer pollutants than a vehicle in need of maintenance.

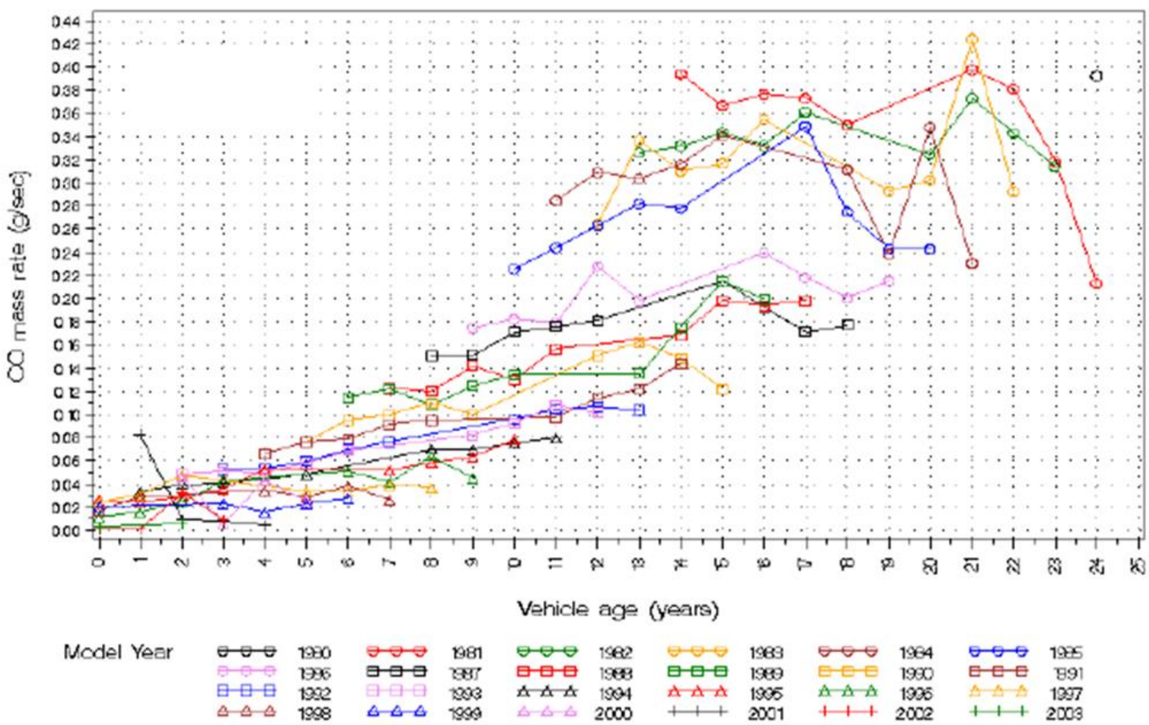

Figure 2.2 CO Emission vs. Vehicle Age for Light-Duty Vehicles

- <u>Fuel Type:</u>

In recent years, the advances in alternative fuel vehicles have greatly changed the emissions of vehicles. Alternative fuel vehicles, including hybrid electric vehicles (HEVs), plug-in hybrid electric vehicles (PHEVs), and all-electric vehicles (EVs) typically produce lower emissions than conventional vehicles with gasoline do. However, although all-electric vehicles are generally considered zero emissions, the production of electricity source to power the vehicles leads to indirect emissions since there are emissions associated with the majority of electricity production in the United States. By taking this indirect emission into account, the U.S. Department of Energy compares the annual CO_2 emissions for the above mentioned alternative fuel type vehicle compared with traditional gasoline vehicles, shown in Figure 2.3 *(25).* Even considering the indirect emissions from electricity production, all-electric vehicles will have 60 percent less CO_2 emissions than gasoline vehicles. However, the percentage of alternative fuel vehicles is still significantly low to make an impact on reducing overall vehicle emissions. Statistics show that by the end of 2015, only about 5.3 percent of vehicles are alternative fuel vehicles *(25).* As the market penetration rates for alternative fuel vehicles may increase during the coming years, it is predictable that overall transportation emissions will further decrease.

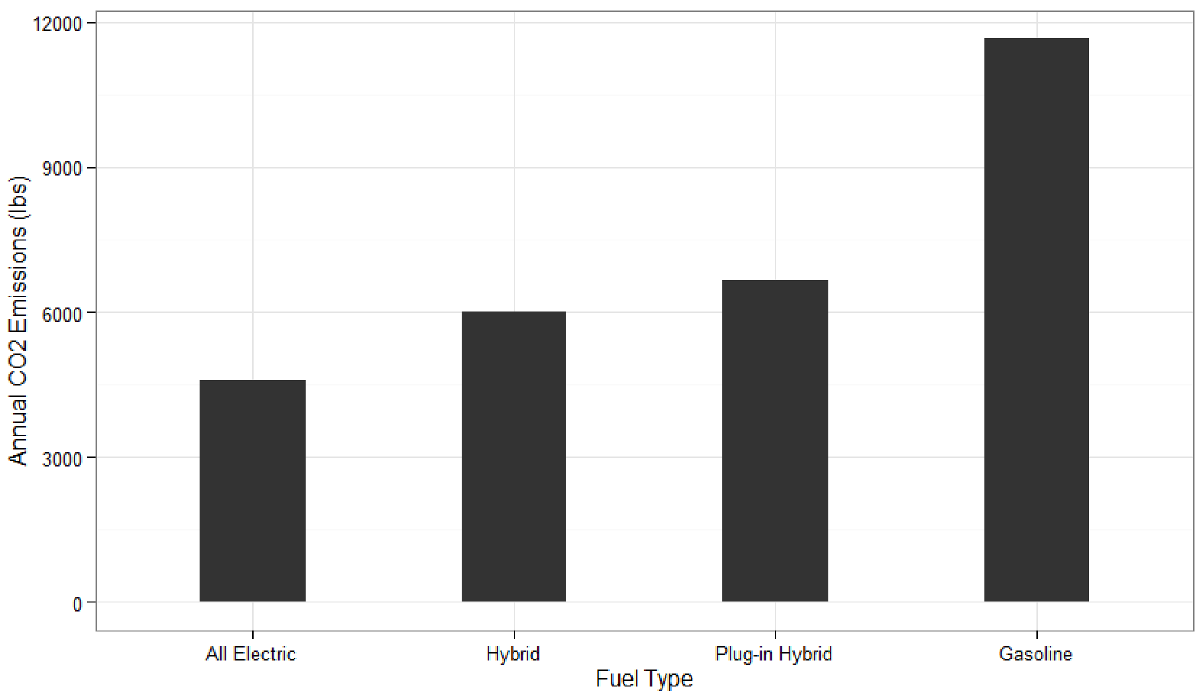

Figure 2.3 Annual CO_2 Emissions by Vehicle Fuel Types

2.2.2 Vehicle Average Speed

Many research efforts have identified vehicle average speed as a key factor in affecting emissions. Therefore, emission factors or rates have been commonly associated with average speed. MOBILE6 model, which was EPA's official emission model prior to the development of MOVES, estimate vehicle emissions mainly based on traffic average speed. The general relationship between average speed and CO_2 emissions can be illustrated in Figure 2.4 *(26).* As can be observed from the figure, the trend can be described as a “U-Shaped” pattern. CO_2 emission rate are high during low speed, decreases as speed increases. The lowest emission rates are within a 40 mph to 60 mph range, higher than 60 mph will cause emission rates to further increase.

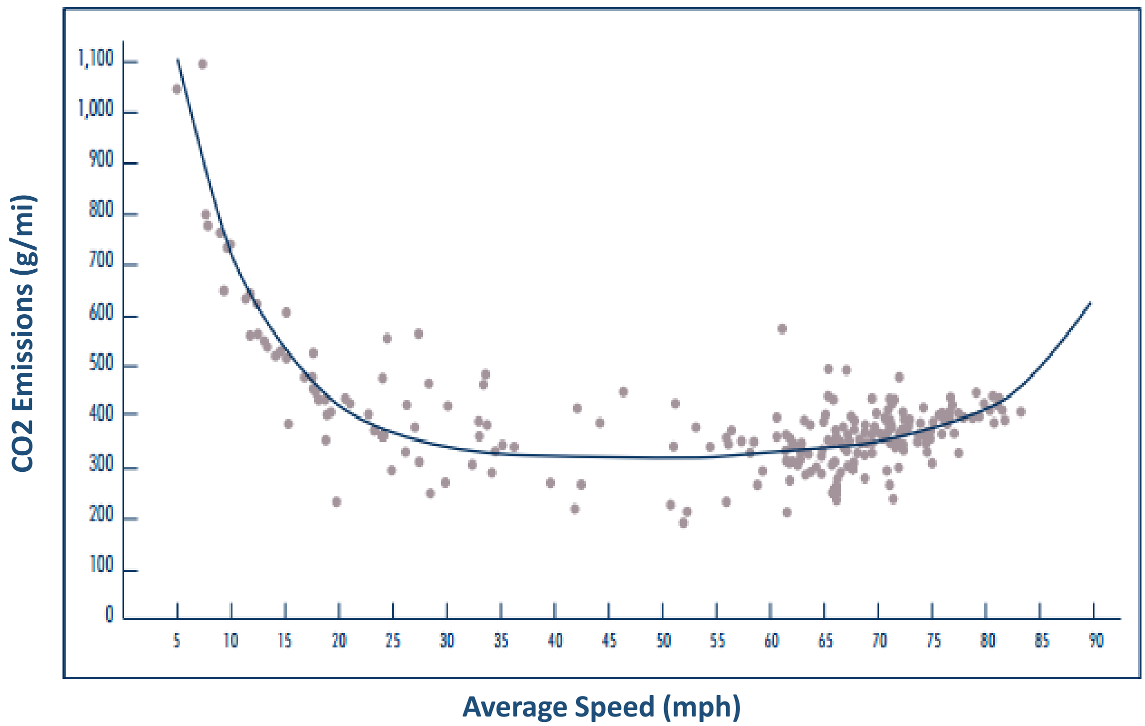

Figure 2.4 Average Speed vs. CO_2 Emissions

2.2.3 Vehicle Driving Cycle

A typical driving trip consists of idling, accelerating, cruising, and decelerating, which is referred to as a driving cycle. The proportion of driving time spent in each of the modes will greatly affect the amount pollutants emitted. This proportion depends on several factors, including driver behavior (e.g., aggressive vs. mild driving habits), roadway type (e.g., freeways, arterials or locals), and the level of traffic congestion. This can be shown graphically through a vehicle speed profile, a chart that shows speed over time for different roadway types, shown in

Figure 2.5 *(26).* The amount of pollutants emitted during the trip will differ based on these factors. Given a specific speed profile and detailed information on the vehicle, emissions can be estimated using a vehicle emissions model.

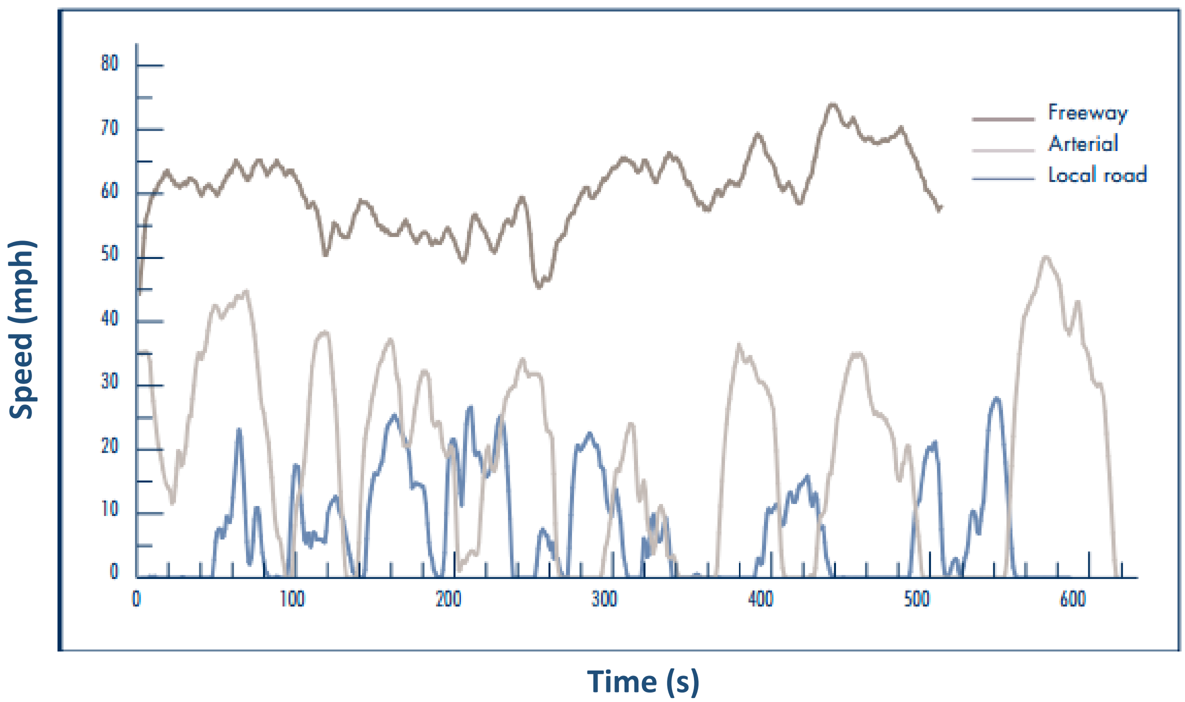

Figure 2.5 Typical Vehicle Speed Profile for Different Roadway Types

The emission rate for each vehicle operating mode can differ significantly. Figure 2.6 illustrates the CO emission rate for each operating mode for light-duty vehicles (passenger cars and trucks) *(Modified based on 23).* As can be observed from the figure, idling has the smallest emission rate in terms of g/time (which is also referred to as emission factor), deceleration comes next with a slightly higher emission rates. Cruise and acceleration have the largest emission rates. They can be further divided by the speed range. Low speed cruise/acceleration will have lower emission rates compared with medium speed and high-speed cruise/acceleration. This fundamental relationship serves as the basis for EPA's MOVES project level analysis.

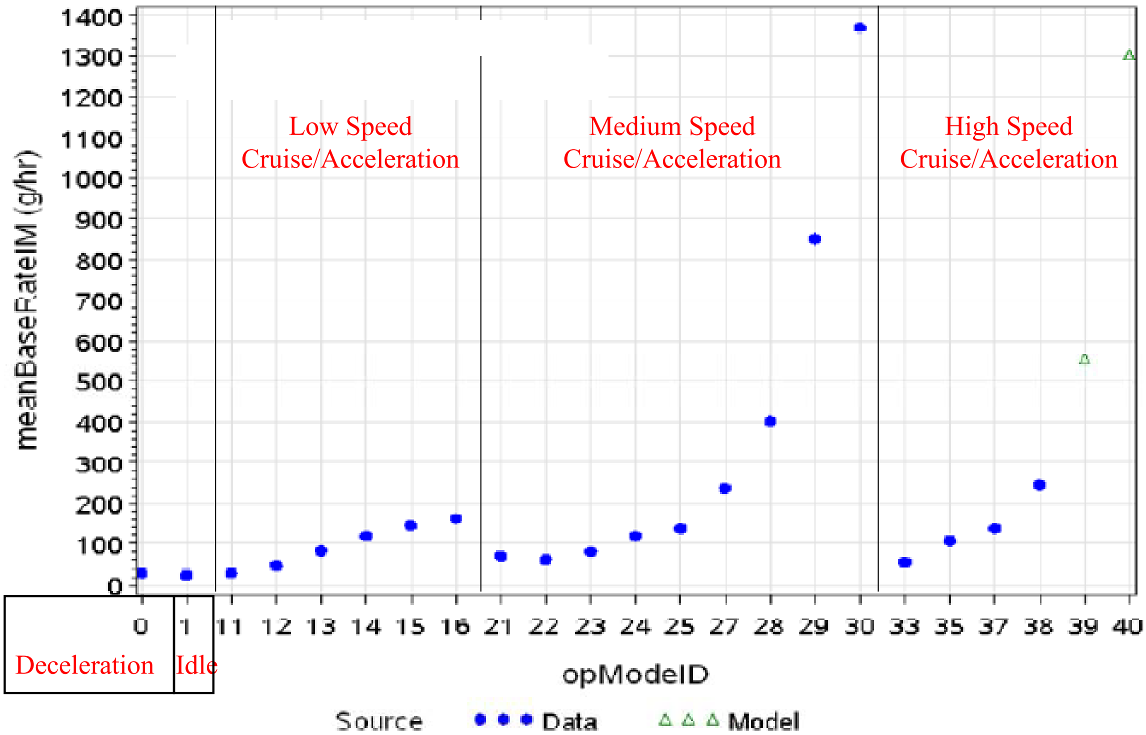

Figure 2.6 CO Emission Rate vs. Operating Modes

2.2.4 Non-Vehicle Factors

Non-vehicle factors that affect vehicle emissions are mainly weather conditions, including temperature, humidity and wind. Emission rates are usually high in very hot weather or in very cold weather.

Besides, roadway grade is also an influencing factor. With a larger upgrade, the vehicle needs to have larger drag force, causing higher emissions, vice versa.

2.3 Transportation Emission Analysis Models

2.3.1 MOVES

MOVES stands for U.S. Environmental Protection Agency's (EPA) Motor Vehicle Emission Simulator. The predecessor of MOVES is a model named MOBILE6. MOBILE6 was designed by the U.S. EPA to address a wide variety of air pollution modeling needs. MOBILE6 is a computer program that estimates HC, CO, NOx, PM, SO_2, NH_3, HAP, and CO_2 emission factors for gasoline-fueled and diesel highway motor vehicles, and for certain special vehicles such as natural-gas-fueled or electric vehicles for calendar years between 1952 and 2050. MOBILE6 estimates emissions mainly based on link average speed. However, this model has been critiqued in numerous researches due to its inaccuracy. For example, Unal et al. stated that the use of standard driving cycles in MOBILE makes it inapplicable for evaluation at microscopic scale *(27).* Yu et al. criticized the model for being constrained by its model frame, which limits the use and refinement for multilevel emissions estimation *(28).*

In 2004, MOVES was launched as EPA's state-of-the-art tool for estimating emissions from highway vehicles. Its latest version up to date is MOVES 2014a *(9).* It is used to create emission factors or emission inventories for both on-road motor vehicles and non-road equipment. The purpose of MOVES is to provide an accurate estimate of emissions from cars, trucks and non-highway mobile sources under a wide range of user-defined conditions.

In the current modeling process, the user specifies vehicle types, time periods, geographical areas, pollutants, vehicle operating characteristics, and road types to be modeled. The model then performs a series of calculations, which have been carefully developed to accurately reflect vehicle-operating processes, such as running, starts, or hoteling, and provide estimates of total emissions or emission rates per vehicle or unit of activity.

2.3.2 EMFAC

The California Air Resources Board developed an Emission Factors (EMFAC) model to calculate statewide or regional emissions inventories by multiplying emissions rates with vehicle activity data from all motor vehicles, including passenger cars to heavy-duty trucks, operating on highways, freeways, and local roads in California *(10)*. The latest version of the model is EMFAC2014. In EMFAC2014, the emission rates are multiplied with vehicle activity data provided by the regional transportation agencies to calculate the statewide or regional emission inventories. The EMFAC2014 model can estimate emission rates for on-road mobile sources for calendar years from 1970 to 2050 operating in California. Pollutant emissions for HC, CO, NO_X, PM_{10}, $PM_{2.5}$, lead, and sulfur oxides are output from the model. Emissions are calculated for thirteen different vehicles classes comprised of passenger cars, various types of trucks and buses, motorcycles, and motor homes. EMFAC is used to calculate current and future inventories of motor vehicle emissions at the state, air district, air basin, or county level. EMFAC models on-road mobile source emissions under multiple temporal and spatial scales. It produces composite emission factors for an average day of a month (from January to December), a season (summer and winter), or an annual average, for specific California geographic areas by air basin, district, and county as well as statewide level. EMFAC can produce $PM_{2.5}$ and PM_{10} emission rates for three exhaust emission processes (running, starting, and idle), tire wear, and brake wear. In summary, EMFAC is only used for conformity purposes in California at the macroscopic level. Therefore, this model is not applicable for project level emission analysis.

2.3.3 CMEM

Comprehensive Modal Emissions Model (CMEM) was initially developed in the late 1990's with sponsorship from the National Cooperative Highway Research Program (NCHRP) and the U.S. EPA to fulfill the need for microscopic emissions modeling *(11)*. The model was developed at the University of California, Riverside as a fine-scale emissions predictions model that was specifically designed to improve the prediction of the variation of the vehicle operating conditions. CMEM was developed to meet the need for an emissions modeling system in response to traffic operational changes (i.e. the various driving ‘modes’, such as idle, steady-state cruise, various levels of acceleration/deceleration).

CMEM integrates with existing micro-simulation software packages that generate second-by-second speed/acceleration vehicle trajectories. CMEM is microscopic because it predicts second-by-second tailpipe emissions and fuel consumption based on different modal operations from in-use vehicle fleet *(11)*. One of the most important features of CMEM is that it uses a physical, power-demand approach based on a parameterized analytical representation of fuel consumption and emissions production. In this type of model, the entire fuel consumption and emissions process is broken down into components that correspond to physical phenomena associated with vehicle operation and emissions production. Each component is modeled as an analytical representation consisting of various parameters that are characteristic of the process. These parameters vary according to the vehicle type, engine, emission technology, and level of deterioration. One distinct advantage of this physical approach is that it is possible to adjust many of these physical parameters to predict energy consumption and emissions of future vehicle models.

2.4 Pollutant Dispersion Models

2.4.1 Dispersion Modeling Introduction

Air pollutant dispersion modeling is a mathematical simulation of emissions as they are transported through the atmosphere. It uses mathematical equations describing the atmosphere, dispersion and chemical and physical processes within the plume to compute pollutant concentrations at various locations. Dispersion models are used to estimate the downwind ambient concentration of air pollutants or toxins emitted from sources such as industrial plants, vehicular traffic or accidental chemical releases. The models are typically used to determine whether existing or proposed new projects are or will comply with the National Ambient Air Quality Standards (NAAQS) (*29*).

Gaussian model is the most popular and is employed in almost all currently available dispersion models. It assumes that the air pollutant dispersion follows a Gaussian distribution, meaning that the pollutant distribution has a normal probability distribution. Gaussian models are most often used for predicting the dispersion of continuous, buoyant air pollution plumes originating from ground level or elevated sources. Gaussian models may also be used for predicting the dispersion of non-continuous air pollution plumes (called puff models). The primary algorithm used in Gaussian modeling is the Generalized Dispersion Equation for a Continuous Point-Source Plume (*30*).

Emission sources in air dispersion models can be categorized into four types according to its shapes, as follows,

- <u>Point source:</u> Single, identifiable source of air pollutant emissions. Point sources are also characterized as being either elevated or at ground level. A point source has no geometric dimensions. Examples include the emissions from a combustion furnace flue-gas stack.
- <u>Line source:</u> One-dimensional source of air pollutant emissions. Examples include the emissions from the vehicles on a roadway.
- <u>Area source:</u> Two-dimensional source of diffuse air pollutant emissions. Examples include the emissions from a forest fire, a landfill or the evaporated vapors from a large spill of volatile liquid. Transportation emissions can also be modeled using area sources.
- <u>Volume source:</u> Three-dimensional source of diffuse air pollutant emissions. Essentially, it is an area source with a third (i.e. height) dimension. Examples include the fugitive gaseous emissions from piping flanges, valves and other equipment at various heights within industrial facilities such as oil refineries and petrochemical plants.

2.4.2 U.S. EPA Preferred and Recommended Models

- <u>AERMOD</u>

AERMOD is U.S. EPA most advanced and currently recommended model. AERMOD is a near field steady state Gaussian plume model based on planetary boundary layer turbulence structure and scaling concepts, including treatment of both surface and elevated sources over both simple and complex terrain. It is able to model multiple sources of different types including point, area and volume. In the stable boundary layer, the distribution is assumed to be Gaussian in both the horizontal and vertical directions. However, in the convective boundary layer, the vertical distribution is described using a bi-Gaussian probability density function, whilst the horizontal distribution is considered to be Gaussian. AERMOD is capable to model buoyant plumes and incorporates a treatment of lofting, whereby the plume remains near the top of the boundary layer. In general, Gaussian models are limited to treatments of flows over a simple terrain; however, AERMOD incorporates a simple method to approximate flows over complex terrain (*12*).

There are two input data processors that are regulatory components of the AERMOD modeling system: AERMET, a meteorological data preprocessor that incorporates air dispersion based on planetary boundary layer turbulence structure and scaling concepts, and AERMAP, a terrain data preprocessor that incorporates complex terrain using USGS Digital Elevation Data (*31*).

- CALPUFF

CALPUFF is a multi-layer, multi-species non-steady-state puff dispersion model that simulates the effects of time- and space-varying meteorological conditions on pollution transport, transformation and removal. CALPUFF can be applied on scales of tens to hundreds of kilometers. It includes algorithms for sub grid scale effects, as well as, long-range effects (*32*).

- CALINE3

CALINE3 is a steady-state Gaussian dispersion model designed to determine air pollution concentrations at receptor locations downwind of highways located in relatively uncomplicated terrain. CALINE3 is incorporated into the more refined CAL3QHC and CAL3QHCR models. It consisted of a series of tables and monographs that enabled the user to predict CO concentrations near roadways based on estimated meteorology and traffic. The transport and dispersion element of the model was a modified form of the Gaussian point source plume dispersion model (*33*).

- CAL3QHC/CAL3QHCR

CAL3QHC is a CALINE3 based CO model with queuing and hot spot calculations and with traffic model to calculate delays and queues that occur at signalized intersections; CAL3QHCR is a more refined version based on CAL3QHC that requires local meteorological data (*34*). CAL3QHC requires all the inputs required for CALINE-3 including roadway geometries, receptor locations, meteorological conditions and vehicular emission rates. In additional, several other parameters are necessary, including signal timing data and information describing the configuration of the intersection being modeled (*34*).

2.5 Real-Time Estimation of Vehicle Emissions

2.5.1 Portable Emission Measurement System (PEMS)

A comprehensive literature search was conducted to identify current practice in real-time vehicle emission monitoring systems. Portable Emission Measurement System (PEMS) have been widely used in previous government testing and academic research *(35)*. PEMS is essentially a lightweight laboratory that can be used to test and assess mobile source emissions for the purposes of compliance, regulation, or decision-making.

The PEMS system is able to continuously and directly measure various gaseous emissions including NO, NO_2, CO, CO_2 and THC. The system can determine exhaust gas mass emissions and vehicular fuel economy of a vehicle operating in the real world in real-time. It employs a novel exhaust gas flow rate measurement technique, integrates Global Position System (GPS) functionality to associate emissions with location, and interfaces with a vehicle's data port to associate emissions with engine operating parameters and driver control *(35).*

The advantages of PEMS system is that it is a much more flexible system compared with laboratory testing. Since the testing can take place during the regular operation of the tested vehicles, a large number of vehicles can be tested within a relatively short period of time and at relatively low cost. In addition, the data obtained is a real-world emission data.

However, only one vehicle can be tested at a time, which is often used as probe vehicle within the traffic flow. This probe vehicle method was employed in a series of researches to collect vehicle operating data and emission data. It is also not applicable for emission estimation for an entire traffic flow, nor continuously monitors emissions at fixed locations on the roadway.

2.5.2 Visual Traffic Monitoring

Video cameras on roadways have been widely used for a variety of transportation purposes, including traffic volume monitoring, red-light running detection, speed detection and incident detection, among others. Early vision-based traffic monitoring researches used video cameras to mimic the inductive loop sensor counts by manually defining virtual loops in the camera field of view *(36)*. Although effective and easy to implement, the virtual loops did not take advantage of the spatial coverage afforded by the camera, reducing the wide field of vision into several small point sensors. Afterwards, most researches began to focus on moving object detection and tracking, through counts for every tracked vehicle *(37)*.

However, video data processing also has its own issues and disadvantages. The placement location of video cameras and its view are critical for successful data collection. Although the images can provide roadway coverage over long distances, it can also cause perspective distortion, which greatly affects the apparent size of vehicles and leads to occlusion. Cameras also have difficulties dealing with changing environmental conditions such as illumination changes, nighttime traffic data is very difficult to obtain and inaccurate. In addition to shadows caused by lighting, it is quite difficult to operate vision systems at night without the use of costly low-light sensitive or infrared cameras, reducing the effective operating time.

Morris et al. developed an enhanced video-based traffic measurement system to monitor the highway operations in real-time *(38).* Researchers acquired velocity, acceleration and vehicle classification data at frequency of 1 Hz or greater through video data. Both CMEM and MOVES were used to generate emission estimates and fuel consumptions. Morris et al.'s system focused on emission monitoring for highway segments. The literature search did not identify any study that has been completed on real-time emission monitoring for intersections.

2.6 Emission Analysis and Modeling Efforts

2.6.1 Emission Analysis

Significant amounts of research have been focused on the impact of traffic control and other variables on intersection emission. Hallmark et al. assessed the impact of traffic signal timing on CO emissions *(39)*. In that study, acceleration, speed and distance data were collected using handheld laser range-finding devices. A mesoscopic MEASURE model was used to estimate the emission rate. Results revealed that signal coordination is an effective traffic control measure in reducing traffic emission at signalized intersections. Hallmark et al. also investigated on-road variables that affect passenger emission at intersections *(40).* Researchers collected second-by-second activity data for individual vehicles at signalized intersections. Using hierarchical tree based regression analysis, they identified queue position, grade, downstream and upstream per-lane volume, percent heavy vehicles and speed limit were the most statistically significant variables that affect the proportion of vehicles operating in each driving cycle (acceleration, deceleration, cruise, idling).

Another identified research focus is on how emission rate changes under various roadway characteristics. Jackson and Aultman-Hall analyzed the emission of an unconstrained lead vehicle using field probe-vehicle data under various roadway curve conditions to better calibrate modal emission models *(41)*. They found that horizontal curves and vertical curves have a significant impact. The same research group further examined driver and road type effects on PM, CO and other gas emissions using an instrumented minivan. They concluded that different driver and road types both significantly affect emissions *(42)*. Zhang et al. analyzed vehicle emissions under free-flow and congested conditions using probe vehicles and GPS collected second-by-second vehicle speed and acceleration data *(43)*. They concluded that the highest emission rates occurred during the transition from free-flow condition to congested condition and vice-versa. Panis et al. investigated the PM, NO_x and CO_2 emission reductions from speed management policies in Europe, they examined the impact on urban versus highway traffic with different modeling approaches (microscopic versus macroscopic). Results indicated that emissions of most classic pollutants do not rise or fall dramatically. The effects of specific speed reduction schemes on PM emissions from trucks were ambiguous but lower maximum speed (e.g., 55-65 mph) for trucks consistently result in lower emissions of CO_2 *(44)*. In an earlier research effort by Panis et al. to model instantaneous traffic emissions and the influence of traffic speed limits, they concluded that the speed management impact on vehicle emissions is complex *(45)*. The frequent acceleration and deceleration movements in the network may significantly reduce the benefits of changing the overall average speed. The conclusion from that study was that active speed management had no significant impact on total pollutant emissions.

Emissions also vary with respect to drivers' attitude, experience, gender, physical condition, and age. De Vliger et al. concluded that aggressive driving increases emissions compared to normal driving *(46).* Sierra Research found that most drivers spend about 2 percent of total driving time in aggressive mode, which contributes about 40 percent of total emissions *(47).*

As emission analysis models such as MOVES and CMEM started to provide options to conduct more detailed and microscopic emission estimation, research that incorporate trajectory data from real-world GPS probe data and traffic micro-simulation model into emission estimation has emerged. The operating mode distribution approach provides an option to utilize vehicle trajectory data (i.e., speed and acceleration rate at second level) to estimate emission to the most of its accuracy. Especially, when using micro-simulation model, the operating mode approach is an ideal way for vehicle emission estimation by taking full advantage of the output trajectory data from micro-simulation. A microscopic simulation platform for estimating vehicle emissions that can capture the vehicles' instantaneous modal activities was developed by Chen et al. They integrated the microscopic traffic-emission simulation platform by using the microscopic traffic simulation model VISSIM and the modal emission model CMEM on a sub-network selected in Beijing to evaluate the network traffic and emission conditions *(48).* Sun et al. proposed trajectory-based energy/emissions estimation method for signalized arterials using mobile sensing data (e.g., GPS traces). The proposed method first estimates the trajectories for the entire traffic population, including free-flow vehicles and queued vehicles. The estimated trajectories reflect not only the traffic state (e.g., queuing and free flowing), but also vehicle driving mode (e.g., cruise, idle, acceleration and deceleration). The estimated vehicle trajectories are then processed through CMEM emission model to estimate the total fuel consumptions and emissions *(49).*

A study conducted by University of Cincinnati developed a video-based software program to extract vehicle trajectory data that were later converted into operating mode distributions as input into MOVES *(50, 51).* Tao et al. collected GPS trajectory data of two probe vehicles, and used Portable Emission Measurement System (PEMS) to investigate the effect of signal coordination on reducing vehicle emissions. Operating mode distribution approach of MOVES was applied to generate emission rates under different scenarios *(52).* Den Braven et al. used both on-board diagnostics and microsimulation tools as two methods to generate input from MOVES emission analysis *(53).* Apart from the mentioned research, few research efforts have been documented to conduct MOVES analysis that is detailed to the operating mode distribution level based on vehicle trajectory data.

2.6.2 Emission Modeling

A few research efforts have constructed models to predict emissions based on traffic variables. For example, Nesamani et al. proposed an intermediate model component that can provide better estimates of link speeds by considering a set of Emission Specific Characteristics for each link. The intermediate model was developed using multiple linear regression and evaluated using a microscopic traffic simulation model. The evaluation results showed that the proposed emission estimation method performed better than current practice and was capable of estimating time-dependent emissions if traffic sensor data are available as model input *(54).*

Abou-Senna et al. developed a microscopic transportation emissions model to investigate CO_2 emission on limited access highways using micro-simulations *(20).* The model is able to achieve an acceptable degree of accuracy as a surrogate model for predicting transportation emissions. The model considered volume, speed, percent trucks, grade and temperature at different levels. Results showed that volume correlation with CO_2 emissions rates revealed an exponentially decaying function toward a limiting value expressed in the freeway capacity. Moreover, at speeds between 55 and 60 mph there was a significant reduction in the emissions rate, yet up to 90% of the freeway capacity was maintained *(20)*.

Shabihkhani and Gonzales developed an analytical model based on kinematic wave theory to model vehicle emissions at signalized intersections *(55)*. The model is able to compute stops, the proportion of time spent idling, and cruising based on the arrival flows. By incorporating the resulting emission factors into the analytical traffic model, total traffic emissions are easily estimated for a wide range of arriving traffic flows without the need for extensive microsimulations or additional data collection *(55)*.

Chen et al. also developed analytical emission models based on macroscopic mobility measures *(56)*. The modeling procedure was based on MOVES operating mode distribution method and microsimulation output through stepwise regression. The final model included VMT and vehicle delay to estimate emissions, which showed to reach an acceptable degree of accuracy compared with operating mode approach *(56)*.

Salamati et al. developed a simplified empirical based macroscopic model to compare emissions in roundabouts and signalized intersections. Traffic variables including intersection capacity, demand-to-capacity ratio (d/c), cycle length, green-to-cycle length ratio, signal progression (i.e., arrival type), and number of lanes were included in the model for analysis and comparison between signals and roundabouts. Total hourly emissions are estimated as the sum of emissions generated by each speed profile (Type A: no stop, Type B: one stop, Type C: multiple stops) multiplied by the proportion of those vehicles that have that speed profile and the hourly entry flow of the approach (*57*).

2.7 Literature Summary

In summary, although emission models such as MOVES has provided options to estimate transportation emissions based on operating mode distribution, only a few studies have adopted this method, which may be due to the lack of reliable vehicle operations data. Among these studies, trajectory data were either collected by probe vehicle equipped with GPS data logger or obtained from the output of micro-simulation. The major issue of using probe vehicle based GPS data is that the trajectory data used are solely based on the trajectories of one or two probe vehicles, which is difficult to fully represent the dynamic characteristics of all vehicles in the entire traffic flow. However, this disadvantage of probe GPS data can be fully addressed by using radar detection data that track all vehicle trajectories within the radar detector's detection range. Due to the limitation of probe GPS data, there is also a lack of research on real-time traffic emission monitoring system based on real world vehicle operations data. Especially, none has been developed for intersection applications.

In addition, only a few recent researches have attempted to develop macroscopic models to directly predict emissions from traffic demand and other variables. Specially, none of them are based on predicting total time spent in each operating mode, which provides more resolution than other previously used methods. In addition, many important variables, including percent of heavy vehicles and impact of roadway grade have not been considered in the models. With the use of radar based vehicle detection data and emission monitoring system, predictive models could be developed to assess the influence various factors on transportation emissions at intersection level.

3 Development of Real-Time Emission Monitoring System at Intersection Level

3.1 Transportation Emission Estimation at Microscopic Level

3.1.1 Project Level Analysis Procedure based on MOVES

As EPA's state-of-the-art emission analysis model, MOVES is able to complete analysis and estimation at national level (macroscopic), county level (macroscopic) and project level (microscopic). Since the proposed real-time emission monitoring system framework operates at the intersection (microscopic) level, only the project level analysis is further discussed below.

MOVES project level analysis is conducted in a series of steps. The first step in completing a project-level analysis using MOVES is to define project links in order to accurately capture emissions where they occur. Within MOVES, a link represents a segment of road where a certain type of vehicle activity occurs. Generally, the links specified for a project should include segments with similar traffic/activity conditions and characteristics. For example, a free-flow highway segment with a relatively stable average speed might be modeled as a single link, while an intersection or interchange will involve several number of links. The next step is to complete the Run-Spec, which include the general information for this project level analysis, including the location, time period, vehicles, roadway type, pollutants and processes to be analyzed, output type and format. The final step is to enter detailed project data using the project data manager. The data that is needed can be categorized in two general types: traffic related information and non-traffic related information. Traffic related information is the key to the accuracy of the emission estimation. For project-level analyses, MOVES allows users to enter specific details of vehicle activity for each link in the highway or transit project. MOVES provides three methods to achieve this objective:

- Link average speed. Using this method, MOVES will calculate emissions based on a default driving cycle for a given speed, grade, and road type. This method requires the least amount of traffic information. However, it also yields the least resolution when analyzing project level emissions due to the fact that default driving cycles within MOVES cannot reflect the traffic characteristics of the project roadway. This is also the method that the predecessor of MOVES, MOBILE6 used, which have been critiqued in several research.
- Link drive schedule. This method allows the user to define the precise speed and grade as a function of time (seconds) on a particular roadway link. It provides more resolution than the link average speed method. However, only one driving cycle can be entered for a run no matter the traffic volume and vehicle types, this method can only represent the path for an “average” vehicle in the traffic flow. Thus, link drive schedules will only represent average vehicle activity, not the full range of activity that will occur on the link.
- Operating mode distribution. This method allows the user to directly import operating mode fraction data for source types, hour/day combinations, roadway links, and pollutant/process combinations that are included in the run specification. Among the three methods, operating mode distribution requires the most detailed input data, which in turn leads to more accurate emission estimation. It is to be noted that, even when using the previous two approaches, MOVES still internally converts the data into operating mode distribution. For example, if using the

average speed approach, MOVES assigns a default drive schedule that corresponds to the average speed provided and coverts to operating mode distribution. If using the drive schedule approach, MOVES converts the second-by-second speed profile to operating mode distribution as well.

As stated in the previous paragraphs, traffic activity input is key to emission estimations. MOVES provides three methods to users, which is summarized and illustrated in Figure 3.1. Operating mode distribution method needs the most detailed input, and yields the most accurate results. Therefore, operating mode distribution method will serve as the basic methodology throughout this research to provide accuracy of estimation.

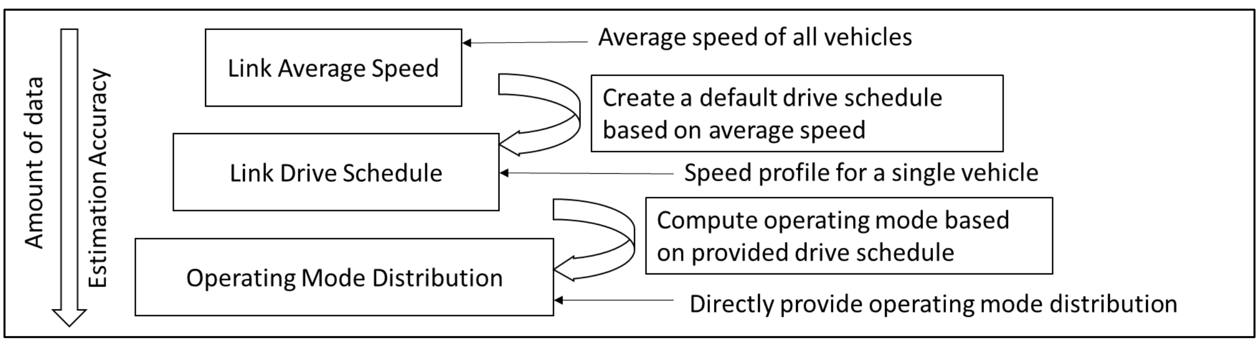

Figure 3.1 Traffic Data Input Methods in MOVES Project Level Analysis

3.1.2 Data Needs for Project Level Analysis

This section summarizes the different types of data needed for microscopic emission estimation, with respect to the MOVES project level operating mode distribution method specifically. As mentioned from previous sections, the data needed for project level analysis can be generally separated into two categories: traffic related and non-traffic related. Figure 3.2 displays the data needed for microscopic emission estimation based on operating mode approach.

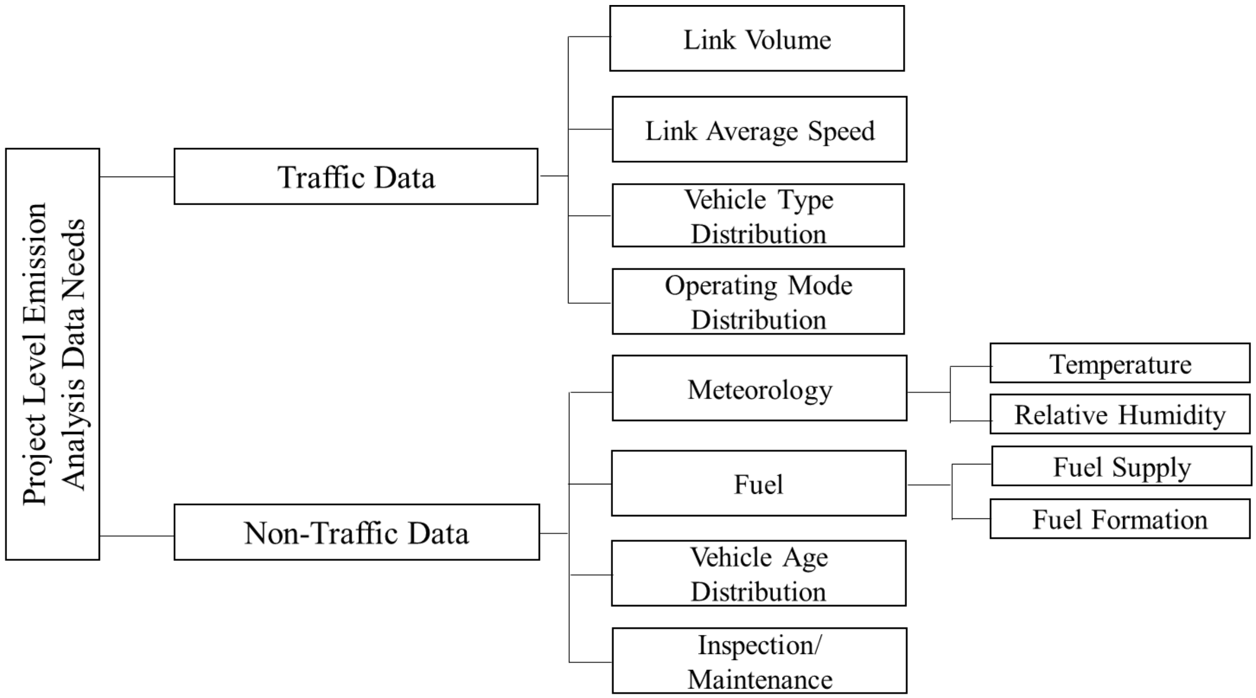

Figure 3.2 Data Needs for Microscopic Emission Estimation

- Non-Traffic Data and Sources

Non-traffic data for transportation emission analysis include meteorological information, fuel information, vehicle age distribution and inspection/maintenance program. Some of the non-traffic related data, such as, meteorological information could be obtained from local measurement or historical data, while others, including fuel, vehicle age distribution are difficult to obtain. Thus, MOVES provides a default database for this information based on the year, month and location selected. Therefore, MOVES default database is used to fill in the non-traffic data needed.

- Traffic Data and Sources

Traffic related data is crucial for accurate estimation of transportation emissions. The typical traffic data needed include roadway traffic volume, average speed, grade, the proportion of different vehicle types and the proportion of time in each operating mode. Traffic volume, average speed and grade are generally easier to obtain due its aggregate nature of measurement. The percentage of different vehicle types may be obtained from a field data collection. On the other hand, operating mode distribution is a type of data that cannot be directly obtained from any data sources. There is a need for a complex computation process from a more detailed vehicle operating information in the traffic, which often takes the form of a vehicle trajectory data, i.e., tracking the speed/location/acceleration of vehicles at every certain time interval. Currently, the source of operating mode data may come from the following sources:

- <u>Probe Vehicles.</u> Probe vehicles or devices are vehicles designed primarily for collecting traffic data in real-time, which is currently primarily used for collecting travel time and traffic operations data, incident detection, and route guidance applications. Probe vehicles collect data based on two primary methods: GPS data and geo-location that leverage cellular phone networks. These data were also used in several researches to estimate and analyze the emission rates for the probe vehicle itself and for the traffic around it. It is flexible to be implemented at any roadways without the need for fixed detectors and video cameras. However, the trajectory for the probe vehicle is used for emission analysis to represent an "average" vehicle's operations, which cannot capture the dynamics of the entire traffic flow, and the "average" conditions are hard to be measured or conducted within the traffic flow.
- <u>Output from microsimulation models</u>. Microsimulation models such as VISSIM and PARAMICS are great tools for the microscopic evaluation of traffic flow and operations. They are often able to generate second-by-second vehicle trajectory files that could be used for computing an operating mode distribution as input for

emissions analysis. However, one issue is that there is a need to calibrate and validate the simulation results in order to improve accuracy. To complete the validation and calibration, significant additional efforts are needed.

- Real-world vehicle trajectories. Ideally, this method will be able to capture all vehicles' operational information at all times. This will greatly improve the accuracy of the emission estimation compared with the other sources mentioned above. Radar based vehicle detection technology has shown the potential of obtaining this type of data, which is the method proposed in this research to achieve a real-time estimation of vehicle emissions.

3.2 Radar Based Vehicle Detection and Data Collection Process

Microwave radar was first developed for detecting objects before and during World War II. Only until recently was microwave radar used for transportation data collection purposes. The radar operating principle is as follows: roadside-mounted microwave radar sensors transmit energy toward an area of the roadway from an overhead antenna. The area in which the radar energy is transmitted is controlled by the size and the distribution of energy across the aperture of the antenna. The manufacturer usually establishes the design constraints of the radar sensor. When a vehicle passes through the antenna beam, a portion of the transmitted energy is reflected back towards the antenna. The energy then enters a receiver where the detection is made and vehicle data, such as volume, speed, occupancy, and length, are calculated *(58)*.

For intersection applications, radar sensor is typically mounted on the signal arm or other utility poles at the intersection, as shown in Figure 3.3. The radar sensor overlooks the approaching traffic, and uses radar wave to scan all oncoming vehicles. Radar based vehicle detection system is able to continuously monitor vehicle trajectories. If a vehicle is within the range of the radar detection, and is traveling toward the radar, the system will constantly keep track of the vehicle position and speed at a very short interval. Currently, the sensor is capable of detecting vehicles up to approximately 500 feet from its location. This distance is large enough to cover the functional area of most urban intersections, which means the radar detector is able to acquire all approaching vehicles operating characteristics. At every scanning instant (0.1s to 0.5s as the interval depending upon different sensors), the sensor obtains the horizontal (Y) and lateral (X) positions of each vehicle within its detection range. Each vehicle's instant speed is then computed based on the distance difference of the vehicle's successive horizontal positions. Based on these features, the sensor is therefore able to track each vehicle's trajectory and speed during the course when the vehicle approaches the intersection. Unlike loop detectors that are placed at limited fixed locations, the radar sensor is more like having a series of contiguous "virtual loop detectors" between its minimum and maximum detection ranges, and can hence accurately estimate each vehicle's real-time position and speed.

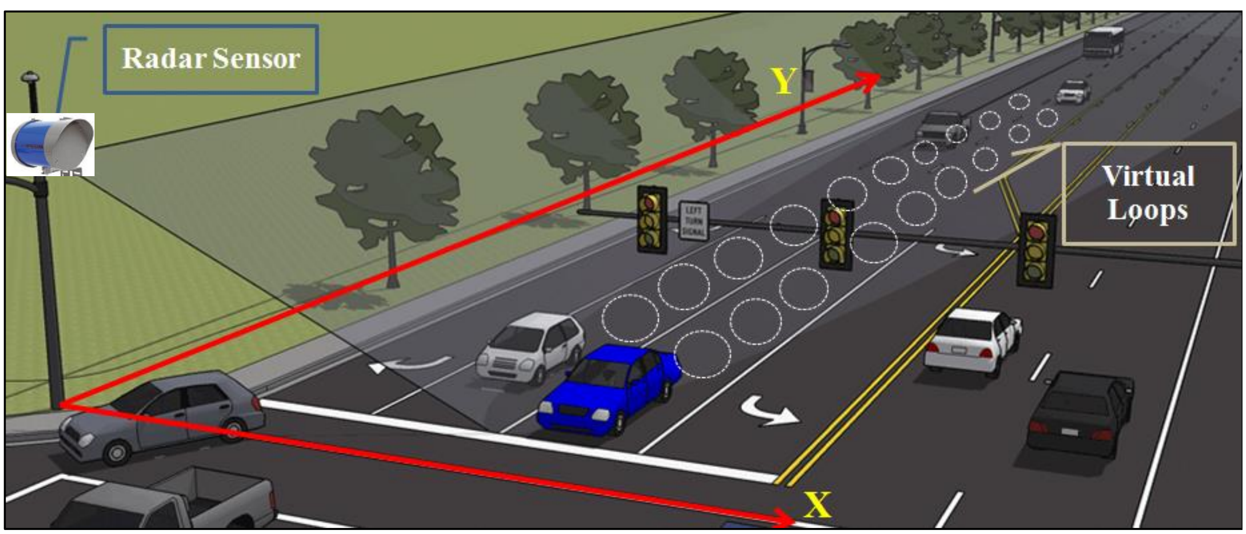

Figure 3.3 Radar Based Vehicle Detection at Signalized Intersections

(Modified based on http://www.wavetronix.com/zh/products/smartsensor/advance/features)

3.3 Development of Emission Computation Tool for Radar Data

With the data collected using radar based vehicle detection devices, it is important to develop an algorithm to use the data to convert to operating mode distribution and eventually compute emissions. In addition, this process ideally will be automatically completed every time new data come in to the system to achieve the real-time computation of transportation emissions. Ideally, the algorithm will not need to run MOVES each time, it will only need to obtain the key parameters (i.e. emission factors) from MOVES and apply these factors during the computation. Therefore, the objectives of the development of the data conversion tool are to implement and automate the process of converting raw vehicle operational data into emission estimates through using emission factors from MOVES model.

The source data is the raw data collected from radar detectors, which contains the following variables:

- Location variables (e.g. intersection name, approach direction);
- Time stamp;
- Unique vehicle ID;
- X and Y coordinates;
- Speed; and
- Vehicle length.

To process raw data into operating mode distribution and proceed with emission computation, interim variables including acceleration rate, vehicle specific power (VSP), and operating mode, need to be computed. The entire emission computation tool was developed using the R programming language, which is a popular language for data analysis and processing

(59). The following paragraphs summarize the internal algorithm used in developing this tool and illustrated in Figure 3.4.

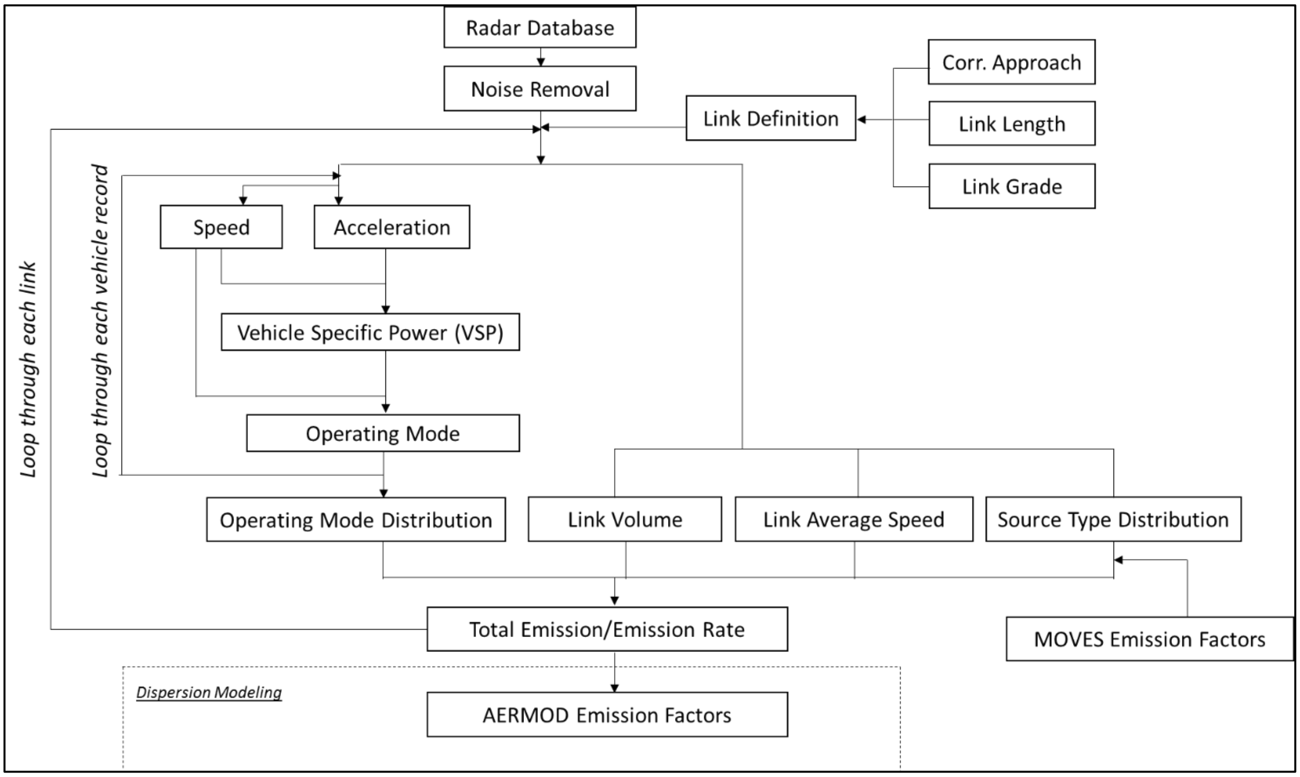

Figure 3.4 Internal Algorithm of Emission Computation Tool

3.3.1 Outlier Removal

The raw radar detector data will contain irrelevant data detected, including pedestrian activity data and other irrelevant information. This is due to the nature that the radar detector is able to detect all types moving objects. Therefore, a preliminary step is to clean the data to remove outlier (noise). However, this procedure will differ by each location. Hence, there is not a universal algorithm for this procedure. An outlier removal procedure is presented in Section 4.2.3 for the case study intersection.

3.3.2 Assign MOVES Link ID

As stated in previous sections, the roadway needs to be separated into different links for MOVES analysis. The radar data will typically be stored in a SQL database. R will then import the data into its workspace. Different approaches are first separated given a link ID number (or range) for each approach. If further division is needed, this tool requires users to import a .txt or.csv file that contains definitions of different links. The file needs to contain information including link ID number, the upper and lower boundary position of the link and the corresponding approach. The tool will then automatically assign each raw vehicle trajectory point to its corresponding link ID number based its x and y coordinates.

3.3.3 Compute Acceleration Rate

As the trajectory data did not contain acceleration rate information for each time stamp, acceleration rate need to be derived using the following equations. Specifically, speeds at successive time stamps were used to compute the acceleration rate, as represented by Equation 3.1. For the first appearance of each vehicle, the acceleration rate for its first time stamp is assumed the same as the acceleration rate at its second occurrence as shown by Equation 3.2.

$$\mathrm{a}_{\mathrm{t,k}} = \frac{v_{t-1,k} - v_{t,k}}{T} \tag{3.1}$$

$$\mathrm{a}_{\mathrm{1,k}} = a_{2,k} \tag{3.2}$$

Where,

$\mathrm{a}_{\mathrm{t,k}}$ = acceleration rate of vehicle k at time t;

$v_{t-1,k} v_{t,k}$ = speed of vehicle k at time t and t-1; and

T = time gap between successive vehicle trajectory data.

3.3.4 Compute Vehicle Specific Power (VSP)

VSP is a significant factor for determining vehicle operating mode. It is first proposed by Jimenez et al, representing the instantaneous tractive power per unit vehicle mass. It can be calculated from roadside measurements, and captures most of the dependence of light-duty vehicle emissions on driving conditions, and is directly specified in emissions certification cycles. The equation of VSP is a mathematical representation of engine load against aerodynamic drag, acceleration, rolling resistance, plus the kinetic and potential energies of the vehicle, all divided by the mass of the vehicle *(60)*. Its original equation is in the following form, as shown in Equation 3.3:

$$VSP = v(1.1a + gsin\theta + gC_r) + \frac{\rho_a C_d A_f v^3}{2M} \tag{3.3}$$

Where,

v = vehicle speed (m/s);

a = vehicle acceleration rate (m/s^2);

g = acceleration due to gravity (9.81 m/s^2);

θ = grade;

C_r = coefficient of rolling resistance;

ρ_a = density of air (kg/m^3);

C_d = coefficient of aerodynamic drag;

A_f = frontal area of vehicle (m^2); and,

M = mass of vehicle (kg);

In practice, a generic set of coefficients values for estimating VSP for a typical light duty fleet is applied as a useful basis for characterization *(61)*. VSP is calculated based on only measured speed, acceleration and road grade. The VSP values for light-duty and heavy-duty vehicles are calculated using the following equations:

$$VSP_{LDV} = v\times[1.1a + 9.81\times grade + 0.132] + 0.000302\times v^3 \quad (3.4)$$

$$VSP_{HDV} = v\times[a + 9.81\times grade + 0.09199] + 0.000169\times v^3 \quad (3.5)$$

Where,

v = vehicle speed (m/s);

a = vehicle acceleration rate (m/s^2); and,

grade = vehicle vertical rise divided by the horizontal run.

3.3.5 Assign Operating Mode

Emission estimation in this research is based on operating mode distribution to determine emission rates for a project level analysis. Operating mode can generally be classified into four categories, deceleration, idling, cruising and acceleration. In total, MOVES has further classified and defined 23 operating modes for estimation of vehicle running exhaust. A vehicle's operating mode is determined through a combination of the vehicle's speed and VSP. The detailed definition of each operating mode bins is list in MOVES User Manual, as shown in Table 3.1 *(9)*.

Each raw trajectory point was assigned a corresponding operating mode number based on its speed range and VSP values.

Table 3.1 Definition of Operating Modes

Category	Op Mode ID	VSP Criteria (kW/ton)	Speed Criteria (mph)
Braking	0	Acceleration <= -2 mph/s or <= -1 mph/s for 3 consecutive seconds	
Idling	1		-1 <= Speed<1
Low Speed Cruise/Acceleration	11	VSP< 0	1<=Speed<25
	12	0<=VSP< 3	1<= Speed<25
	13	3<=VSP< 6	1<=Speed<25
	14	6<=VSP< 9	1<=Speed<25
	15	9<=VSP<12	1<=Speed<25
	16	12<=VSP	1<=Speed<25
Medium Speed Cruise/Acceleration	21	VSP< 0	25<=Speed<50
	22	0<=VSP< 3	25<=Speed<50
	23	3<=VSP< 6	25<=Speed<50
	24	6<=VSP< 9	25<=Speed<50
	25	9<=VSP<12	25<=Speed<50
	27	12<=VSP<18	25<=Speed<50
	28	18<=VSP<24	25<=Speed<50
	29	24<=VSP<30	25<=Speed<50
	30	30<=VSP	25<=Speed<50
High Speed Cruise/Acceleration	33	VSP< 6	50<=Speed
	35	6<=VSP<12	50<=Speed
	37	12<=VSP<18	50<=Speed
	38	18<=VSP<24	50<=Speed
	39	24<=VSP<30	50<=Speed
	40	30<=VSP	50<=Speed

3.3.6 Compute Operating Mode Distribution

Operating mode distribution uses a percentage values to show the proportion of a specific operating mode within the entire data for each combination of link and vehicle type. It is computed using the following equation:

$$p_{l,v,o} = \frac{n_{l,v,o}}{\sum_o n_{l,v}} \tag{3.6}$$

Where,

$p_{l,v,o}$ = proportion of vehicle time operating in operating mode o, in link l, for vehicle type v.

$n_{l,v,o}$ = number of vehicle trajectory points in operating mode o, in link l, for vehicle type v.

3.3.7 Compute Total Emissions and Emission Rates

In traditional approach, the results (i.e. data tables) obtained could be used as input into the MOVES model along with the RunSpec files created with location, road type and other information. Many other data, such as meteorological data, vehicle age, and fuel type used MOVES default values, as no exact local data could be obtained for these inputs. Although MOVES is able to estimate emission by considering several factors, including running exhaust, start exhaust, and tire wear, only running exhaust is considered in this research, as it is the most significant type of emission on roadways. However, one issue that exists for this traditional approach is that, MOVES needs to be run for each analysis, which is not only time consuming, but also preventing the automatic process to obtain emission estimates.

During the development of this tool, an improved method is implemented to use emission factors generated by MOVES, thus eliminating the need to run MOVES for each analysis. MOVES only need to run once for each location and month combination to generate emission factors for each operating mode and source type. Emission factors come with the unit of g/hr or g/s, specific to each vehicle type and operating mode. The detailed procedure to generate emission factors from MOVES for a specific location is presented in the case study chapter.

With the availability of emission factors, total emissions for each link can be computed using the following model. All data can be obtained from intermediate variables computed in the previous steps in the algorithm.

$$E_{l,p} = \frac{L_l}{v_l} * V_l * \left(\sum_{st} \sum_{opmode} \left(EF_{o,t,p} * p_o * p_t\right)\right) \tag{3.7}$$

Where,

$E_{l,p}$ =total emission for link l, and pollutant p, in grams;

L =link length for link l, in miles;

v =link average speed for link l, in mph;

V =link traffic volume for link l, in veh/time;

$EF_{o,t,p}$ =emission factors for pollutant p, operating mode o and source type t, in g/s;

p_o =operating mode fraction for operating mode o;

p_t =vehicle type fraction for vehicle type t;

In addition, per-vehicle emission rate can be computed using the following equation:

$$ER_{p,l} = \frac{E_{p,l}}{V_l * L_l} \tag{3.8}$$

Where,

ER_p = per vehicle emission rate, for link l, pollutant p, in g/veh-mile (g/VMT);

$E_{p,l}$ = total emission for link l, pollutant p, in g;

V = traffic volume for a certain period of time (veh/time); and

L = length of link defined for emission analysis (mile);

With the computed total emissions and emission rates, the tool will also be able to compute AERMOD emission factors as input to dispersion modeling. These factors will provide the critical connection between emission analysis and dispersion modeling. This procedure is presented in Section 3.4.1.

3.3.8 Graphical User Interface (GUI)

The graphical user interface of the data conversion tool is shown in the Figure 3.5. The web application was developed using R Shiny Package, a web development framework for R *(62)*. Users can select specific radar data based on a specific date and time period and specific approaches. Various pollutants can be processed as outputs. The GUI will then proceed with the calculations and display various outputs. Basic traffic parameters including traffic volume and average speed for each link can be displayed; total emissions and emission rate per vehicle-mile (g/VMT) are also displayed. Operating mode distributions are graphically displayed as well which can greatly help users visualize the data.

Figure 3.5 GUI of the Emission Computation Tool for Radar Data

3.4 Integration with Air Pollutant Dispersion Models

The computed emission quantity and rates for various criteria pollutants provide detailed and valuable insight on vehicle emissions. Furthermore, if air pollutant concentration could be computed using the emissions rates through air dispersion models, this system could provide additional functionalities. Average pollutant concentration data can be used for quantitative hotspot analysis and NAAQS air quality conformity purposes. This section introduces the procedure and data needed for completing such analysis.

3.4.1 AERMOD Dispersion Analysis Procedure

As EPA's preferred and recommended dispersion model, AERMOD is a steady state Gaussian plume model for analyzing air pollutant dispersion from various sources, including industrial and transportation sources. In the stable boundary layer, it assumes the concentration distribution to be Gaussian in both the vertical and horizontal directions. In the convective boundary layer, the horizontal distribution is also assumed to be Gaussian, but the vertical distribution is described with a bi-Gaussian probability density function. AERMOD incorporates algorithms to account for enhancements of lateral dispersion resulting from plume meander. It characterizes the planetary boundary layer through surface and mixed layer scaling. Vertical profiles of wind speed, wind direction, turbulence, temperature, and temperature gradient are constructed by using measurements and extrapolations of those measurements. AERMOD accounts for the vertical inhomogeneity of the planetary boundary layer in its dispersion calculations. The latest version of AERMOD, as of 2016, version 15181 was used in this air dispersion analysis.

The Gaussian plume model serves as the basis of the AERMOD. The equation is shown as follows (*63*),

$$\mathrm{C} = \frac{q}{2\pi u \sigma_y \sigma_z} * \exp\left(\frac{-y^2}{2\sigma_y^2}\right) * [\exp\left(\frac{-(z-H)^2}{2\sigma_z^2}\right) + \exp\left(\frac{-(z+H)^2}{2\sigma_z^2}\right)] \tag{3.9}$$

Where,

C = concentration of receptor at (x, y, z) in g/m3;

q = emission factor in g/s;

u = wind speed in m/s;

H = source height in m and,

σ_y, σ_z = horizontal and vertical dispersion parameters in m.

AERMOD is a command line based model using a keyword-parameter approach. To complete the AERMOD analysis, users need to provide an input text file that contains most necessary options for modeling. Additional text files may be needed to supplement the input information. This input file is structured to have five components, which are listed as follows. An example of contents of AERMOD input file is shown in Figure 3.6.

- <u>CO</u>ntrol: this segment defines the title and modeling options including the pollutant type, average concentration time period etc.
- <u>SO</u>urce: this segment defines the source type, location, size and emission factors. Multiple sources of different types can be defined and modeled in a single run.
- <u>RE</u>ceptor: this segment defines the locations at which air pollutant density needs to be computed. Again, multiple sets of receptors can be defined and modeled in a single run.
- <u>EV</u>ent: this segment is optional for input and not usually applicable for roadways as emission sources.
- <u>OU</u>tput: this segment configures the types of output options for pollutant concentrations. Output options include computing average or first-highest, second-highest, etc. concentrations for each receptor locations, or a list of receptors with highest concentrations.

```
CO STARTING
   TITLEONE Air Dispersion Modeling for Appleton Int
   MODELOPT  CONC   FLAT
   AVERTIME  1  3  8  24  PERIOD
   POLLUTID  CO
   RUNORNOT  RUN
   ERRORFIL  ERRORS.OUT
CO FINISHED

SO STARTING
   ELEVUNIT  METERS
   LOCATION  STACK1  LINE  -134.0   0.0   18.0   0.0
   ......
   SRCPARAM  STACK1  0.01  2.5  11
   ......
   SRCGROUP  ALL
SO FINISHED

RE STARTING
   GRIDCART POL1 STA
                 XYINC -150 15 10 10 15 10
   GRIDCART POL1 END
   ......
RE FINISHED
ME STARTING
   SURFFILE  aermet2.sfc
   PROFFILE  aermet2.pfl
   SURFDATA  XXXXX  2015  XXXXXXXXX
   UAIRDATA  XXXXX  2015  XXXXXXXXX
   PROFBASE  XXX  METERS
ME FINISHED

OU STARTING
   RECTABLE  ALLAVE  FIRST
   MAXTABLE  ALLAVE  50
   SUMMFILE  AERTEST.SUM
OU FINISHED
```

Figure 3.6 Example Contents of AERMOD Input File

3.4.2 Data Needs for Dispersion Analysis

This section summarizes the different types of data needed for air pollutant dispersion analysis, with respect to AERMOD model for transportation emission sources. Figure 3.7 provides an overview of data needs. The input data for air dispersion analysis can be classified into three general categories, which are introduced below.

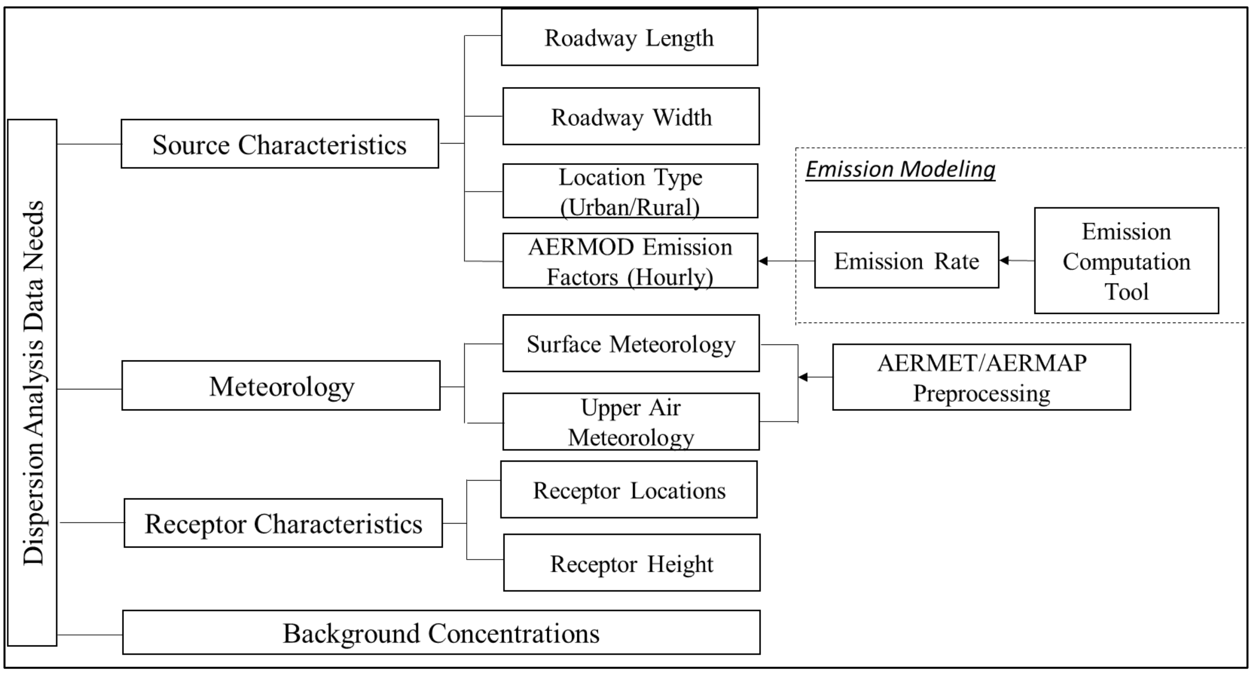

Figure 3.7 Data Needs for AERMOD Dispersion Analysis

Emission Source (Roadway) Characteristics

For transportation air pollutants dispersion analysis, roadways are the sources of emissions and air pollutions. The required source characteristics include roadway segment lengths, widths and urban/rural location. For intersection analysis, multiple sources can be separately defined for each approach or at even more detailed level. Roadways are conventionally modeled as LINE or rectangular AREA sources. The separation of different emission sources can generally follow the link definition in emission analysis.

Emission Factors

An emission factor is one of the most important inputs for dispersion analysis. This also provides the connection between emissions computed using radar based vehicle detection data and dispersion modeling. A more detailed variable emission factors will lead to more resolution for dispersion analysis. Therefore, the radar-based emission modeling procedure introduced in the previous sections can provide such detailed emission factors information.

AERMOD requires composite emission factors in the units of g/s/m^2. Therefore, there is a need to convert emission rates computed to the units required by AERMOD. The equation for computing composite emission factors is listed below:

$$EF_{comp,l} = \frac{ER_l * V_l * L_l}{3600 * A_l} \tag{3.10}$$

Where,

$EF_{comp,l}$ = Composite emission factor, in g/s/m^2;

ER_l = Emission rate computed using Emission Computation Tool for Radar Data, in g/veh-mile (VMT);

V = Source traffic volume, in vph;

L = Source length, in m, and

A = Source area, in m^2.

Meteorological Information

Meteorological data directly uses the results from the two preprocessors AERMET and AERMAP based on local data. Weather data can be obtained from National Weather Service database.

Receptors

Receptors are virtual monitoring stations where air pollutants concentration data is estimated. Receptors are general placed at a height of 1.8 m above the ground to simulate the human breathing height. Generally, near a source, receptors are placed with finer spacing and farther from a source with wider spacing.

Background Concentrations

The background concentration includes emissions from all sources other than the project, which affects concentrations in the project area. The concentrations obtained from AERMOD should be added to the background concentration to get the total representative concentration, called the design value; this value describes the future air quality concentration in a project area, which can be compared with the National Ambient Air Quality Standards. Several options for obtaining the background concentration can be found in an EPA publication (*12*).

Output Options

The dispersion output options including highest 1-hour, 3-hour, 8-hour, 24-hour average concentrations in order to compare with NAAQS standards for each criteria pollutant. The concentration computed have the units of $\mu g/m^3$, while NAAQS criteria are provided as ppm (particles per million). There is a need to convert between units, shown in the following equation. Other output options include identify the Top X receptors locations with the highest average concentrations, which can be used for quantitative hot spots analysis.

$$Conc\ \left(\frac{\mu g}{m^3}\right) = Conc\ (ppm) * \frac{Molecular\ Mass\ \left(\frac{g}{mol}\right)}{Molar\ Volume\ (L)} * 10^3 \tag{3.11}$$

3.5 Real-Time Emission Monitoring System Framework

Based on the characteristics of the radar based vehicle detection system, emission computation tool and dispersion analysis procedure, a full-scale framework for a system that monitors vehicle emission at intersections in real time, and provides visualization and decision-making support for transportation authorities to react to high emission levels, is proposed. The system is named as Real-Time Intersection Emission Surveillance System (RETIESS). The feasibility of RETIESS is based on incorporation of MOVES emission factors, radar detection data and AERMOD dispersion modeling.

Figure 3.8 shows the system framework of RETIESS with data flow indicated. According to the figure, RETIESS is composed of the following six components: Configuration Module (CM), Data Collection Module (DCM), Data Processing Module (DPM), Emission Computation Module (ECM), Dispersion Analysis Module (DAM) and Emission Visualization and Decision Support Module (EVDSM).

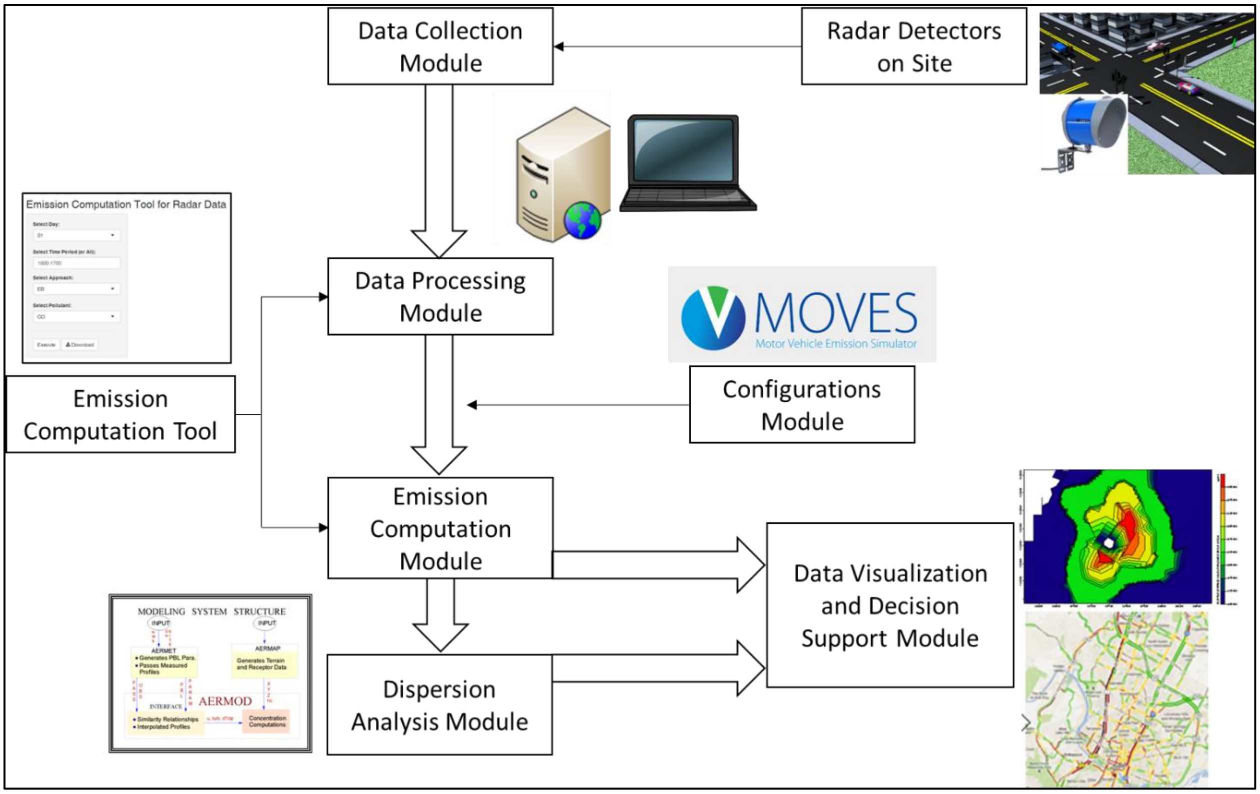

Figure 3.8 Real-Time Emission Monitoring System Framework

The functionality of each module is presented in the following paragraphs:

3.5.1 Configuration Module

The configuration module (CM) provides a GUI (Graphical User Interface) to define the MOVES links, and MOVES project parameters, and collect all non-traffic related information. The configurations are eventually stored in a Run-Spec file in MOVES database, many non-traffic parameters could apply MOVES default database values.

3.5.2 Data Collection Module

In this data collection module (DCM), data collected from radar detectors are continuously stored into a SQL database on a real-time basis to prepare for data processing.

3.5.3 Data Processing Module

The data processing module (DPM) retrieves real-time trajectory data of all vehicles traveling on all legs of an intersection at a certain frequency (e.g. 0.5 second) from the radar detector. The collected trajectory data are stored immediately in the database of RETIESS. The DPM then retrieves the trajectory data from the database at certain analysis interval (e.g. 1 minute), processes and converts the trajectory data into interim processed data including acceleration rates, average speeds of links, volumes, VSPs and operating mode distributions.

3.5.4 Emission Computation Module

The emission computation module (ECM) eventually runs the Emission Computation Tool using emission factors generated from MOVES model to estimate the emission rate for specified types of pollutants. This entire process can be repeated at a fixed time interval (e.g., 1 minute or 5 minutes), so that real time emission surveillance can be realized.

3.5.5 Dispersion Analysis Module

The dispersion analysis module (DAM)s converts the emission computation result into AERMOD input format and configures the receptors and other needed information. AERMOD will be run in this module and concentration values will be computed using the defined sets of receptors.

3.5.6 Emission Visualization and Decision Support Module

The emission visualization and decision support module (EVDSM) is responsible of the emission rate surveillance by providing a GUI that displays the emission rates of various intersection approaches. The emission alarm server of the EVDSM monitors the emission rate in real time and initiates alarm as warnings if the emission rate exceeds the preset threshold, for example using EPA's light duty vehicle emission standard. The system can also display other traffic information, such as traffic volume, average speed, and operating mode distribution. Air dispersion results can be used for air quality analysis and transportation conformity purposes by comparing to NAAQS standards.

In summary, this uniqueness in terms of completeness of dataset for computing the operating mode distribution assures accurate estimation of vehicle emission using Emission Computation Tool for Radar Data and in a real-time manner. The next chapter will implement this proposed system at an urban signalized intersection as a case study to test the feasibility and validity of this system.

4 System Implementation - Case Study

4.1 Study Site

The objective of this case study is to implement the proposed real-time emission monitoring system and evaluate its applicability and performance for an urban signalized intersection scenario. The study intersection is an urban signalized traditional four-leg intersection located in Appleton, WI. The intersecting roadways are Wisconsin Avenue and Meade Street, in which Wisconsin Avenue is an arterial and Meade Street is a collector road. The average annual daily traffic (AADT) on Wisconsin Avenue is approximately 11,000 veh/day, while AADT on Meade Street is approximately 10,000 veh/day *(64)*. The speed limit on all approaches is 30 mph. Each of the four approaches has one exclusive left turn lane and two through lanes (right turns are shared in the right most lane), as shown in Figure 4.1.

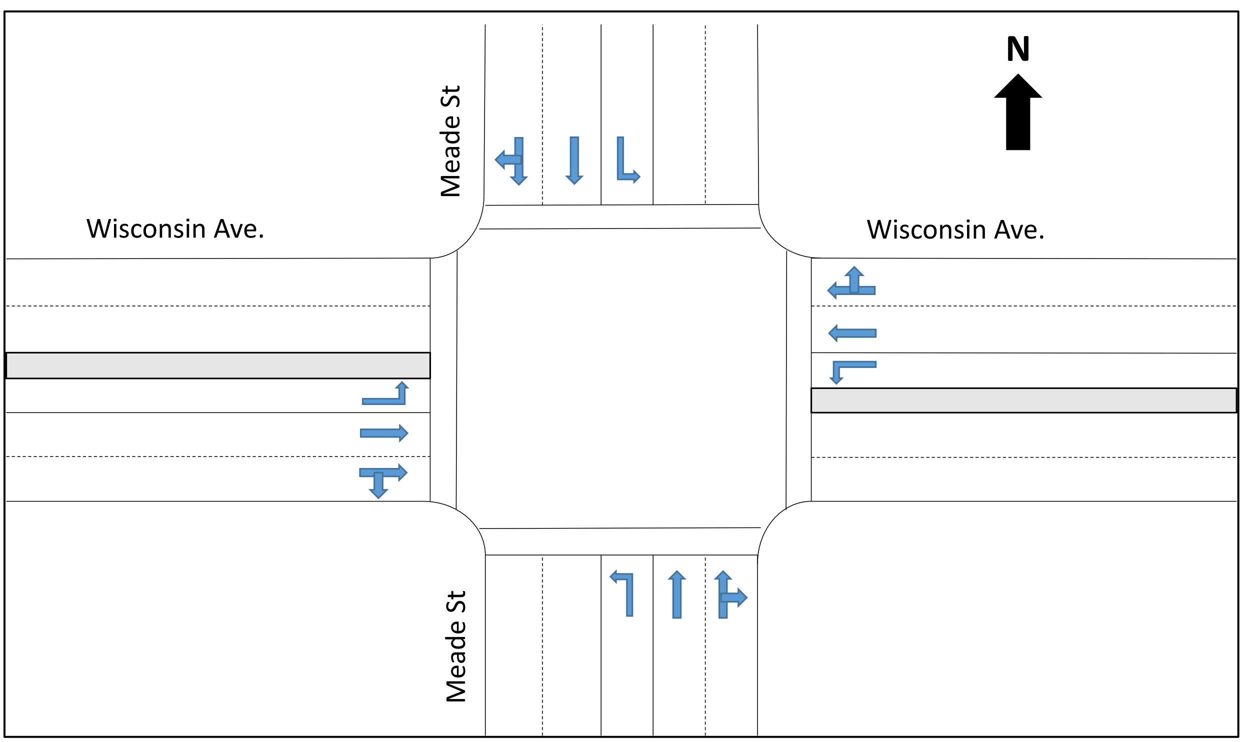

Figure 4.1 Case Study Intersection Configurations

4.2 Data Collection and Processing

4.2.1 Data Collection Overview

In order to collect raw vehicle's operational data at each intersection approach using radar based vehicle detection, one radar detector was placed on the signal pole to monitor each approach. As can be shown through Figure 4.3, each red circle indicates the location of the radar detector at the intersection approaches, which are installed on signal poles. The radar detector used is called Intersector™, a commercially available radar based vehicle detection system manufactured by MsSedco. Figure 4.2 illustrates the actual Intersector™ device. The advantages of the device include not affected by weather conditions, the ability to detect in multi-lanes, and easily installable, among others *(65)*. The data collection was conducted during the months of January and February 2015.

Figure 4.2 Intersector™ Radar Detector by MsSedco *(65)*

(a) Southbound Approach

(b) Northbound Approach

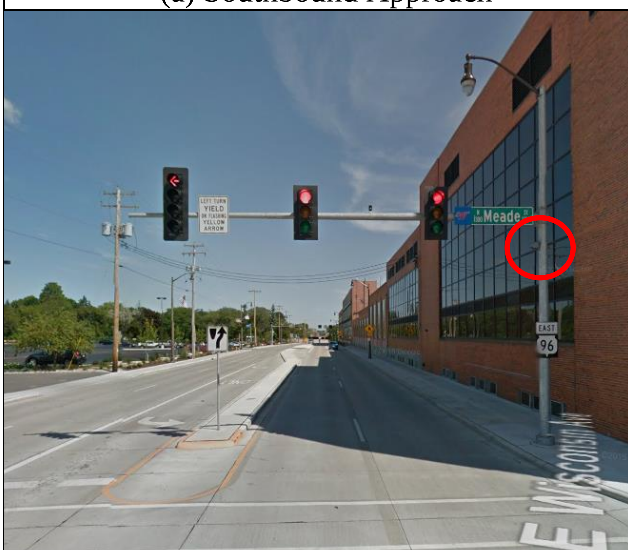

(c) Westbound Approach

(d) Eastbound Approach

Figure 4.3 Study Site Data Collection Photos

In order to log radar data for all four intersection approaches, a laptop computer running custom data collections software was placed inside the signal cabinet. The software used for logging vehicle trajectory data from radar detectors relies on the technology developed by Santiago-Chaparro et al *(66)*. The data collection software monitors the underlying data stream of the radars without interfering with the main function of the vehicle detection system.

4.2.2 Raw Trajectory Data

A sample of the raw vehicle trajectory data collected by the radar detector is presented in Figure 4.4. The raw is stored in a MySQL database, subsequently imported into R for data analysis. It can be observed from the figure that one vehicle trajectory record is generated for approximately every 0.5 seconds for each vehicle within the detection range. Each raw record contains the following information that enables data query and manipulations based these attributes.

- Data collection site;
- Unique Vehicle ID;
- Detailed timestamp (date and time);
- Approach;
- X, Y coordinates representing the location of the vehicle on the Cartesian plane;
- Speed (mph); and
- Vehicle length (ft).

site	vehicleid	timestamp	approach	xcoord	ycoord	speed	length
WiscMeade	SB_49_2015_1_1_4_49_4	2015-01-01 04:49:17.352202	SB	16.1	140.4	4.3	11.2
WiscMeade	SB_49_2015_1_1_4_49_4	2015-01-01 04:49:17.867003	SB	16.1	134.2	4.3	11.2
WiscMeade	SB_49_2015_1_1_4_49_4	2015-01-01 04:49:18.381804	SB	16.4	129.9	4.5	11.2
WiscMeade	SB_49_2015_1_1_4_49_4	2015-01-01 04:49:18.896604	SB	16.4	124.7	4.7	11.2
WiscMeade	SB_49_2015_1_1_4_49_4	2015-01-01 04:49:19.395805	SB	16.1	120.7	4.9	11.2
WiscMeade	SB_49_2015_1_1_4_49_4	2015-01-01 04:49:19.895006	SB	16.1	120.4	5.6	11.2
WiscMeade	SB_49_2015_1_1_4_49_4	2015-01-01 04:49:20.386407	SB	15.7	119.7	6.3	11.2
WiscMeade	SB_49_2015_1_1_4_49_4	2015-01-01 04:49:20.909008	SB	14.8	112.5	6.7	11.2
WiscMeade	SB_49_2015_1_1_4_49_4	2015-01-01 04:49:21.423809	SB	12.8	107.3	6.7	11.2
WiscMeade	SB_49_2015_1_1_4_49_4	2015-01-01 04:49:21.938610	SB	10.2	103.0	6.7	11.2
WiscMeade	SB_49_2015_1_1_4_49_4	2015-01-01 04:49:22.445611	SB	7.5	100.4	6.0	11.2
WiscMeade	SB_49_2015_1_1_4_49_4	2015-01-01 04:49:22.968212	SB	2.6	97.1	5.4	11.2
WiscMeade	SB_49_2015_1_1_4_49_4	2015-01-01 04:49:23.483012	SB	-1.0	95.5	4.3	11.2
WiscMeade	SB_49_2015_1_1_4_49_4	2015-01-01 04:49:23.982213	SB	-5.2	92.8	3.8	11.2

Figure 4.4 Raw Radar Detector Data Sample

In order to visualize the raw vehicle trajectory data, a randomly selected sample of data was plotted based on its X and Y coordinates for each approach and presented in Figure 4.5. The y-coordinate is measured approximately parallel to the roadway direction of travel. A zero y-coordinate represents the location of the radar detector. As Y increases, it indicates that the actual vehicle location at the specific time stamp is farther away from the intersection. The farthest data points detected is slightly above 500 ft., which confirms the radar detector's detection range. The x-coordinate is measured approximately perpendicular to the roadway direction of travel. It can indicate the lane that the vehicle is traveling on. It can be seen from the figure that, the plot of this raw data sample generally conforms to the configurations of each intersection approach, which shows its plausibility of being a valid and strong data source for transportation emission analysis. However, a number of data points seem to be to out of the roadway range, which are considered outliers and noises. These data points need to be removed before starting data processing and emission analysis to improve validity and accuracy.

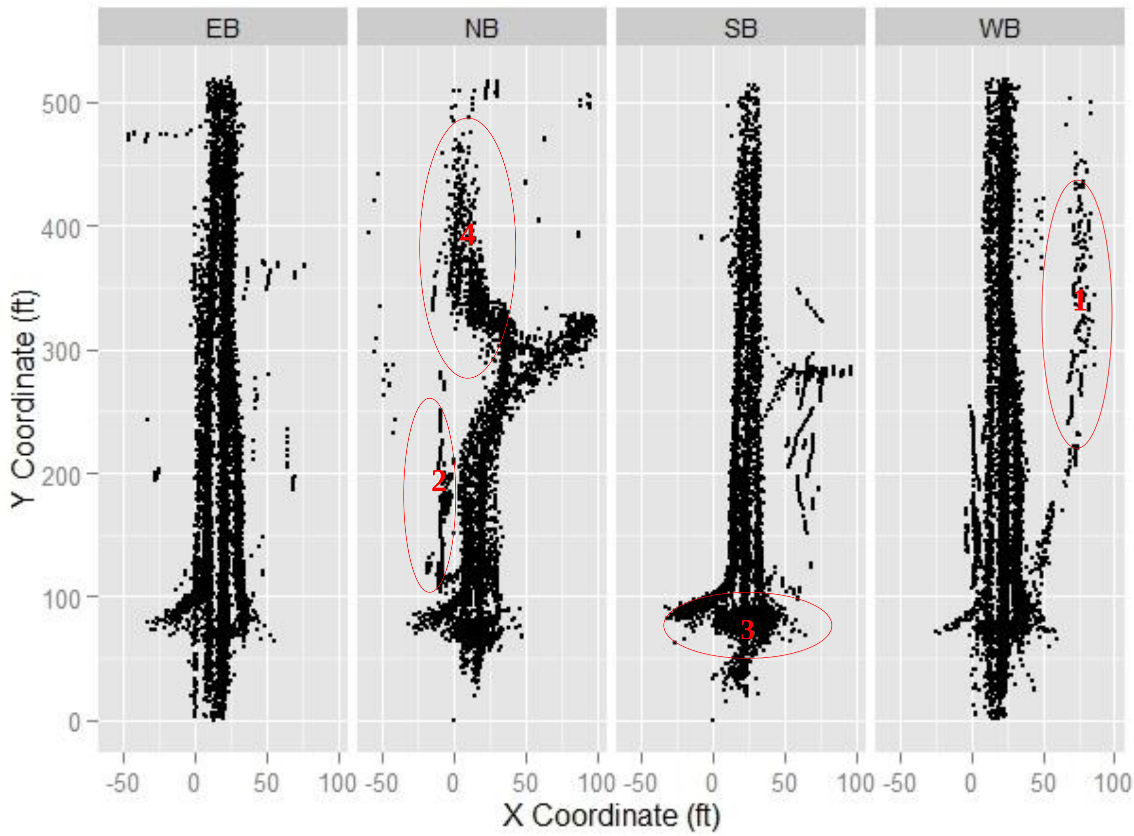

Figure 4.5 Vehicle Trajectory Points Examples

4.2.3 Outlier Removal

The objective of the outlier removal is to identify the noise sources and remove data that are irrelevant to vehicle operations near the case study intersection. Through investigating the surrounding land use and intersection configurations, three major sources of data noise are identified, which are listed below. Each noise source is also indicated in Figure 4.5 using the corresponding number.

1. Vehicles operating in nearby business parking lots detected;
2. Pedestrian and bicyclists activities detected;
3. Cross traffic detected (duplicate detection);

4. In addition, the geometry at the northbound approach becomes complicated beyond 300 ft. from the intersection, as the roadway is curved and there exists another immediate unsignalized three-leg intersection.

Each of the different noise source needs to have separate criteria for removing the data and associated trajectory. An important parameter to consider before defining noise removal criteria is to identify the location (i.e. y-coordinate in the radar data) of the stop bar. Through intersection measurement, the stop bar has a y-coordinate of approximately 120 ft for all approaches. With the stop bar location for each approach identified, noise removal criteria can be defined, introduced in the following paragraphs.

First, remove all trajectory points on the northbound approach where y-coordinate of the point is larger the 300 ft threshold. This step aims at removing the data from the local road that is irrelevant to this intersection. Next, remove all trajectory points on all approaches where the data has a y-coordinate greater than the y-coordinate of the stop bar (y_{sb}) and whose x-coordinate is outside of the range of the traveled lanes (defined by x_{low} and x_{upp}), shown through the following equation.

$$\text{Remove: } \mathrm{y} > \mathrm{y}_{\mathrm{sb}} \ \& \ (x < x_{low} \mid x > x_{upp}) \tag{4.1}$$

This step can remove the vehicle activity data in the nearby parking lot and some pedestrian and bicycle data. Then, remove all data associated with a vehicle id that only appears with y smaller the y_{sb} or only y larger than y_{sb}, shown in the following equations.

$$\text{Remove all: } \max(y_{id1}) < y_{sb} \mid \min(\mathrm{y}_{id2}) > y_{sb} \tag{4.2}$$

The former is able to remove cross traffic from other approaches, while the latter is able to remove vehicles entering into nearby businesses. Finally, remaining pedestrian data are removed with the following criteria,

$$\text{Remove all: length}_{\text{id}} < 6 \;\&\; \text{mean}(\text{x}_{\text{id}}) < \text{x}_{\text{low}} \tag{4.3}$$

Figure 4.6 graphically illustrates the outlier removal process. As a result of this process, the remaining data contains the best possible trajectory data that can be used for further analysis. This ensures that the best available data is used to achieve the highest accuracy in analysis results.

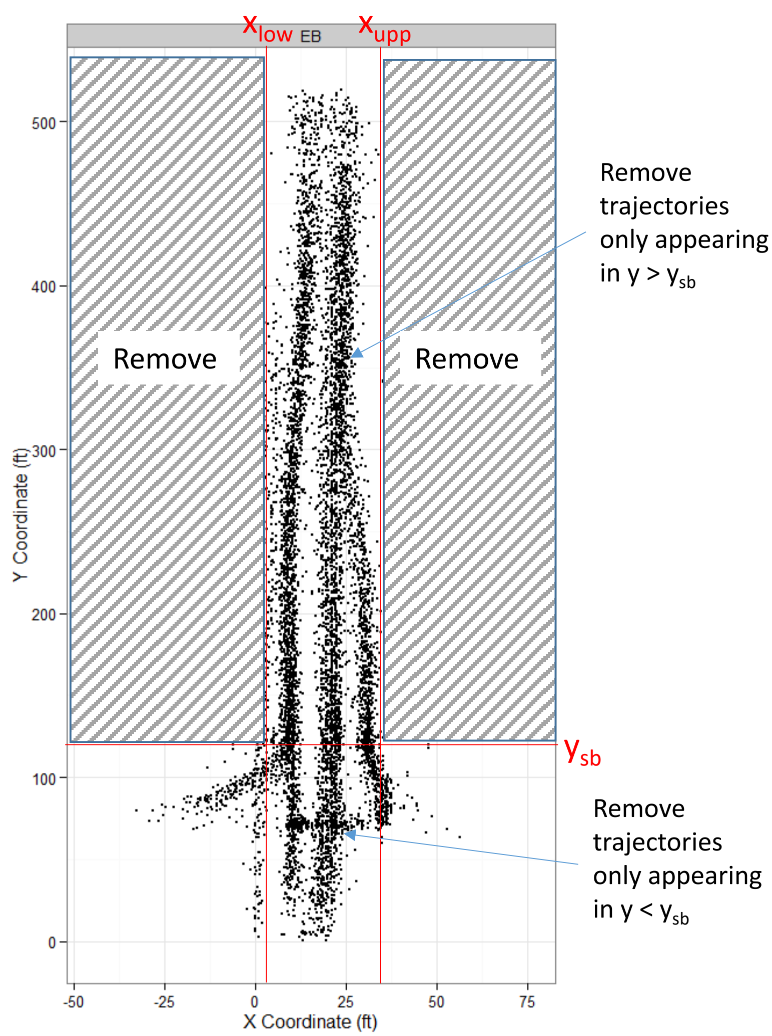

Figure 4.6 Noise Removal Procedure Illustration

4.3 Results Analysis and Validation

4.3.1 Traffic Volume

With raw vehicle trajectory data cleaned up from outliers and ready for data processing and analysis, a series of analyses were designed and conducted in this case study. To start with, fundamental traffic parameters, including traffic volume and average speed could easily be obtained from the radar detector data in real-time, which is analogous to the data obtained from conventional loop detectors.

Traffic volume can be computed using the number of unique vehicle ids that exist during a certain time period. Figure 4.7 illustrates the traffic volume variations during a weekday at the study site based on the collected data grouped by each approach. One traffic volume count is generated every 15 minutes. The traffic volume trend over the day is a typical pattern that can be commonly observed, with very low traffic during midnight to 6 AM, and high volume during morning and evening peak hours. All approaches have rather similar number of entry vehicles into the intersection, with northbound and southbound approaches having larger volume during morning peak hours and eastbound approach having the greatest number of vehicles during evening peak hours.

The average weekday intersection entering volume during the data collection period is to 21,069 vehicles, which closely matches with the intersection AADT of approximately 21,000 veh/day. To be more specific, the average weekday EB and WB entering volume is 10,753 (AADT 11,000) and NB and SB entering volume is 10,285 (AADT 10,000). This can show that the radar based vehicle detection system is able to detect vehicle operating data with a very high degree of accuracy.

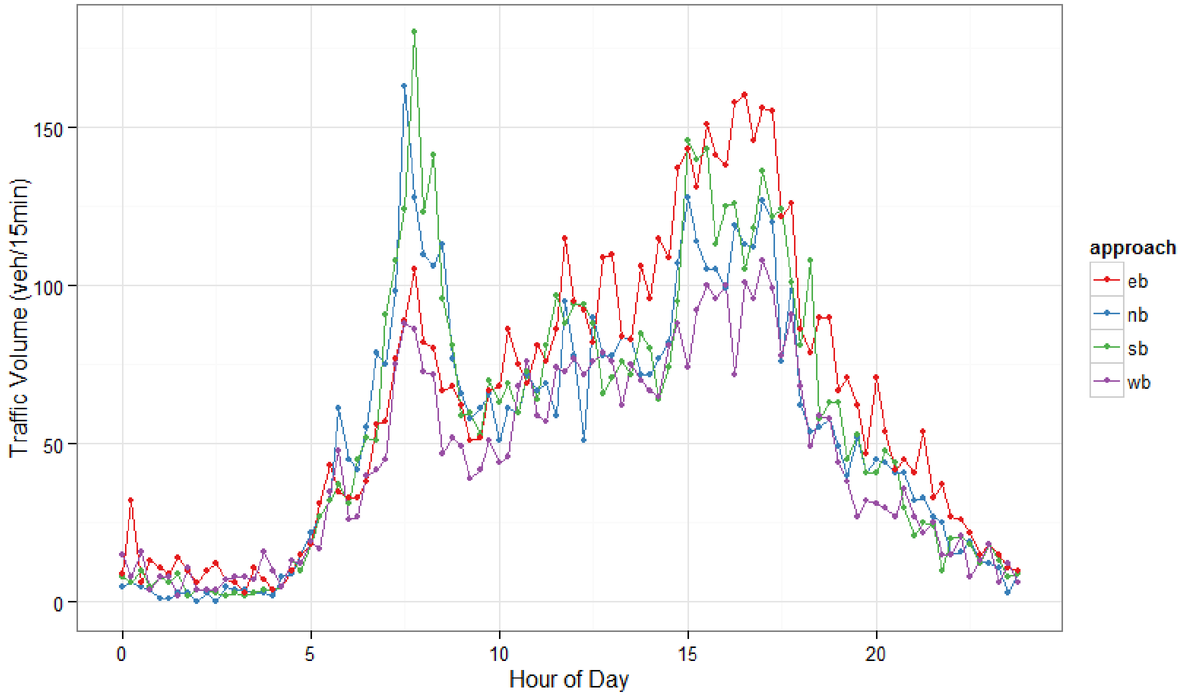

Figure 4.7 Traffic Volume by Hour of Day

4.3.2 Average Speed

Average speed is computed by taking the mean speed of all vehicle trajectory point with a specific period. Again, one average speed for each approach is computed every 15 min. Figure 4.8 illustrates the results. A commonly seen daily speed pattern can be observed with high average speed during nighttime due to less number of stops and deceleration. Eastbound and westbound approaches have generally larger average speed than northbound and southbound approaches dues to their higher speed limit (35 mph). Northbound approach has the lowest average speed due to its different shorter intersection distance measurement from the intersection compared with other approaches.

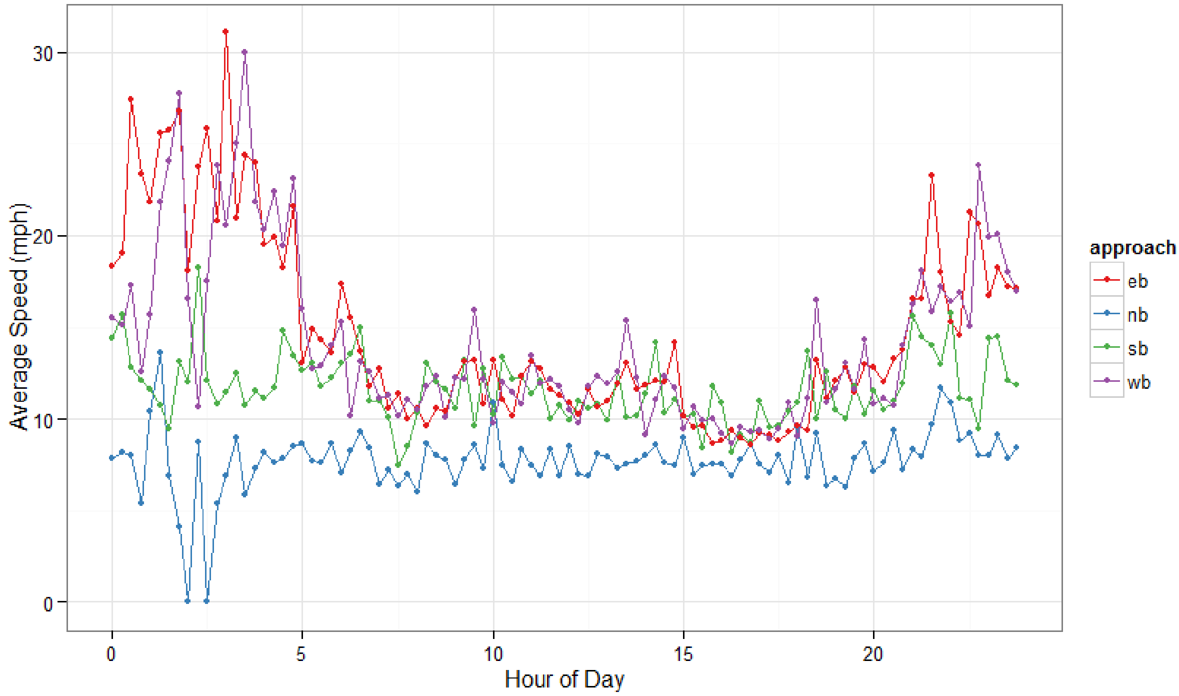

Figure 4.8 Average Speed by Hour of Day

4.3.3 Operating Mode Distribution

The proposed real-time emission monitoring system is used to estimate the emissions of various pollutants for each intersection approach. As an intermediate step, operating mode distributions during different time periods was first analyzed. Each operating mode distribution is calculated and obtained as an intermediate result using the Emission Computation Tool for Radar Data. As a result, figures were generated to compare the operating mode distributions in short time interval during a typical peak and off-peak hour.

Figures 4.9 compare the operating mode distribution during consecutive 10-minute intervals in a typical peak hour (4 PM to 5 PM) and off-peak hour (10 AM to 11 AM) by corresponding intersection approaches. Note that operating modes 33 through 40 are not shown in this figure and subsequent figures. These operating modes represent high-speed acceleration/cruising modes (>=50 mph) which is not applicable for this intersection due to low speed limits. These comparisons aim at revealing the change in operating mode distribution during different short time intervals within an hour. According to these figures, change in operating mode distribution can be seen in both peak-hour intervals and off-peak hour intervals. For example, in Figures 4.9, percentages of different operating modes vary in different figures among different approaches and time intervals. The patterns are significantly different for operating mode 1 (i.e. idling), with higher percentage during peak hours. This indicates that during peak hour, larger percentage of vehicle need to stop at the intersection approach. In addition, it can be observed that non-peak hour has generally a higher proportion of operating mode 21 through 30, which indicates that during non-peak hours, traffic operates more smoothly and more vehicles are able to maintain their operating speed while traveling through the intersection.

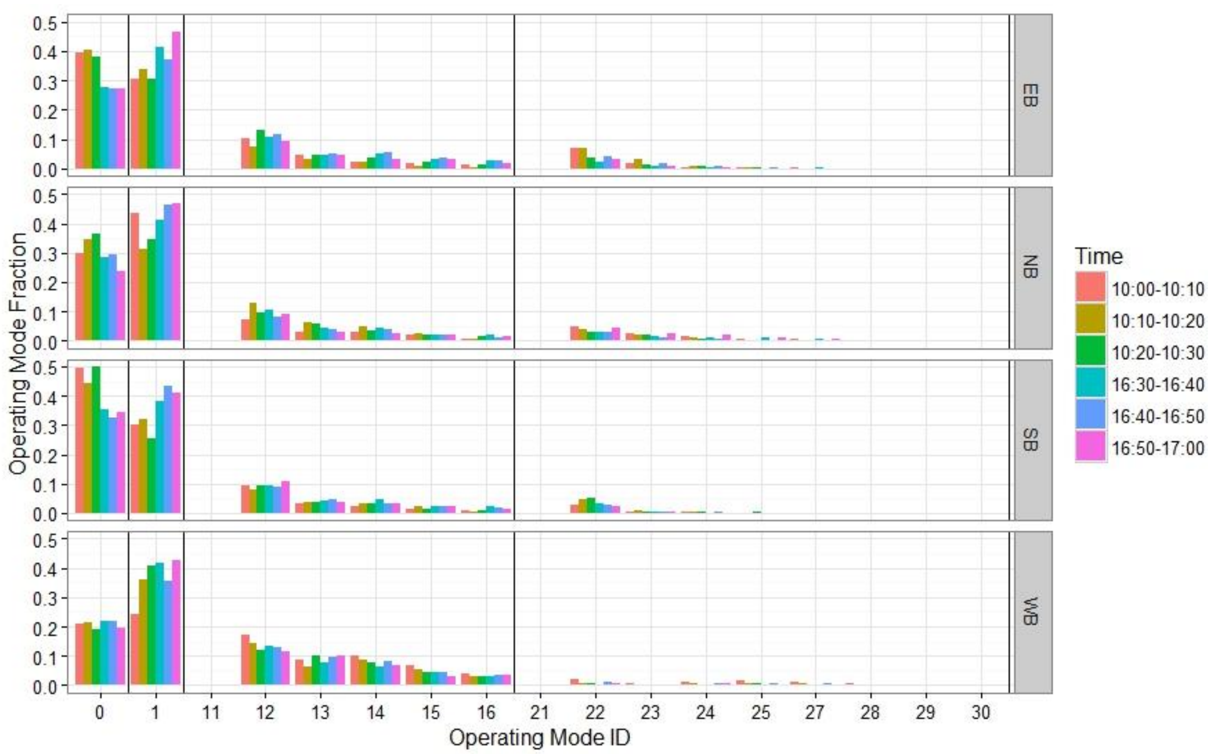

Figure 4.9 Operating Mode Distribution during Peak and Non-Peak Hour Periods by Approach

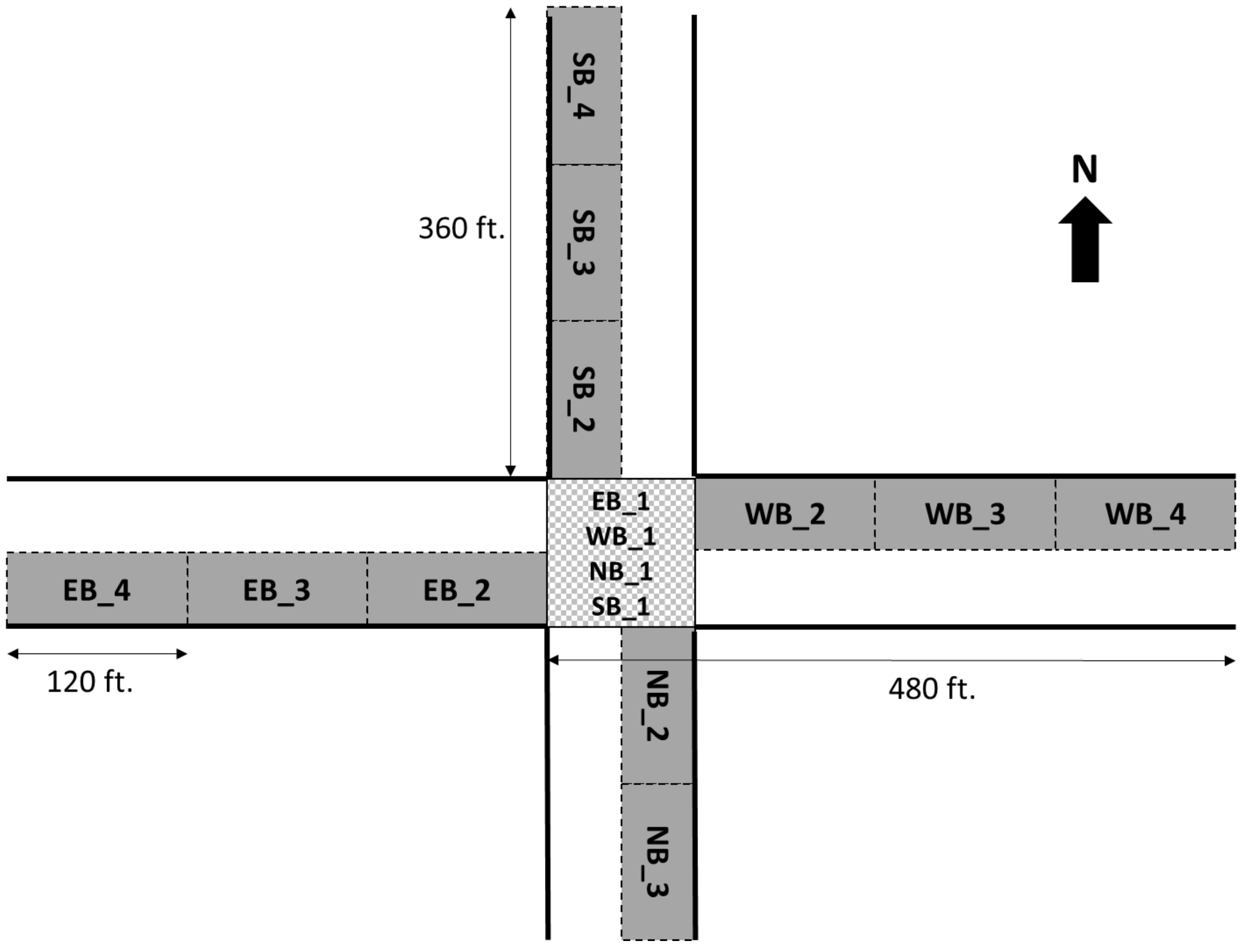

Figure 4.10 Link Classification Diagram

Next, each approach is further divided into links to analyze the operating mode difference with respect to distance to intersection. Figure 4.10 graphically displays the link classification for this test intersection. Specifically, each approach was divided into four separate links (3 for NB approach), with each link having a length of 120 ft. Link 1 of each approach represent the area within the intersection, link 2 represent the section that is nearest the approach stop bar, 4 being furthest away for intersection. Each operating mode distribution was illustrated for each approach and peak/non-peak hour with respect to each link. It can be shown from Figure 4.11 that link 2 of each approach mainly consist of vehicle idling, while link 3 has the largest proportion of vehicle decelerating, link 4 has the largest proportion of vehicle mid-speed cruising/acceleration.

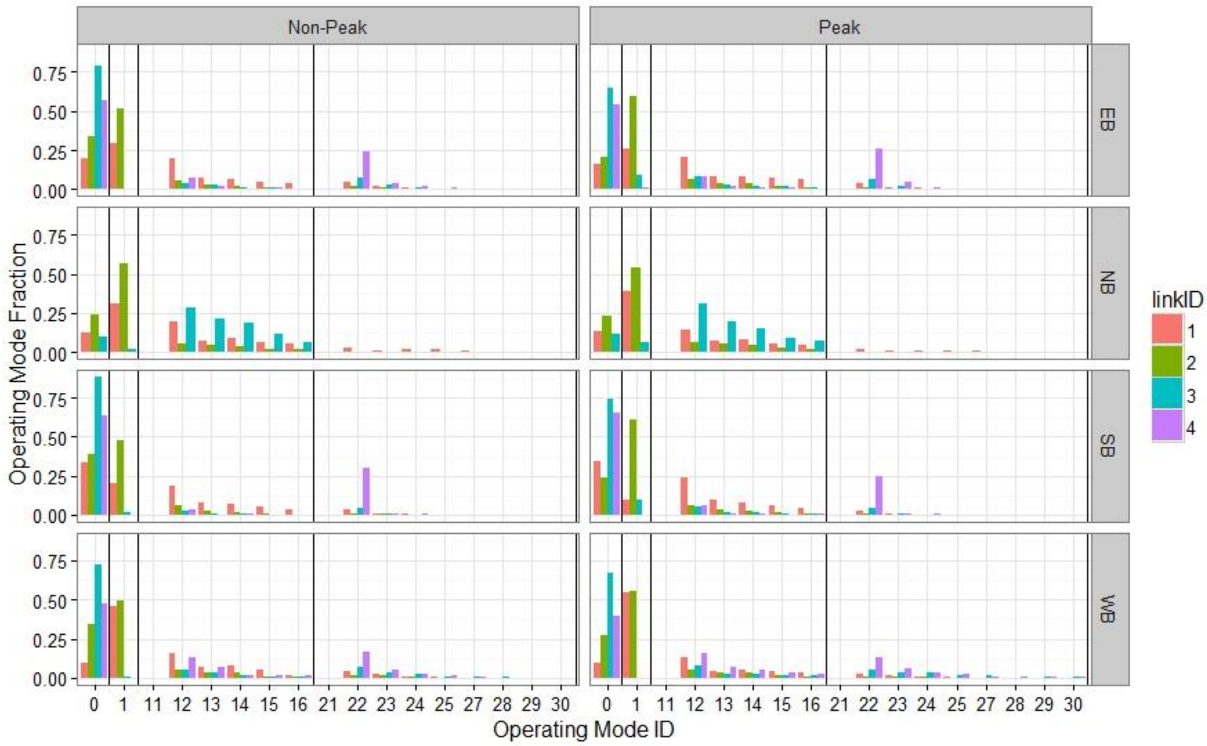

Figure 4.11 Operating Mode Distribution during Peak and Non-Peak Hour by Link

These figures have proven that operating mode distribution patterns did change over short periods at the study intersection approach and differ by approaches and distance to intersections. This difference results from the change of traffic flow state, and showed to be well captured by the radar detector. The above finding further validates the necessity of real-time emission monitoring at intersections, as the change in operating mode distribution will accordingly result in a change in emission rate. To verify the results, Chi-squared test was used to test homogeneity between different operating mode distributions. The test statistic and the expected frequency count can be computed using the following equations:

$$\chi^2 = \sum \frac{(O_{r,c} - E_{r,c})^2}{E_{r,c}} \tag{4.4}$$

$$E_{r,c} = \frac{n_r * n_c}{n} \tag{4.5}$$

Where,

$O_{r,c}$ = the observed frequency count in population r for level c of the categorical variable;

$E_{r,c}$ = the expected frequency count in population r for level c of the categorical variable.

n_r = total number of observations from population r;

n_c = total number of observations at level c; and

n = total sample size.

Specifically, selected periods from peak hour and non-peak hour in Figure 4.9 and 4.11 were compared to each other. Finally, the peak hour and non-peak hour data were compared. Comparisons were not conducted separately for each link due to the limited sample size within each link, since chi-squared test generally requires at least five counts for each mode type. The chi-squared test results are shown in Table 4.1, showing most pairs of distributions are significant different even at 0.001 significance level. This result further indicates that different links at different time periods will yield significantly different operating mode distribution patterns.

Table 4.1 Chi-square Test for Homogeneity Result

Comparison Type	Trajectory Data Sample Size		df	χ^2	p-Value
Peak 1 VS. Peak 2	680	915	7	54.6	<0.001
Peak 1 VS. Peak 3	680	893	7	17.8	0.013
Peak 2 VS. Peak 3	915	893	7	45.9	<0.001
Non-Peak 1 VS. Non-Peak 2	3008	3207	11	180	<0.001
Non-Peak 1 VS. Non-Peak 2	3008	4393	11	55.8	<0.001
Non-Peak 2 VS. Non-Peak 3	3207	4393	11	336	<0.001
Peak Hour VS. Non- Hour			14	897	<0.001

4.3.4 Total Emissions and Emission Rates

With the computed intermediate variables such as volume, speed, and operating mode distribution, total emissions and emission rates are computed using the proposed methodology. The advantage of this method is to extract emission factors for the case study intersection so that there is no need to run MOVES for each analysis. MOVES emission factors are generated by assuming one single vehicle on each link and only operating on a single operating mode for one hour. The resulting total emission can then be used as emission factors with the unit of g/hr for each operating mode. Figure 4.12 graphically illustrates the emission factors for a passenger vehicle and truck for common pollutants including CO, CO_2, NO_x and $PM_{2.5}$ for the case study intersection only. Equation 3.7 can then be applied to compute the total emission for a link during a certain period of time. To validate the proposed method, a few test cases have been performed to compare the emission results from using the proposed method and fully running MOVES for each analysis. The comparison results showed that the proposed method yielded the exact same result with fully running MOVES. This indicates the proposed method is valid and can automatically and continuously compute emissions without the need of manually running MOVES each time.

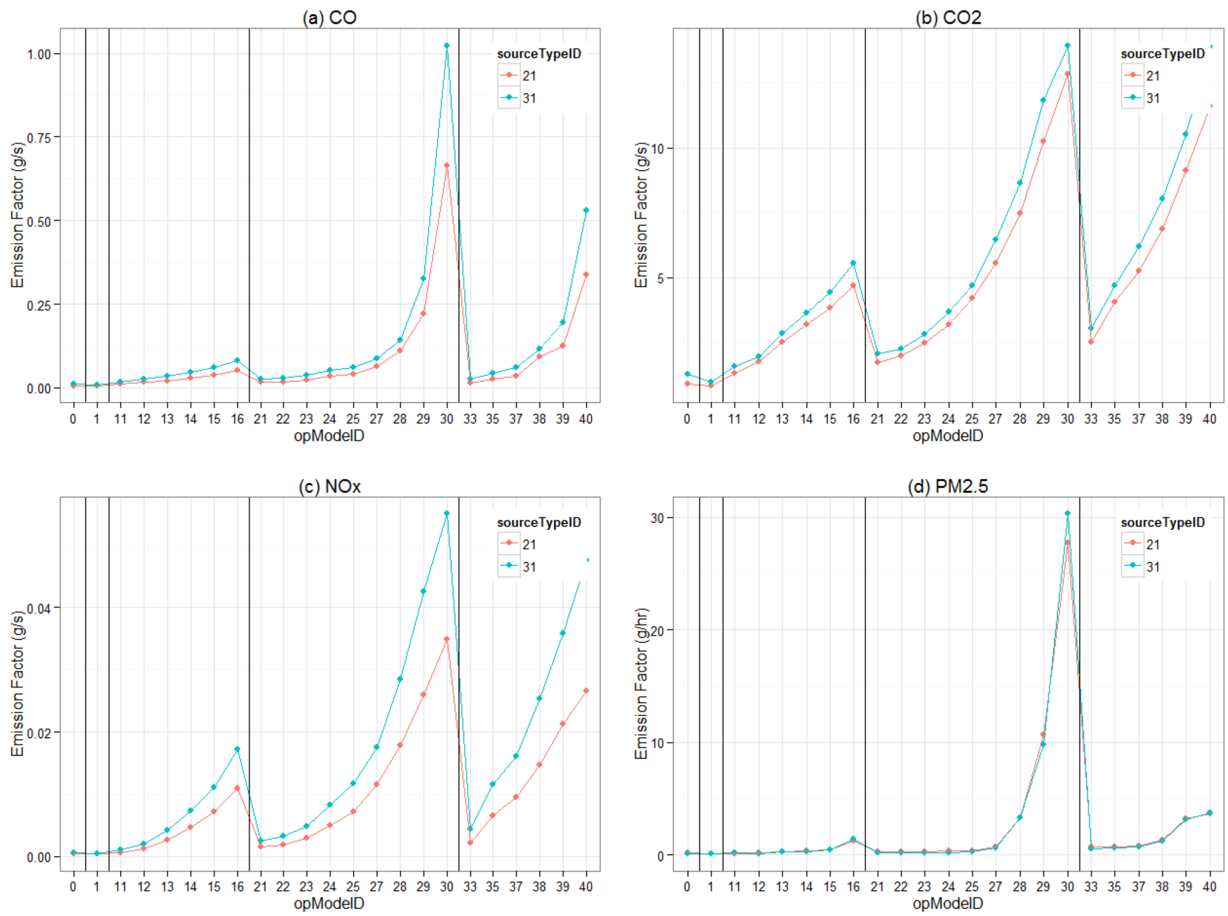

Figure 4.12 Emission Factors by Operating Mode for Major Pollutants

Total emissions and emission rate per vehicle for various pollutants were then computed for each link using the Emission Computation Tool for Radar Data. Figure 4.13 show how CO emission rates during a typical peak and non-peak hour for each link of each approach, respectively. According to the figure, the emission rates for different links have different magnitudes, which is an expected result due to the difference in operating mode distributions. The reason behind the phenomenon is that emission rate should vary by the distance from the intersection. This is due to the more complex driving behavior (e.g., idling, acceleration, and deceleration) at a closer distance from the signalized intersection. To be more specific, link 3 has the lowest emission rate, since a majority of operating modes is composed of braking which usually causes a low CO emission rate. On the other hand, Link 1 shows a higher CO emission rate than the remaining links. As Link 1 represents part of the within-intersection portion of the case study site, vehicles traveling on Link 1 are typically high-acceleration-rate traffic from stopping condition or relatively high-speed traffic which passes the intersection during the green signal. There are usually no low-emission breaking conditions associated with Link 1. As higher speed and higher acceleration rate lead to higher VSP, Link 1 is mainly composed of vehicles with higher VSP that results in a higher emission rate. In addition, by comparing emission rates during peak and non-peak hours shows that peak hours have slightly larger emission rate due to lower average speed.

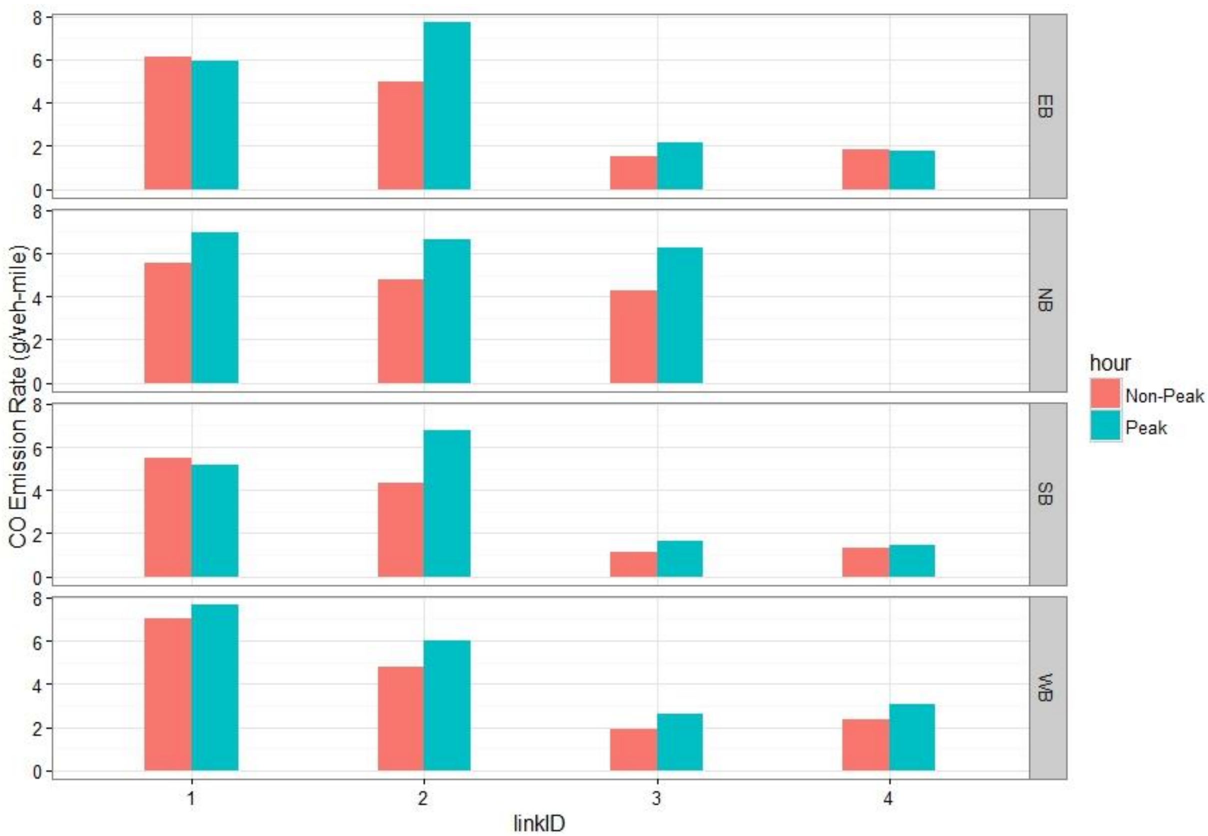

Figure 4.13 CO Emission Rate during a Typical Peak and Non-Peak Hour by Link

On the other hand, Figure 4.14 shows the distribution of various pollutant emission rates at a more aggregated level. Each data point in the figure represents the emission rate during a 15-min interval for a specific link. Data for time period from 6 AM to 10 PM are shown. These figures can be combined with a threshold line to apply the concept of the Emission Visualization and Decision Support Module, which is responsible for displaying the emission rate in real time and provide warnings when the emission rate exceeds a certain threshold.

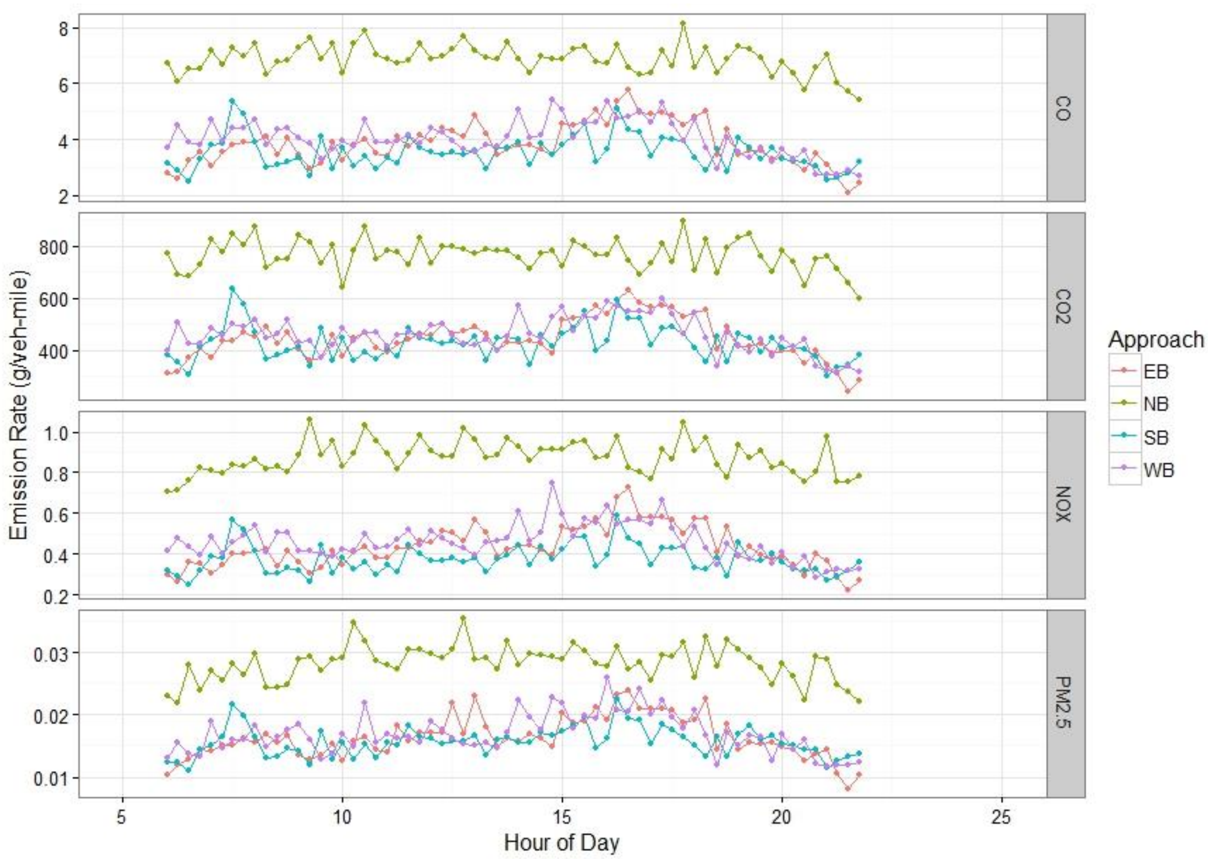

Figure 4.14 Emission Rate of Various Pollutants during a Typical Day

4.3.5 System Validation

Although no ground truth emissions are available to validate total emissions and emission rates computed, the validation process is still needed and can completed through multiple indirect methods. The validation process using different aspects of data is presented in the following paragraphs,

- First of all, the average daily traffic volume computed closely matches with recent AADT data from Wisconsin Department of Transportation. This indicates that there is no significant over counting or under counting of vehicle activities.
- Secondly, the emission computed using the proposed method are identical to fully running MOVES for each analysis. This indicates that the proposed methodology is valid and is able to automatically replicate the MOVES computation process.
- Finally, the emission rates computed are compared with the recent EPA's light duty vehicle emission standards. It stated a 3.4 to 4.2 g/mile for CO emissions, and 0.4 to 0.6 g/mile from a single vehicle standpoint. The computed emission rates closely match with the EPA criteria, although somewhat towards the higher end due larger volume and longer time to cross the intersection.

4.4 Pollutant Dispersion Analysis

4.4.1 Dispersion Modeling Setup

AERMOD input file setup consists of several components including defining sources, characterizing receptors, input meteorological information and select modeling options. Sources are separated identically with the separation of links during the emission computation process. Each intersection approach is defined as a separate emission source, whose length is identical to the coverage area of the radar detectors which is approximately 500 ft. Initial emission release height is assumed to be approximately 1.7 times the average vehicle height to account for the effects of vehicle induced turbulence according to U.S. EPA documents (*12*). The base elevation of the intersection was determined using USGS Geographic Names Information Systems (GNIS) for Appleton, WI (*67*). The specific characteristics of the sources can be found in Table 4.2.

Table 4.2 Source and Receptor Characteristics of the Study Site

Items	Characteristics	Values
Sources	Number of Sources	4
	Source Length	152 m
	Source Width	7 m
	Base Elevation	240 m
	Release Height	2.5 m
Receptors	Sets of Receptors	8
	Receptor Spacing	10 & 25 m
	Receptor Height	1.8 m
	Total No. of Receptors	564

Receptors are virtual monitoring stations where air pollutants concentration data is estimated. Receptors are placed at a height of 1.8 m above the ground to simulate the human breathing height. Eight sets of receptors are defined for this case study intersection. The first four sets of receptors are placed 10-meter from each other on grid scale. These are placed directly adjacent to the intersection approaches. Another four sets of receptors are placed further apart from the intersection, with a 25-meter interval. Figure 4.15 visually displays the receptors setup.

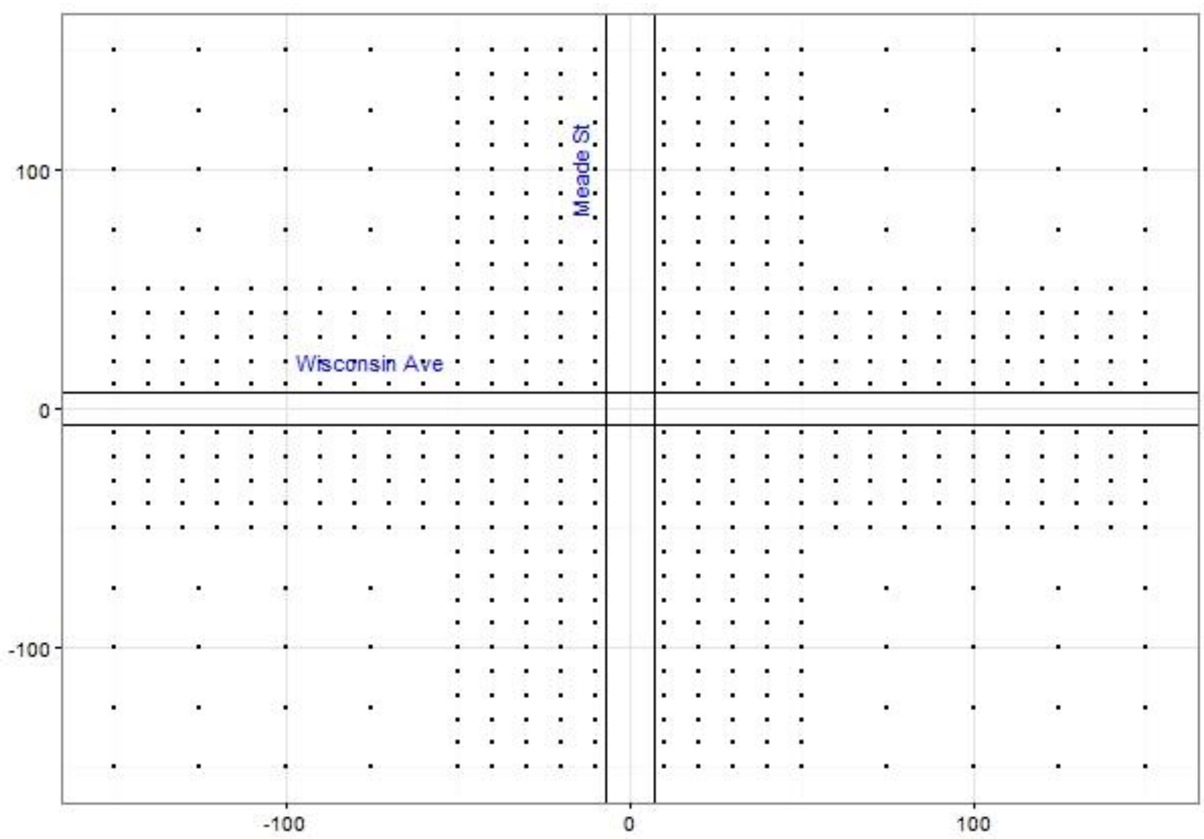

Figure 4.15 AERMOD Receptors Setup

Composite emission factors were computed based on emission rates computed above using the procedure introduced in the previous chapter. Emission factors were computed on an hourly basis for each source as input to dispersion modeling. Figure 4.16 shows the composite emission factors over an entire day for each intersection approach. The pattern for composite emission factors generally follows the trend of approach vehicle volume, which is the highest during morning and afternoon peak hours.

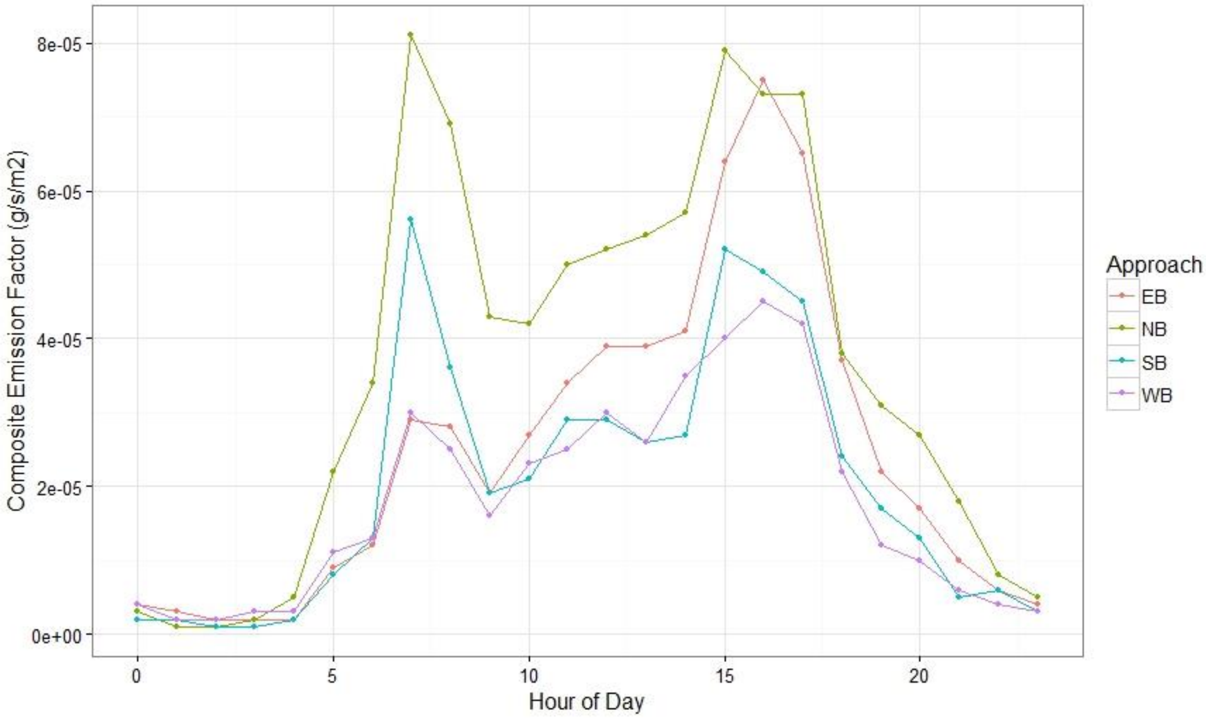

Figure 4.16 Hourly AERMOD Emission Factors

Detailed meteorological information and background concentrations levels could not be obtained through publicly available sources. Background concentration were thus not specified in AERMOD modeling, leading to results that only measures the impact of this intersection vehicle emissions. Meteorological information from a similar location was used, thus the results is not representative of the actual meteorological conditions of the local area.

4.4.2 Pollutant Concentration Results

Highest 1-hour average and 8-hour average CO concentrations are selected as output concentrations for this study intersection since NAAQS standards uses these two average periods' concentrations for CO in their standards. Figure 4.17 shows the plotted 1-hour CO concentrations for receptors defined without considering background concentrations. The concentrations were found to be higher near the sources and gradually decreased as the distance from the sources increased. In addition, these high concentration locations were concentrated toward the northeast quadrant, which matches the directions of the prevailing winds from southwest to northeast for the case study intersections. The receptor with the highest 1-hour concentration is 1,334 $\mu g/m^3$, is far below NAAQS 1-hour CO standards of 35 ppm (43,200 $\mu g/m^3$).

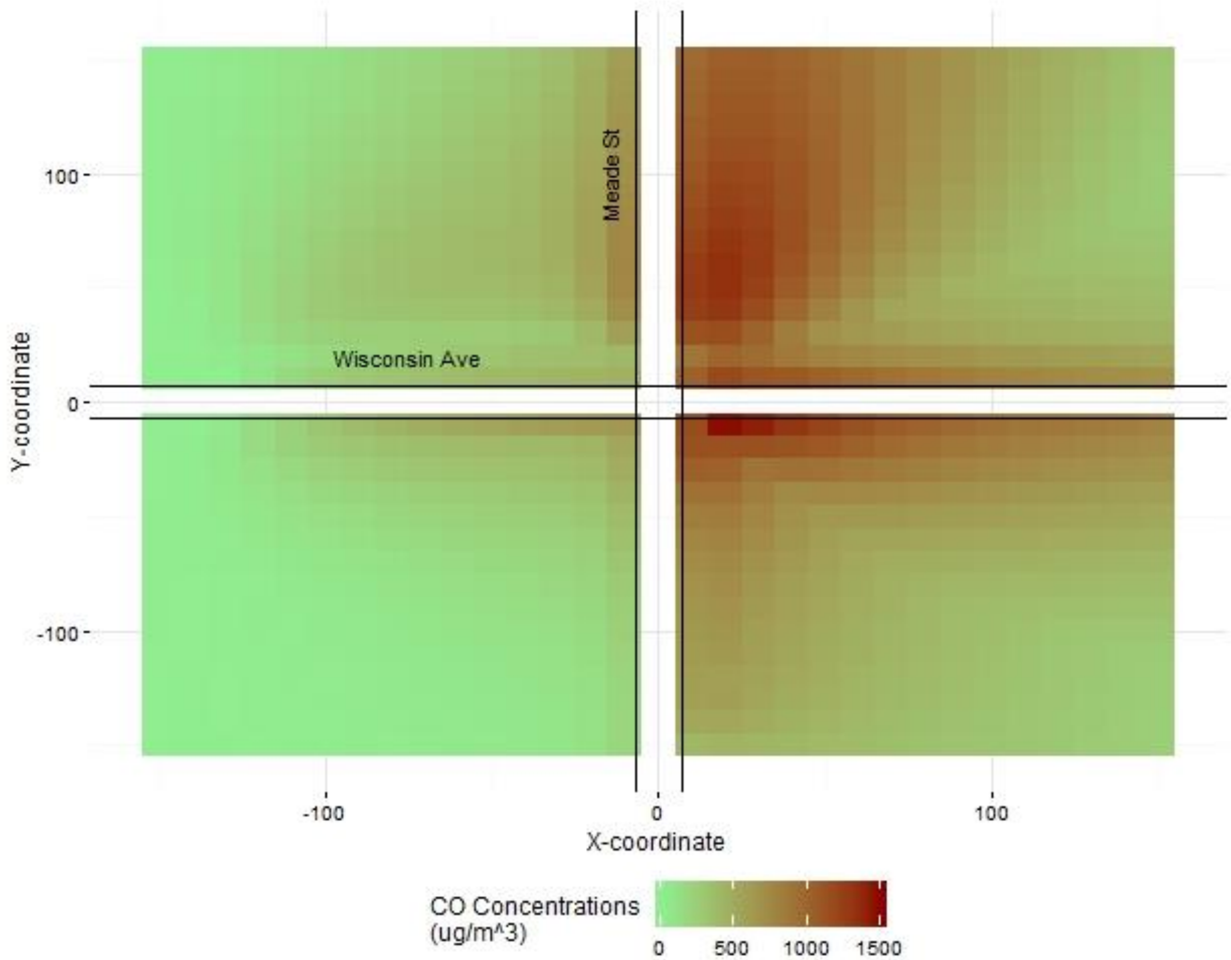

Figure 4.17 Highest 1-hour CO Concentrations Plot without Background Concentrations

The concentration results presented in this section shows that emission computed using radar based vehicle detection data can be further integrated with dispersion models to provide additional functionalities to the entire system.

5 Operating Mode Based Emission Modeling

5.1 Comparison with Probe Vehicle Methods

5.1.1 Qualitative Comparison

Many previous researches used probe vehicle GPS data to analyze transportation emissions. The assumption behind this approach is to use trajectory data of an individual probe vehicle to represent the characteristics of the entire traffic flow. To validate this assumption, a comparison was conducted to compare the difference of traffic characteristics and operating mode distribution between a platoon of vehicles and individual probe-like vehicles. This difference can be both understood qualitatively and analyzed quantitatively. If significant difference exists, the assumption used by the GPS probe data based methods would be invalid.

In order to visualize the difference between operating characteristics of platoon and probe-like vehicles in the platoon, a platoon of four vehicles traveling through the intersection in the same lane during peak hour was selected for analysis. The trajectories of all vehicles within the platoon was plotted and shown in Figure 5.1. The different colors in each trajectory represent the instantaneous speed of each vehicle at different time stamps. Observing the figure, although the four vehicles have somewhat similar trajectories, significant differences can be observed from the different deceleration and accelerations rate for different vehicles.

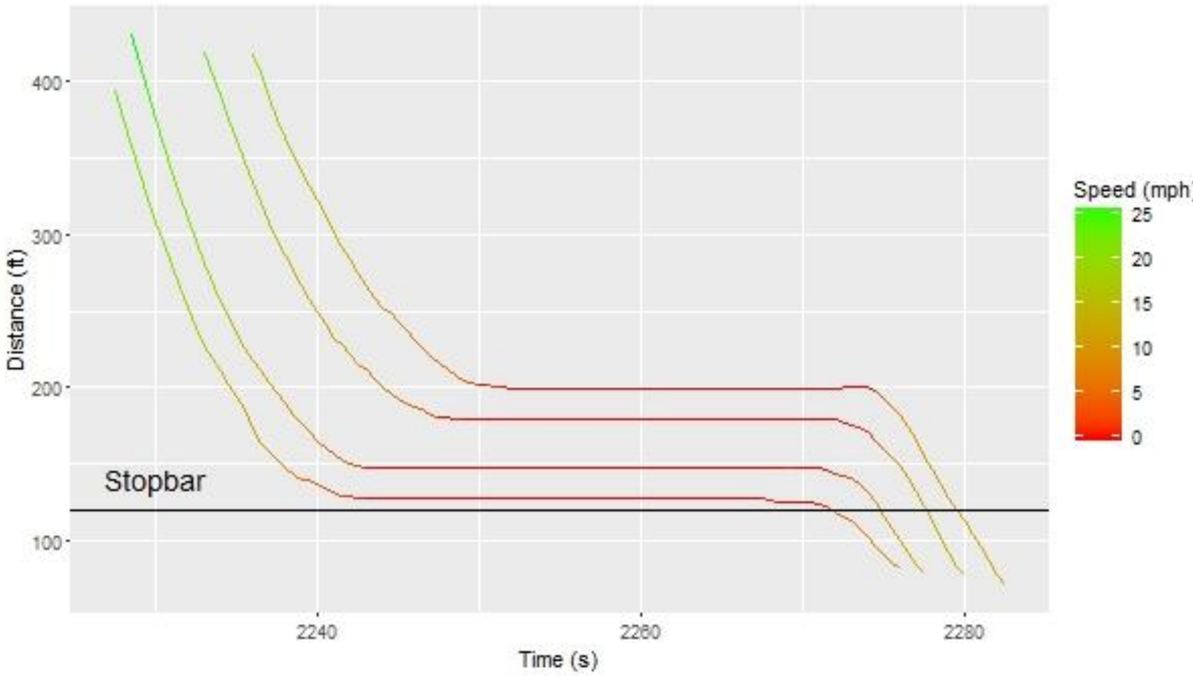

Figure 5.1 Vehicle Platoon Trajectory Plot

To further understand the underlying difference between individual probe-like vehicles and vehicle platoons, an experiment was designed to qualitatively compare the operating mode difference. Specifically, trajectory data of the platoon approaching to the intersection was used to compute the operating mode distribution of the platoon. At the same time, trajectory data of each individual vehicle in the platoon was used to compute the operating mode distribution of individual probe-like vehicle. Comparison results are illustrated by Figures 5.2. The upper subfigures show the speed and acceleration rate distributions of the entire platoon, and each individual vehicle. It can be seen that the speed patterns of the platoon are different from that of individual vehicles. The shapes of the acceleration rate distribution curves are more similar between the entire platoon and individual vehicles. Based on the speed and acceleration rate data, operating mode distributions of entire platoon and the individual vehicles were computed. These operating mode distributions of individual vehicles and the platoon were then compared to each other. The lower subfigure shows the comparison results. It shows that the operating mode distribution of the platoon is substantially different from that of individual vehicles. Furthermore, a one-by-one comparison of operating modes between individual vehicles and the entire platoon shows that approximately 20 to 25 percent of all operating modes within the platoon have been classified differently compared with corresponding individual vehicle data.

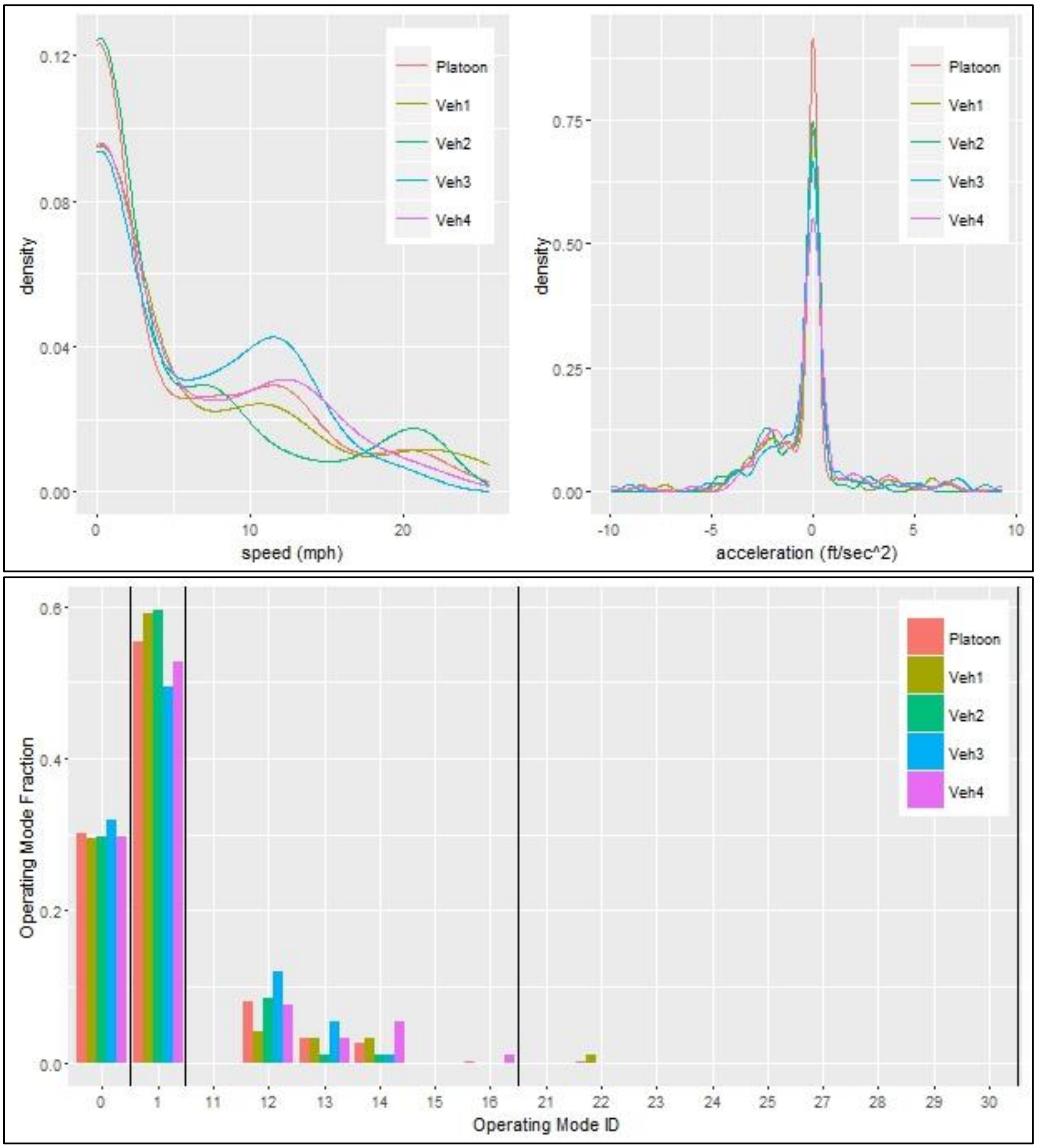

Figure 5.2 Platoon and Individual Vehicles: Speed/Acceleration and Operating Mode Comparisons

Chi-squared tests are further used to validate the aforementioned findings by testing the homogeneity of different operating mode distributions. A pair of operating mode distributions was compared to determine if one distribution is significantly different from the other using the Chi-squared test. Each distribution contains a count of trajectory data point conforming to each of the 23 different operating modes. Table 5.1 summarizes the test results. Statistically significant difference was found between the operating distribution curves of (1) the platoon and this first vehicle of the platoon; (2) the platoon and the second vehicle of the platoon; and (3) the first vehicle and the second vehicle.

Table 5.1 Results of Chi-square Test for Homogeneity

Comparison Type	**Trajectory Data Sample Size**		**df**	χ^2	**p-Value**
Platoon VS. Vehicle 1	651	45	7	38.2	<0.001
Platoon VS. Vehicle 2	651	108	7	54.1	<0.001
Vehicle 1 VS. Vehicle 2	45	108	7	28.6	<0.001

5.1.2 Quantitative Analysis

To further understand the underlying cause that ultimately lead to the difference in emissions estimated using probe vehicle and platoon data, the following equations are used to illustrate the sources of difference. The root cause lays in that the instantaneous speed and acceleration rate values at each time stamp may be different for probe-like vehicle and other vehicles in the platoon. This difference will lead to the different values of VSP computed. The difference in VSP will have a certain probability of being classified as a different operating mode than the probe vehicle. This probability largely depends on the classification criteria of different operating modes. Adding up the total number of operating modes that has been differently classified will result in the difference of emission rate calculated.

$$\varepsilon_v = v_i - v_{probe} \tag{5.1}$$

$$\varepsilon_a = a_i - a_{probe} \tag{5.2}$$

$$\varepsilon_{VSP} = VSP_i - VSP_{probe} = f(\varepsilon_v, \varepsilon_a) \tag{5.3}$$

$$\varepsilon_{OM} = \; P(OM_i \neq OM_{probe}) = f(\varepsilon_{VSP}, \varepsilon_v) = f(f(\varepsilon_v, \varepsilon_a), \varepsilon_v) \tag{5.4}$$

$$\varepsilon_{ER} = |ER_i - ER_{probe}| = f(\sum \varepsilon_{OM}) \tag{5.5}$$

Where,

ε =difference in probe-like vehicle and platoon for a specific variable;

v_i, v_{probe} =speed for vehicle i in a platoon and probe-like vehicle;

a_i, a_{probe} =acceleration rate for vehicle i in a platoon and probe-like vehicle;

VSP_i, VSP_{probe}=VSP of vehicle i in a platoon and probe-like vehicle;

OM_i, OM_{probe} =operating mode for vehicle i in a platoon and probe-like vehicle; and

ER_i, ER_{probe} =emission rate for vehicle i in a platoon and probe-like vehicle;

Finally, an experiment was designed to quantify the difference in emission rate estimated between using probe vehicle and platoon data. Twenty platoon trajectory data were randomly selected and extracted. Within each platoon, a probe-like vehicle was selected that could most closely represent the operating characteristics of the entire platoon. Each probe-like vehicle and its corresponding platoon was considered as a comparison pair. Emission was then computed for all probe-like vehicle trajectory data and platoon trajectory data. To complete the analysis, the following three variables were computed for each comparison pair.

- Absolute difference in emission rate: representing the difference of emission rate using platoon and probe-vehicle, calculated using the Emission Computation Tool for Radar Data, shown in the following equation.

$$\varepsilon_{ER} = |ER_{probe} - ER_{platoon}| \tag{5.6}$$

Where,

$ER_{probe}, ER_{platoon}$ = Emission Rate computed using probe vehicles and platoon.

- Mean absolute error of VSP: representing the mean absolute difference in VSP between probe-like vehicle and platoon, shown in the following equation.

$$MAE_{VSP} = \frac{1}{N}\sum_{i=0}^{N} |VSP_i - VSP_{probe}| \tag{5.7}$$

Where,

MAE_{VSP} =mean absolute error of VSP;

VSP_i, VSP_{probe} =VSP of vehicle i in a platoon and probe vehicle; and

N =number of vehicles in a platoon.

- Percentage difference in operating mode: computed as the proportion of operating mode in a platoon that has been classified differently than its corresponding probe-like vehicle, shown in Equation 5.8.

$$\varepsilon_{OM} = \frac{N(OM_{probe} \neq OM_{platoon})}{N_{total}} * 100\% \tag{5.8}$$

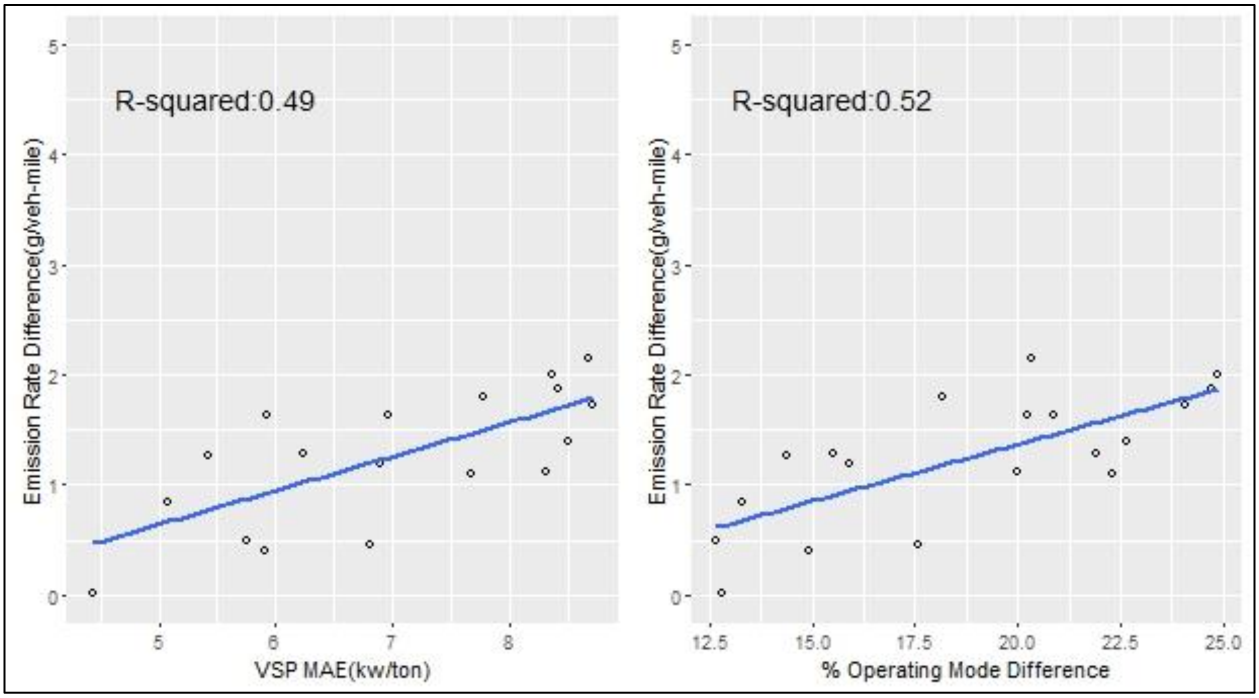

Figure 5.3 Relationship between CO emission rate, VSP and operating mode differences

Scatterplots between the difference in CO emission rate and MAE of VSP and Percentage difference in operating modes were plotted and linear model were built based on the data and are illustrated in Figure 5.3. The figure showed that the difference of emission increases with both a larger mean VSP difference and percentage operating mode difference, although the r-squared value is not as strong.

In summary, all these results validate that individual probe-like vehicles cannot represent a platoon of vehicles, in terms of both traffic flow characteristics and operating mode distribution. Emission rates estimated using the two approaches are different by approximately 15 to 25 percent. Therefore, emission estimated using the GPS probe data based method cannot be accurate enough to describe the entire traffic flow at the intersection. However, this limitation can be overcome by the proposed method based on radar based vehicle detection data.

5.2 Sensitivity Analysis

5.2.1 Roadway Grade

This section conducts sensitivity analysis of two important variables that directly or indirectly affect vehicle emissions. Roadway grade is a variable used in computing Vehicle Specific Power (VSP). VSP represent the instantaneous tractive power per unit vehicle mass. The higher the upgrade, the larger amount of tractive power is needed to maintain vehicle speed. VSP then affects operating mode distribution, eventually impacting the total emissions and emission rates. Specifically, grade only affects the percentage of cruising and acceleration operating modes, but has no influence on the percentage of braking and idling modes.

In this analysis, grade is set to nine different values, ranging from -5 percent downgrade to 5 percent upgrade, in 1 percent interval. Firstly, the impact of grade on computed VSP values was tested at different speed levels. In this analysis, it was assumed that vehicles maintain a cruising state (i.e. zero acceleration). Figure 5.4 shows that the relationship between VSP and grade with respect to different speed levels. VSP will generally increase along with speed keeping grade constant. In general, a positive grade will lead to a larger VSP by keeping the same speed, vice versa. Furthermore, the level of grade impact grows as speed increases.

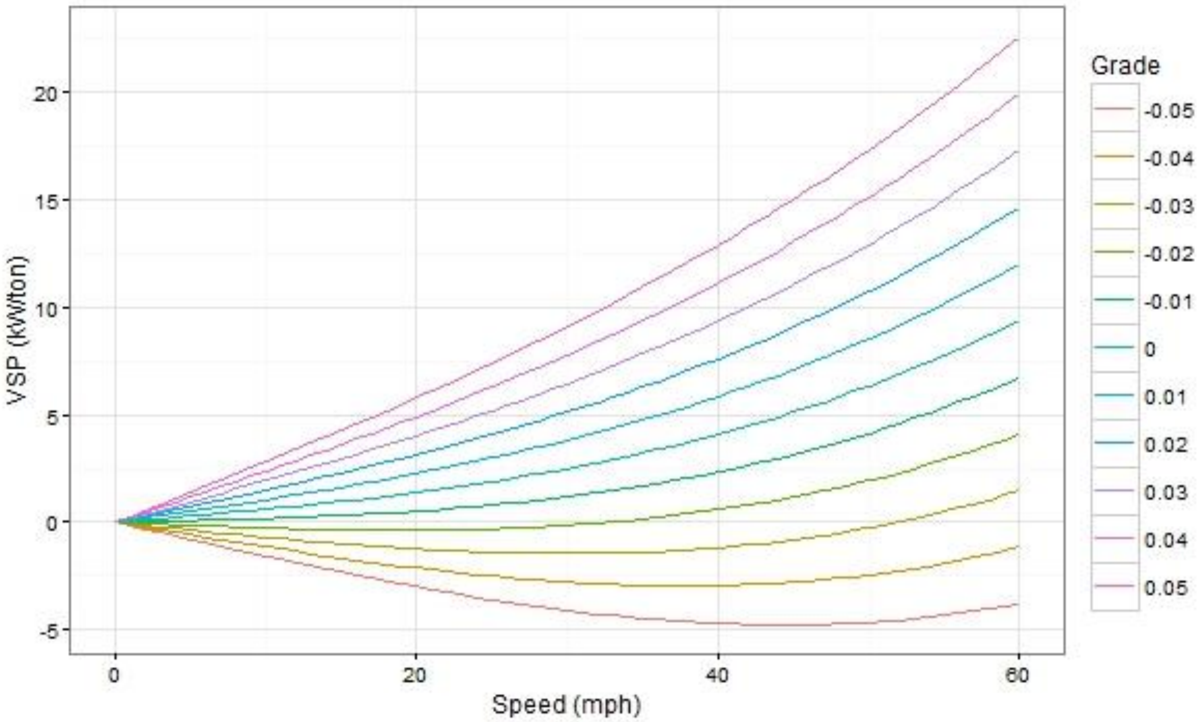

Figure 5.4 VSP vs. Roadway Grade

To help further understand the impact of grade, emission factor vs. grade at different speed levels is plotted. Again, acceleration is assumed to be zero. Grade directly affects VSP, VSP affects operating mode classification, which in turn affect emission factor. However, this change in operating mode classification is a stepwise change, thus the relationship is a piecewise constant function, as can be seen from Figure 5.5.

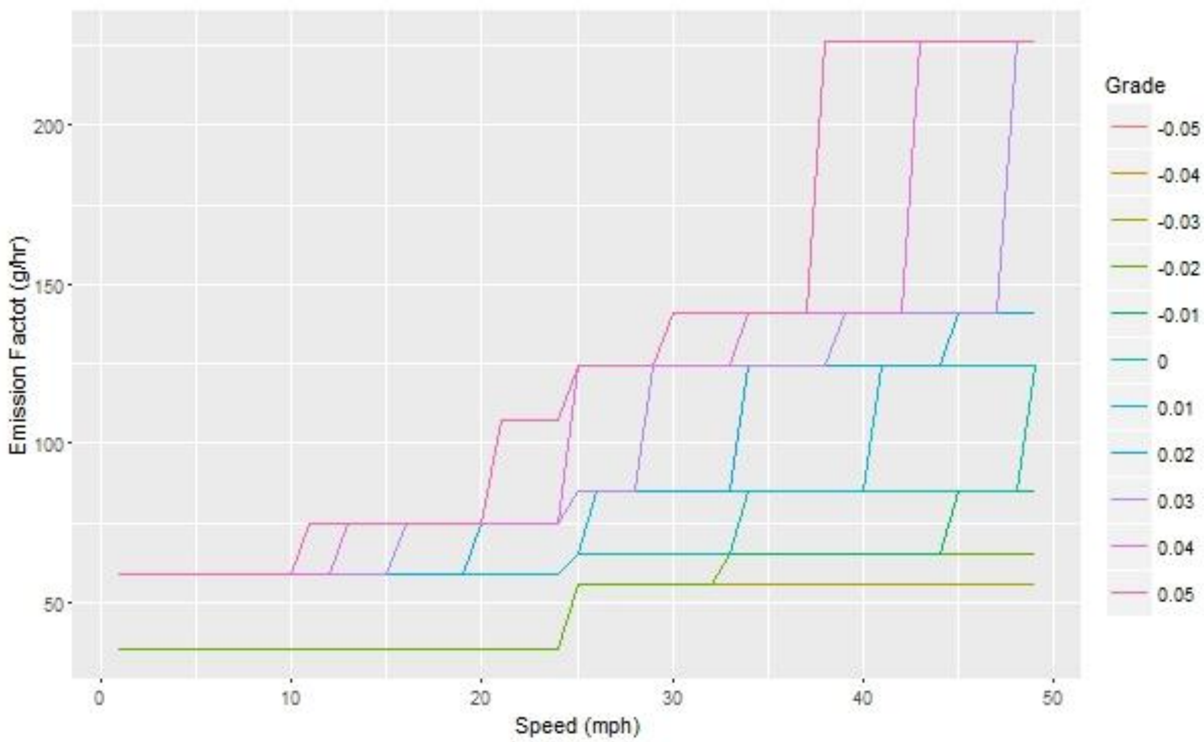

Figure 5.5 Emission Factor vs. Grade

5.2.2 Heavy Vehicle Percentage

As stated in the literature review chapter, vehicle type significantly affects the amount of emissions. In this research, vehicle type is classified only into two types: passenger cars and heavy vehicles since the radar based vehicle data cannot distinguish between specific vehicle types as defined in MOVES. The percentage of heavy vehicle in this sensitivity analysis is set from 0 percent to 16 percent, in 2 percent intervals. Three typical operating mode distributions were selected, including a high braking/idling scenario, a high cruising/acceleration scenario and a balanced scenario. Figure 5.6 displays the emission result with the percentage of heavy vehicles in the three scenarios. Emission rate index was used as the dependent factor, with 100 representing the baseline condition with zero heavy vehicles. Results showed that the high braking/idling condition, which is usually reflected by high traffic volume condition, would have a faster rate of increase in emission rates with respect to percent of heavy vehicles. This indicates that heavy vehicles will have a higher impact on emissions during congested periods.

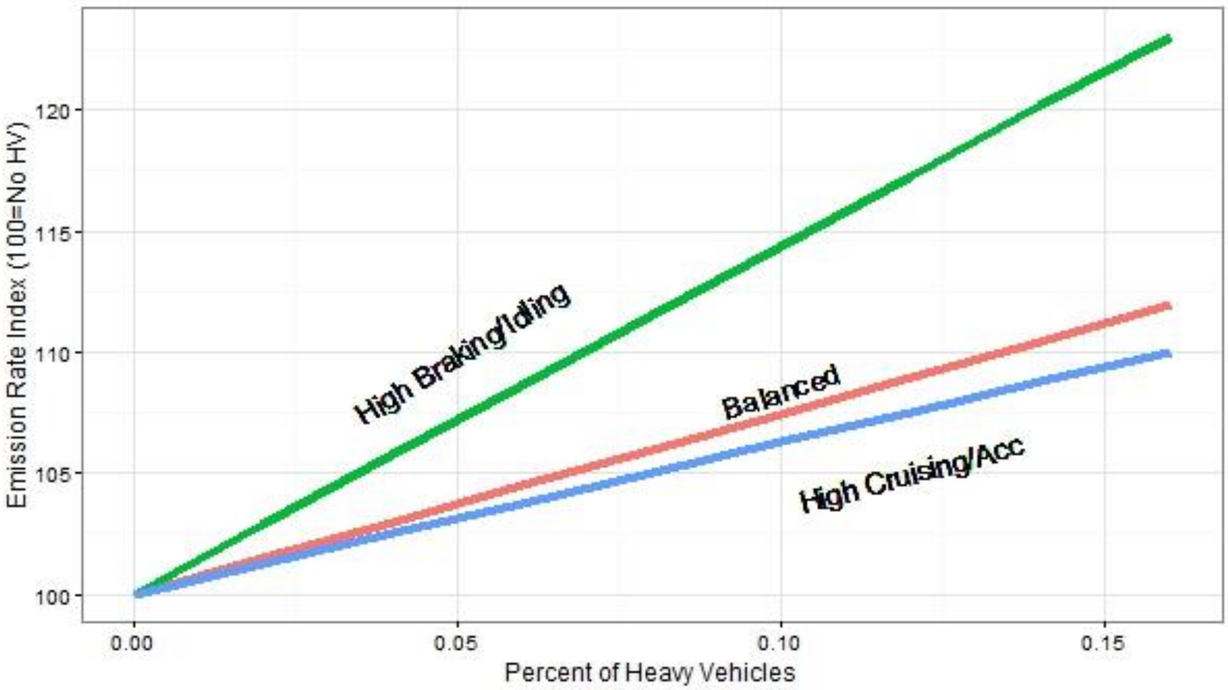

Figure 5.6 Emission Rate vs. Percent of Heavy Vehicles

5.3 Delay and Emissions

5.3.1 Direct Delay Computation Using Radar Data

Delay is an important performance measure in traffic operations analysis. Delay also directly determines the level of service (LOS) of roadway segments or intersections. In this analysis, the relationship between emission rate and delay at signalized intersections is investigated using radar based vehicle detection data collected at the study intersection.

In the traditional approach, the computation of delay at signalized intersections needs to follow the Highway Capacity Manual (HCM) procedures. However, with the radar based vehicle detection data, it is possible to directly compute intersection using the vehicle trajectory data collected without going through the analytical process. The computation procedure for intersection delay using radar based vehicle detection data is summarized below. The procedure accounts for the fact that the first detection of a vehicle may occur at slightly different locations (i.e. y-coordinates).

- Step 1: For each vehicle id, compute actual travel time,

$$\mathrm{TT}_{\mathrm{act,i}} = \max(\mathrm{t_i}) - \min(\mathrm{t_i}) \tag{5.9}$$

Where,

$\mathrm{TT}_{\mathrm{act,i}}$ = actual travel time for vehicle id i, in sec; and

$\mathrm{t_i}$ = vector of time stamps for vehicle id i;

- Step 2: For each vehicle id, compute ideal travel time,

$$\mathrm{TT}_{\mathrm{ideal,i}} = \frac{\max(y_i) - \min(y_i)}{v_{lim} * 1.467} \tag{5.10}$$

Where,

$\mathrm{TT}_{\mathrm{ideal,i}}$ = ideal travel time for vehicle id i, in sec;

$\mathrm{y_i}$ = vector of y-coordinates for vehicle id i, in ft; and

v_{lim} = speed limit of intersection approach, in mph.

- Step 3: Compute the individual delay for each vehicle id and loop through all vehicle ids. If actual travel time is less than ideal travel time, individual delay is considered zero.

$$d_{Tot} = \sum_{i=0}^{N} \begin{cases} TT_{act,i} - TT_{ideal,i} & \text{if } \mathrm{TT}_{\mathrm{act,i}} \geq \mathrm{TT}_{\mathrm{ideal,i}} \\ 0 & \text{if } \mathrm{TT}_{\mathrm{act,i}} < \mathrm{TT}_{\mathrm{ideal,i}} \end{cases} \tag{5.11}$$

- Step 4: Divide total delay by traffic volume yields average delay per vehicle for this approach and time period.

$$d_{Avg} = \frac{d_{Tot}}{V} \tag{5.12}$$

Where,

d_{Avg} =average delay per vehicle, in s/veh;

d_{Tot} =total delay during the analysis time period, in s; and

V =traffic volume during analysis the time period.

5.3.2 Total Delay and Total Emissions

Through this computation procedure, total delay and average delay per vehicle can be directly obtained without going through the complex analytical procedure. It is to be noted that due to the unavailability of full downstream vehicle operations data, delay computed in this section may be systematically underestimated. In this analysis, a total of 3,950 15-min period data was used to compute delay. These 15-min periods are composed of daytime, nighttime, peak/non-peak hours, weekdays and weekend, thus representing a broad range of traffic conditions. Most average delay per period falls into the 10 to 20 s/veh range, corresponding to LOS B, with a few falling into LOS C. CO emission rate is also computed for these periods.

A scatterplot is created to investigate the relationship between total delay and total CO emissions, shown in Figure 5.7. Total delay is shown in the x-axis, total CO emission on the y-axis, and color of the points represent the corresponding level of service (LOS). As can be seen from the figure, total emissions increase along with an increase total delay. The correlation coefficient of these two factors is 0.91, which further shows the significant impact of congestion delay on transportation emissions.

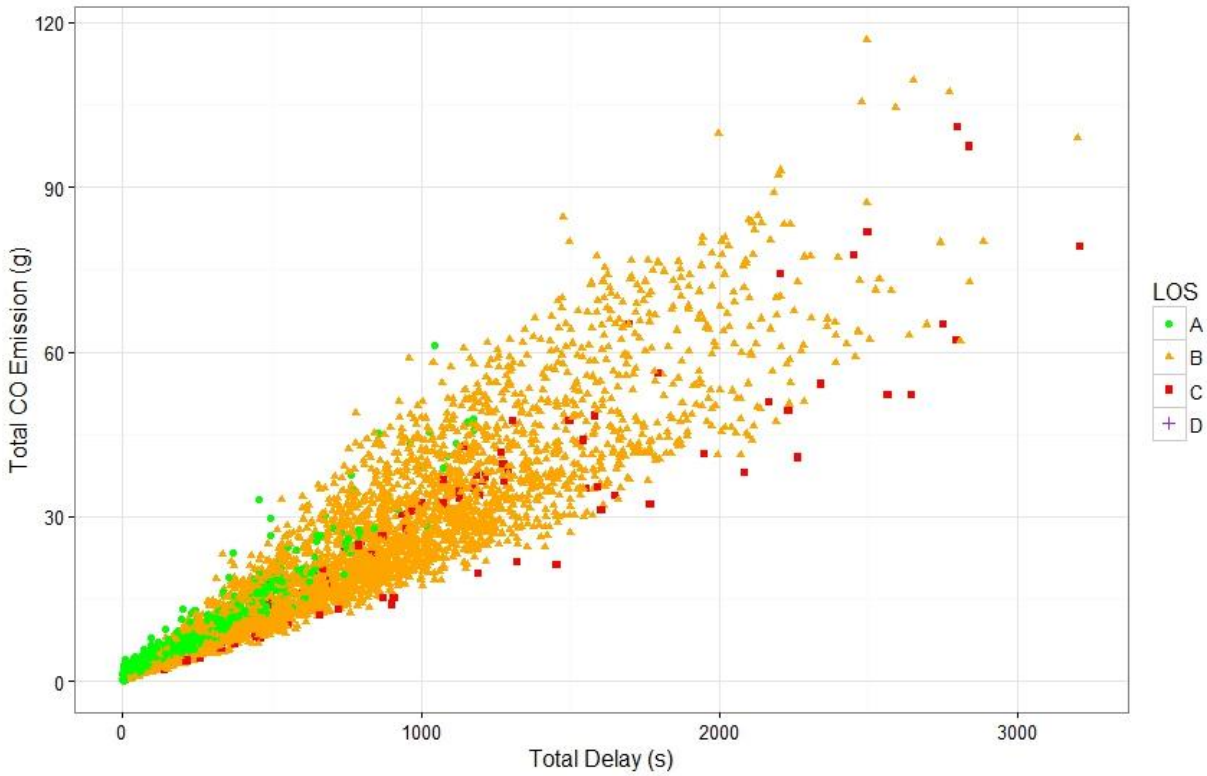

Figure 5.7 Relationship between Total Delay and Total CO Emissions

5.4 Model Development

5.4.1 Model Data Preparation

With the large amount of radar based vehicle detection data collected at the study intersection, and the validated emission monitoring system, it is possible to gain more insight on the nature of transportation emissions at signalized intersections based on empirical observations and modeling.

To start with, the overall assumptions of this macroscopic model are as follows:

1. The speed limits of the approaches do not exceed 35 mph (low speed intersection approaches).
2. Under-saturated conditions (i.e. demand<capacity), with no residual queue.
3. The analysis time interval covers at least five signal cycles, preferably at least 15 min.
4. Vehicle arrivals are uniform.

Empirical data from radar based vehicle detectors shows that all approaching vehicle trajectories can be classified into two categories according to changes in speed and number of stops. The first type is approaching vehicle travels through the intersection without stopping, though it may or may not involve certain level of decelerations. The second type is approaching vehicles stopping once while traveling through the intersection. In theory, though, there is a third type, which is vehicles have to stop two or more time. However, this scenario is extremely rare for this case study intersection. In terms of emissions, the third type will generate the most emissions as a result of the multiple acceleration and deceleration cycles and longer vehicle operating hours.

The basic approach behind this predictive modeling is still based on operating mode distribution and total vehicle operating time to compute the total emissions for an approach during a certain period of time. To be more specific, there is a need to develop a predictive model to identify the total vehicle time spent in each mode category, which is braking (operating mode 0), idling (operating mode 1), low speed cruising/acceleration (operating modes 11 through 16), medium speed cruising/acceleration (operating modes 21 through 30) and high speed cruising/acceleration (operating modes 33 through 40).

In the modeling process, the 80/20 method is used, which is commonly used in machine learning and statistical modeling procedures. This means that 80 percent of available data will be used as training data and 20 percent of available data will be used as testing data. Also, it is noted that all northbound approach data is excluded from the modeling since it has a non-typical special roadway geometry (immediate non-signalized intersection) that is not able to represent the typical characteristics of an intersection approach.

The modeling data is prepared as follows. To ensure an as large as possible sample size, the minimum desirable analysis period is used, which is 15-minute interval as stated in the model assumptions. Also, data from 12 AM to 5 AM is excluded due to the extremely low traffic volume, which will also likely to be considered as outliers. For each 15-min analysis period, the list of parameters computed is listed in Table 5.2. Traffic volume, average speed, operating mode distribution and emission quantities and rates are obtained directly from Emission Computation Tool for Radar Data. The remaining variables are calculated based on the above variables. For example, total vehicle time is computed as follows:

$$\mathrm{T_{tot}} = V * \frac{L}{v} * 3600 \tag{5.13}$$

Where,

$\mathrm{T_{tot}}$	=Total vehicle operating time, in sec;
V	=Traffic volume, in veh/time;
L	=Segment length, in miles; and
v	=Segment average speed, in mph.

Total time idling, deceleration, and cruising/acceleration are then computed by splitting the total vehicle time based on operating mode percentages. The total 15-min sample size is more than 4,000. They are randomly split between 80 percent modeling and 20 percent validation data. Besides, in actual modeling procedure, all traffic volume is expressed through traffic flow rate, which bear the unit of vehicle per hour per lane (vphpl). All total times are expressed through seconds per lane per hour to ensure consistency of units.

Table 5.2 List of Variables in the Modeling Data

Variable Name	Notes
Day	Day of Month
Time Period	15-min period
Approach	Excluding NB
Total CO Emissions	In grams
Emission Rate	In g/veh-mile
Flow Rate	In vphpl
Average Speed	In mph
Percentage of Heavy Vehicles	In decimals
Grade	In decimals
Total Vehicle Time	In sec
Total Idling Time	In sec
Total Deceleration Time	In sec
Total Low Speed Cruising/Acc Time	In sec
Total Medium Speed Cruising/Acc Time	In sec
Total High Speed Cruising/Acc Time	In sec

5.4.2 Total Time Decelerating Sub-Model

The first relationship to investigate is between traffic flow rate and total vehicle time spent in deceleration. A scatterplot plot is generated to have traffic flow rate on the x-axis, total time decelerating per lane per hour on the y-axis. The flow rate and total vehicle time are extrapolated based on a 15-min interval basis according to the model preparation procedure. The scatterplot is shown in Figure 5.8. It can be generally observed that these two variables show a strong linear relationship. Correlation analysis of these two variables shows that the correlation coefficient is 0.957, which confirms their strong linear relationship.

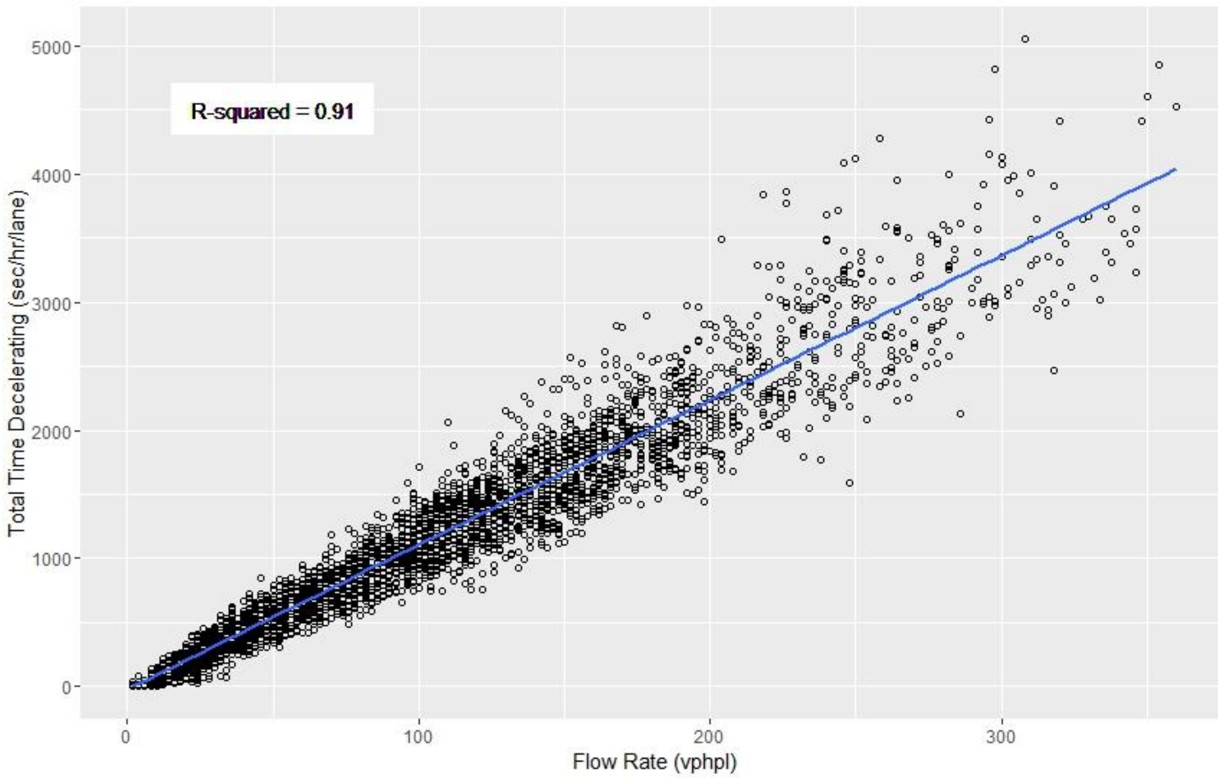

Figure 5.8 Total Time Decelerating vs. Approach Flow Rate

A least square linear is then fit for these two variables. The intercept is fixed to zero to reflect actual conditions. The R-squared value of this model is this linear model is 0.91, which indicates a strong explanatory power of this model. The fitted model line is then added to the scatterplot, as shown in the blue line in Figure 5.8. By multiplying the number of lanes and analysis period, total time decelerating for the analysis period can be computed. This sub-model is shown in the following equation:

$$T_{dec} = 11.15 * V * N_{lane} * T \tag{5.14}$$

Where,

T_{id} =Total vehicle time decelerating per analysis period, in sec;

V =Traffic Flow Rate, in vphpl;

N_{lane} =Number of through lanes for the intersection approach; and

T =Analysis time period, in hours.

5.4.3 Total Time Idling Sub-Model

There are two options considered for modeling total time idling at intersection approach. One method is to completely use empirical data, by relating traffic volume directly with total time idling. However, this method did not consider some very important variables, since total time idling is highly dependent on traffic signal cycle and effective green and red time. Therefore, the second method is used, which is to apply existing traffic flow dynamics and kinematic wave theory.

In this modeling process, it is assumed that the approach is a homogenous road section displaying a triangular fundamental diagram. This method follows the analytical model of kinematic wave theory for signalized intersections. The triangular fundamental diagram is shown in Figure 5.9. It includes free flow speed, saturation flow and jam density as key factors. Again, it is assumed the arrival flow is less than saturation flow, which indicates unsaturated conditions.

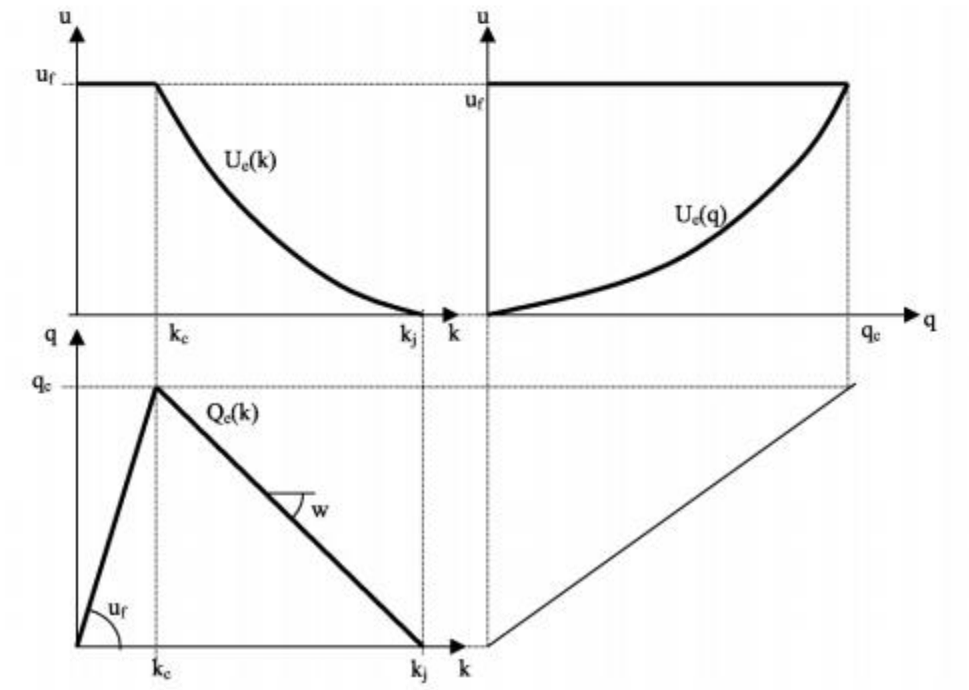

Figure 5.9 Triangular Fundamental Diagram

For intersection applications, traffic signal cycle data significantly affects the operations of vehicle traffic. The key traffic signal parameters include cycle length, effective red time and effective green time. Additionally, there may be a residual queue of vehicles that were not served in the previous cycle. A time-space diagram of the traffic states of the intersection approach both upstream and downstream is shown in Figures 5.10.

The assumptions of the kinematic wave theory are that vehicles will instantly transition from free flow speed to idling, which means that vehicles accelerate and decelerate infinitely fast, as can be seen from the figure. However, in reality, the vehicles at an intersection need to decelerate from cruising speed to a stop and to accelerate from a stop up to the free flow speed. If the vehicle speed changes at a constant rate for the duration of acceleration, then the curvature of the more realistic trajectory is parabolic as shown in Figure 5.10. It can be assumed that half of the vehicle hours traveled while accelerating are taken away from the idling state and the other half are taken away from the cruising state. Therefore, the idling time per vehicle would be reduced from the average deceleration time and acceleration time.

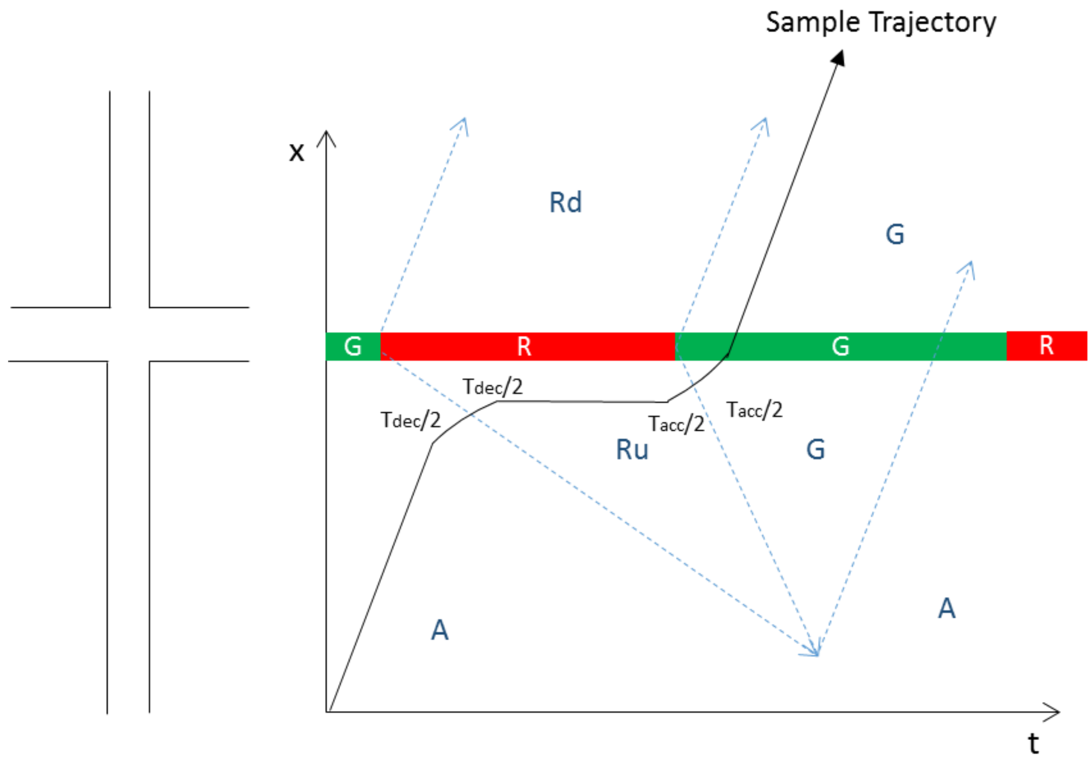

Figure 5.10 Kinematic Waves for Signalized Intersections with Sample Trajectory

Based on the length of the queue, including the vehicles in the residual queue, it is possible to estimate the number of vehicles that stop during the cycle, which follows from the geometry of the triangular queued state:

$$N_{s,cycle} = N_r + \frac{RsV}{s-V} \tag{5.15}$$

Where,

$N_{s,cycle}$ =Number of vehicles that stop per signal cycle;

$N_{r,cycle}$ =Residual queue per signal cycle;

R =Average effective red time per signal cycle, in sec;

s =Saturation flow rate, in vph; and

V =Demand flow rate, in vph.

The total vehicle time spent idling can then be calculated by adding the time that vehicles in the residual queue spend idling to the time that vehicles arriving at the back of the queue spend idling. Without accounting for the effects of acceleration and deceleration, the times would be based on effective red time. However, by accounting for acceleration and deceleration time, the longest time spent completely idling would be removing half of deceleration and acceleration time from the effective red time. Thus, the total time spent idling per signal cycle and per analysis period assuming no residual queue can be computed using the following models:

$$T_{id,cycle} = \frac{sV}{2(s-V)}\left(R - \frac{t_{acc}+t_{dec}}{2}\right)^2 * N_{lane} \tag{5.16}$$

$$T_{id} = \frac{T}{C} * T_{id,cycle} \tag{5.17}$$

Where,

$T_{id,cycle}$ =Total time idling per signal cycle, in sec;

T_{id} =Total time idling per analysis period;

T =Analysis period;

C =Cycle length, in sec;

R =Average effective red time per signal cycle, in sec;

t_{acc}, t_{dec} =Average per vehicle acceleration/deceleration time;

s =Saturation flow rate, in vphpl; and

V =Traffic flow rate, in vphpl.

This model to compute total time idling would account for the important impact of traffic signal cycle.

5.4.4 Total Time Low/Medium/High Speed Cruising/Acceleration Sub-Models

Due to the placement locations of radar detectors, they are not able to fully grasp the downstream vehicle operational characteristics of vehicles accelerating to free flow speed. Therefore, empirical modeling method is used to model total vehicle time spent cruising and acceleration. Total time cruising/acceleration for low speed (0-25 mph), medium speed (25-50 mph) and high speed (50 mph+) are separately modeled to purposefully match with operating mode definitions.

To start with, the relationship between total time low speed cruising/acceleration and traffic flow rate is investigated. A scatterplot of the two variables is displayed in Figure 5.11. As can be seen from the figure, the relation between the two variables most likely follows a second order polynomial model (i.e. parabolic curve). Thus, an empirical model is created for the two variables based on this observation. The intercept is fixed to zero to match realistic conditions. The model results are shown as follows, and the fitted curve is plotted in Figure 5.11. Again, there is a need to multiply that result with number of lanes and analysis period.

$$T_{low} = (0.0336 * V^2 + 3.4258 * V) * N_{lane} * T \tag{5.18}$$

Where,

T_{low} =Total time low speed cruising/acceleration during the analysis period, in sec;

V =Traffic flow rate during analysis period, in vphpl;

N_{lane} =Number of through lanes for the intersection approach; and

T =Analysis time period, in hours.

This model has a R-squared value of 0.88, which indicates a high goodness-of-fit.

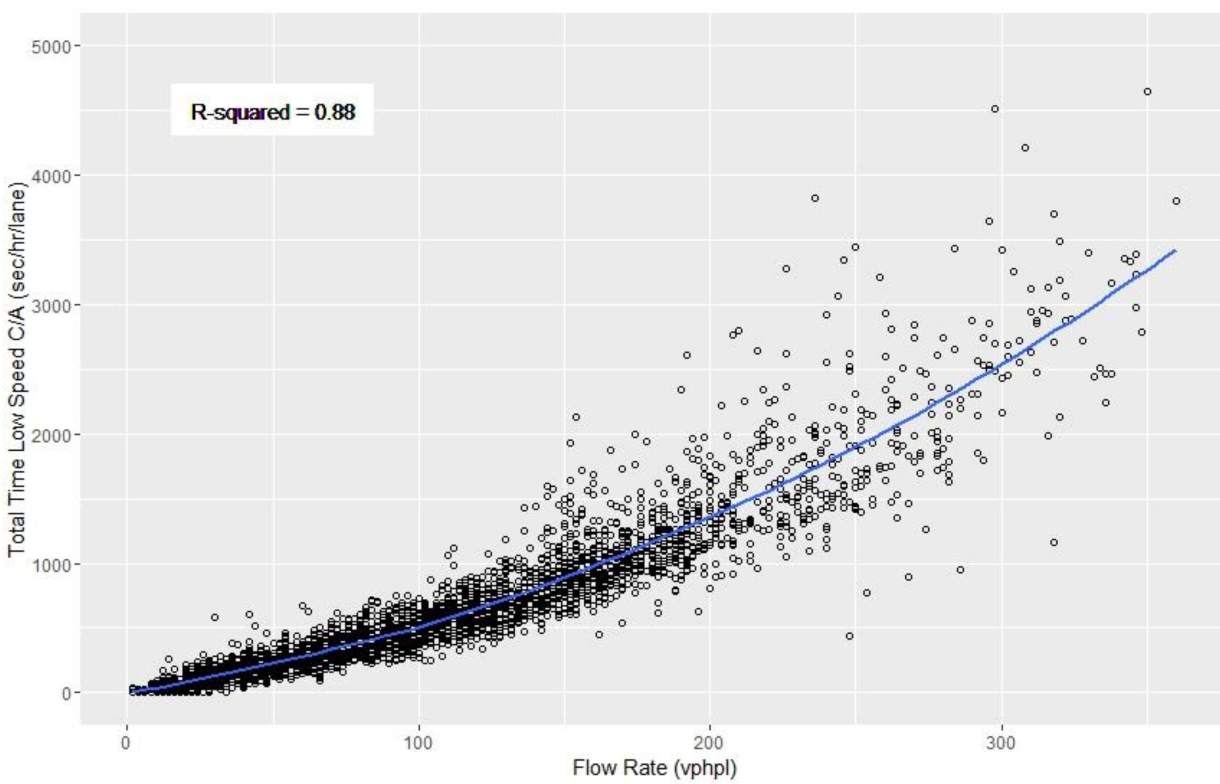

Figure 5.11 Total Time Low Speed C/A vs. Approach Flow Rate

Next, a similar modeling procedure is conducted for medium speed cruising and acceleration. A scatterplot of traffic volume vs. total time medium speed cruising/acceleration is shown in Figure 5.12. Again, observations from scatterplot show that a parabolic model would be the best fit. Again, intercept is fixed to zero to match realistic conditions. The model result is shown as follows:

$$T_{med} = (-0.073 * V^2 + 3.0978 * V) * N_{lane} * T \qquad (5.19)$$

Where,

T_{low} =Total time low medium cruising/acceleration during the analysis period, in sec;

V =Traffic flow rate during analysis period, in vphpl;

N_{lane} =Number of through lanes for the intersection approach; and

T =Analysis time period, in hours.

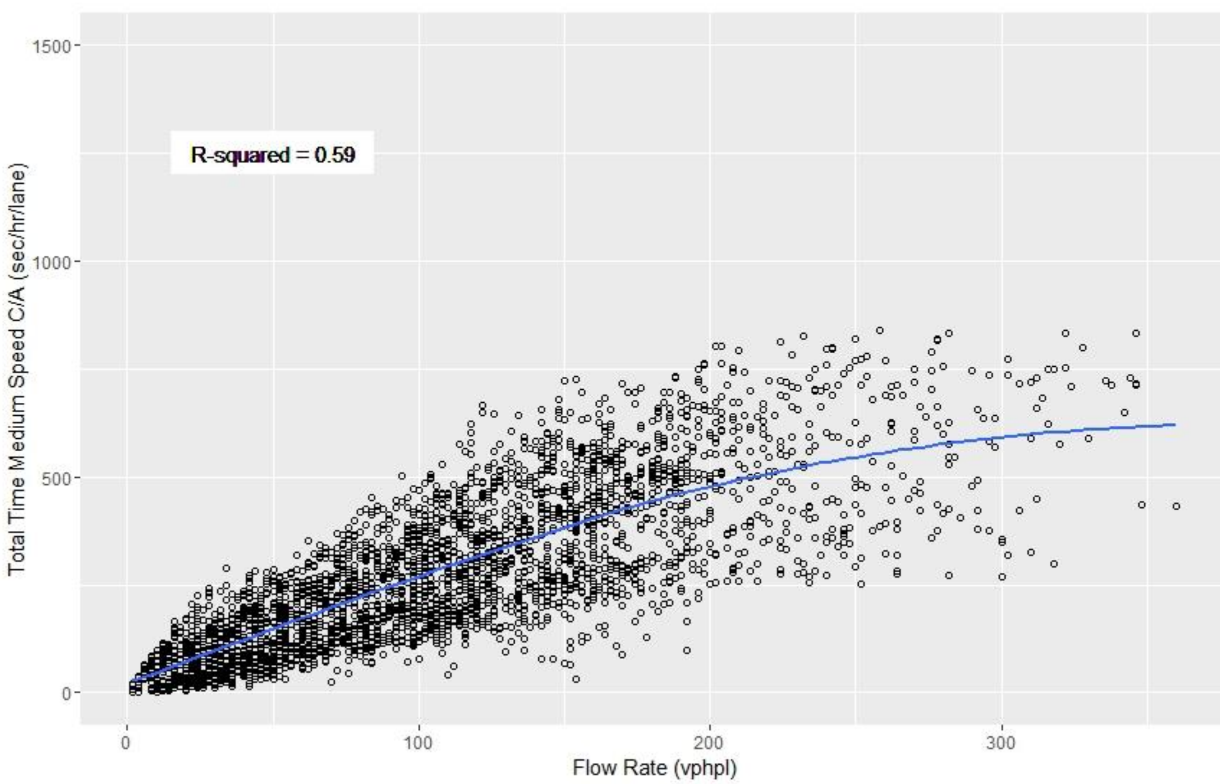

Figure 5.12 Total Time Medium Speed C/A vs. Approach Flow Rate

For low speed intersection approaches, which have speed limits of 35 mph or less, the total time spent in high speed cruising/acceleration modes is assumed to be zero. This can be confirmed from case study data, since the average percentage of operating modes 33 through 40 is less than 0.005%.

5.4.5 Classify Cruising/Acceleration Modes

With the models developed in the previous sections, it is possible to compute the total time spent in each operating mode category. However, in order to gain more insight into the cruising and acceleration modes, further separation into each specific mode is necessary (operating modes 11 through 16, 21 through 30). This necessity is further enhanced by the fact that different operating modes have significantly different emission factors that varies by its VSP ranges.

The operating mode percentages within cruising/acceleration modes are calibrated using empirical data by computing its average distribution. This calibration may be needed for different locations or areas since the magnitude of VSP is highly dependable on driving behavior of local drivers. All percentages assume a zero roadway grade condition.

Table 5.3 shows the operating mode percentages within low speed cruising/acceleration modes based on case study data computation. The mean percentages of modes 11 through 16 should add up 100% to represent the total time in low speed cruising/acceleration conditions. Operating mode 11 has zero percentage since this mode represent conditions where VSP is negative. This situation mostly occurs in downhill conditions. The standard deviation of each operating mode is fairly small compared to its mean value, representing a centered distribution.

Therefore, it is acceptable to use the average percentage for each low speed cruising/acceleration mode.

Table 5.3 Percentage of Mode Distribution within Low Speed Cruising/Acceleration

Speed Range	Operating Mode	Mean	St. Dev.
0-25 mph	11	0%	0
	12	44.2%	0.094
	13	21.3%	0.053
	14	16.1%	0.047
	15	10.1%	0.043
	16	8.2%	0.051
Total Low Speed	11-16	100%	

Table 5.4 shows the operating mode percentages within medium speed cruising/acceleration modes based on case study data computation. Again, the mean percentages of modes 21 through 30 should add up 100% to represent the total time in medium speed cruising/acceleration conditions. Operating mode 21 has zero percentage since this mode represent conditions where VSP is negative. This situation mostly occurs in downhill conditions. The standard deviations values are somewhat larger compared with their mean values, which indicates that the percentage distributions are more dispersed. However, considering the total time spent in medium speed cruising/acceleration on average accounts for less than 6 percent of total vehicle times, the author believes that this method is an acceptable way of distributing among operating modes 21 through 30.

Table 5.4 Percentage of Mode Distribution within Medium Speed Cruising/Acceleration

Speed Range	Operating Mode	Mean	St. Dev.
25-50 mph	21	0%	0
	22	52.1%	0.094
	23	20.3%	0.053
	24	11.5%	0.047
	25	7.1%	0.043
	27	6.5%	0.051
	28	1.5%	
	29	0.5%	
	30	0.5%	
Total Medium Speed	21-30	100%	

5.4.6 Full Model Form

An additional important input for applying the final model is the emission factors for each operating mode and vehicle type. The emission factors can be extracted by running MOVES only once for each specific location and year/month combination. This procedure was also completed during the development of the Emission Computation Tool for Radar Data as presented in Section 3.3.

With the development of interim models above and the emission factors available, it is necessary to combine the results from all previous sub-models and incorporate them using a single final model to compute total emissions and emission rates for specific pollutants.

The final model form shown in the following equation. This final model generally follows the one used in emission computation for radar data, and is a modified version of equation 3.7. The advantage of this revised model is to use total vehicle time instead of volume and average speed. Total vehicle time is then dependent on traffic volume. In this method, there is no need to specifically compute average speed, which is also dependent on traffic volume.

$$E_p = \sum p_{st} \, [T_{id} EF_{id,st,p} + T_{dec} EF_{dec,st,p} + T_{low} \left(\sum p_{low} EF_{low,st,p} \right) + T_{med} \left(\sum p_{med} EF_{med,st,p} \right) + T_{high} \left(\sum p_{high} EF_{high,st,p} \right)] \quad (5.20)$$

Where,

E_p =Total emissions for pollutant p, in g;

T =Total vehicle time idling, decelerating etc., in sec;

$EF_{st,p}$ =Emission factors at each operating mode for each vehicle type for pollutant p, in g/s;

p_{st} =Vehicle type percentage.

With the computed total emissions, emission rates can also be computed using equation 3.8. This completes the entire modeling procedure. The next section will validate the proposed model using the testing data.

5.5 Model Evaluation

5.5.1 Validate Total Time Idling

The first step in the model evaluation process is to evaluate total time idling sub-model. This part of the model is developed based on kinematic wave theory instead of empirical data from the case study. Therefore, all available model data can be used for evaluation purposes.

Since total time idling involves several parameters, especially traffic signal parameters, their values need to be identified. Based on observations from radar data, the following values are used in the evaluation process:

- Average signal cycle length: 90 sec;
- Average effective red time: 50 sec;
- Deceleration/Acceleration Time: 11.15 sec; (according to total time decelerating model)
- Adjusted saturation flow rate: 1600 vphpl.

The relationship between traffic flow rate and total time idling is plotted in Figure 5.13. The scattered points in black represent the case study data, while the blue line represents the calculated values using the proposed model. From visual observation, the proposed model fits the empirical data fairly well. In low flow rate conditions, however, the proposed model seems to have some overestimation of total time idling, which may be due to the values of hard-to-justify adjusted saturation flow rate of each specific location.

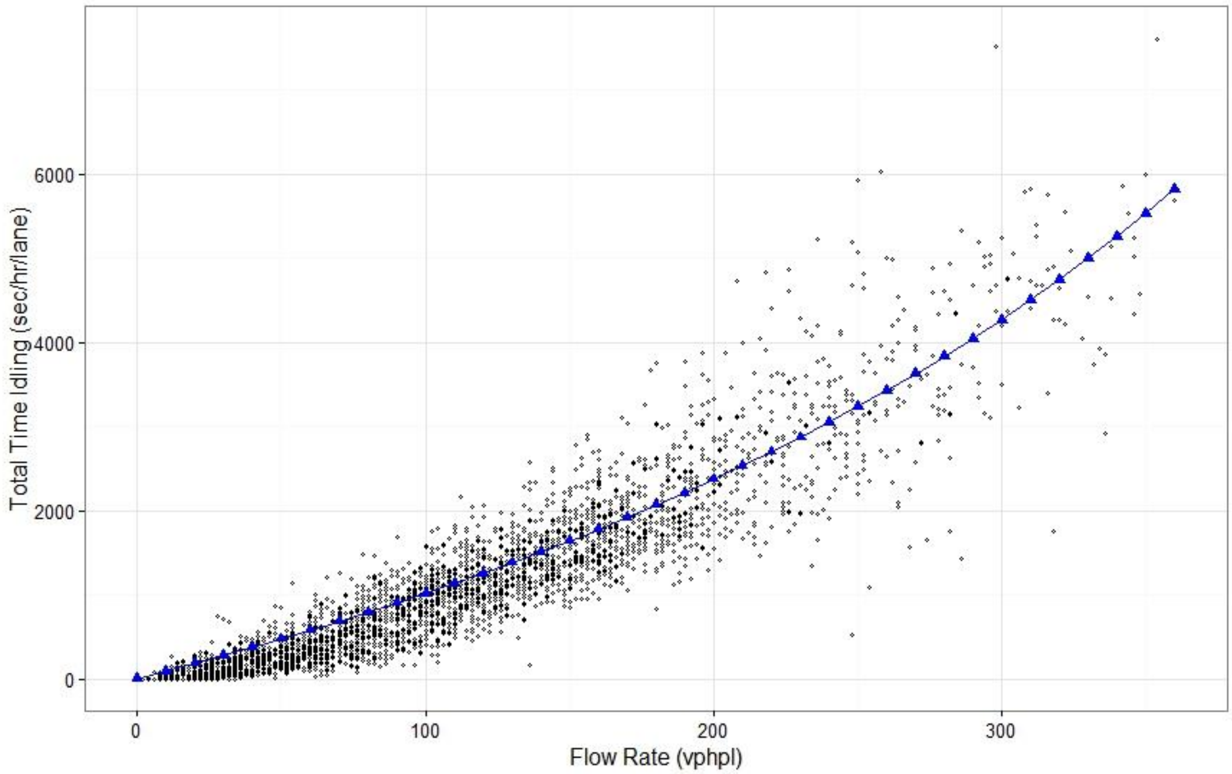

Figure 5.13 Total Time Idling Validation

5.5.2 Validate Total Emissions

The second validation is to evaluate the full model predictability by comparing the total CO emissions computed using the radar based vehicle detection data and proposed model. In the computation of emissions using the proposed model, percentage of heavy vehicles is assumed zero. Data of two analysis period is compared, 15-min aggregation and 1-hour aggregation.

Two parameters are selected to evaluate the full model performance in predicting total CO emissions. First, the Root-Mean-Square-Error (RMSE) is used to quantify the model performance as a scale-dependent parameter. A second scale-independent parameter is Mean Absolute Percentage Error (MAPE). This parameter indicates the average percentage difference between predicted data and empirical data. The RMSE and MAPE values can then be computed using the following equations:

$$RMSE = \sqrt{\frac{\sum_{t=1}^{N}(\widehat{y_t} - y_t)^2}{N}} \tag{5.21}$$

$$MAPE = \frac{\sum_{t=1}^{N}(\widehat{y_t} - y_t)/y_t}{N} * 100\% \tag{5.22}$$

Where,

$\widehat{y_t}$ =Predicted value using proposed model;

y_t =Observed value from case study; and

N =Number of observations.

The relationship between traffic flow rate and 15-min total CO emissions is plotted in Figure 5.14. The scattered points in black represent the case study data, while the red line represents the calculated values using the proposed model assuming zero heavy vehicles. From visual observation, the proposed model fits the empirical data fairly well. The sample size for this validation dataset is 638 data points. The RMSE of this 15-min CO emission is 3.46 g, and the MAPE value is 11.9%. This value is significantly small to show the strong predictive power of this proposed model.

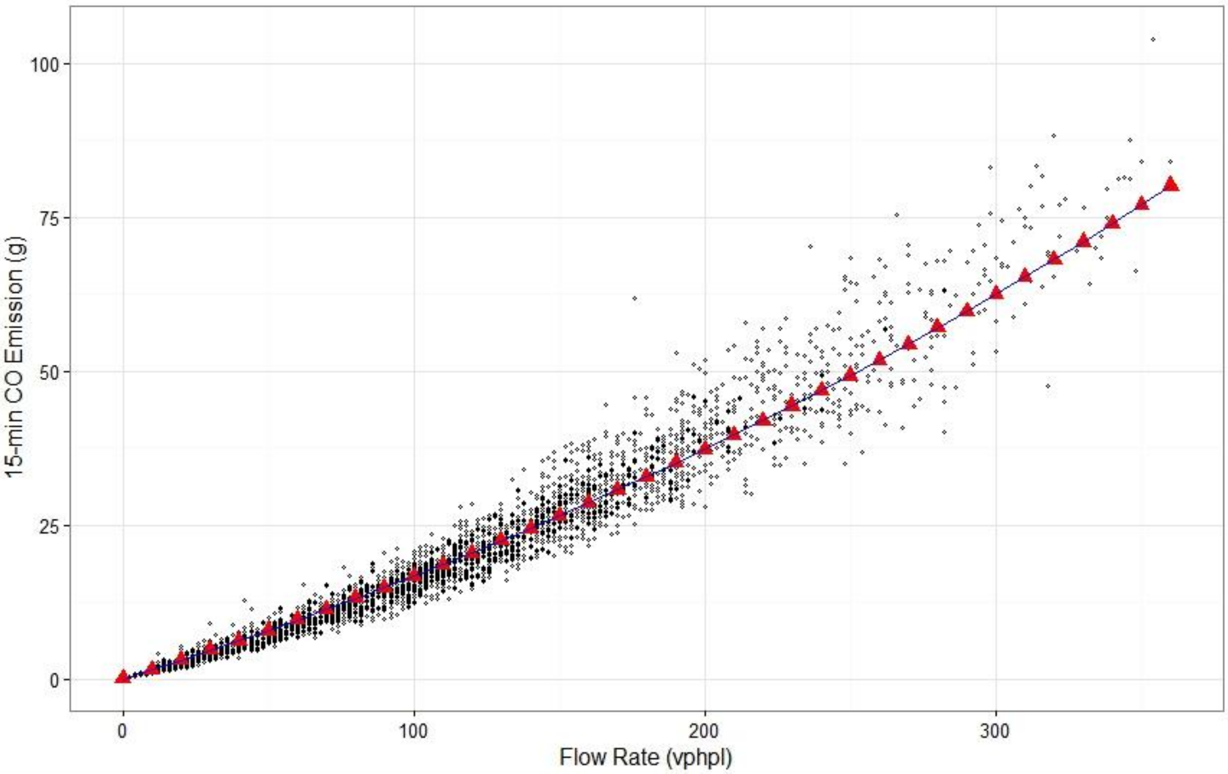

Figure 5.14 15-min Total CO Emissions Validation

The relationship between traffic flow rate and 1-hour total CO emissions is plotted in Figure 5.15. The scattered points in black represent the case study data, while the green line represents the calculated values using the proposed model assuming zero heavy vehicles. From visual observation, the proposed model fits the empirical data fairly well. The sample size for this validation is 798. The RMSE of this 1-hour CO emission is 10.47 g, and MAPE is 9.0%. This value is significantly small to show the strong predictive power of this proposed model in the 1-hour analysis period as well. And it indicates that with a more aggregated analysis period, the average percentage error rate is smaller due to less fluctuations in arrival types and other non-modeled factors.

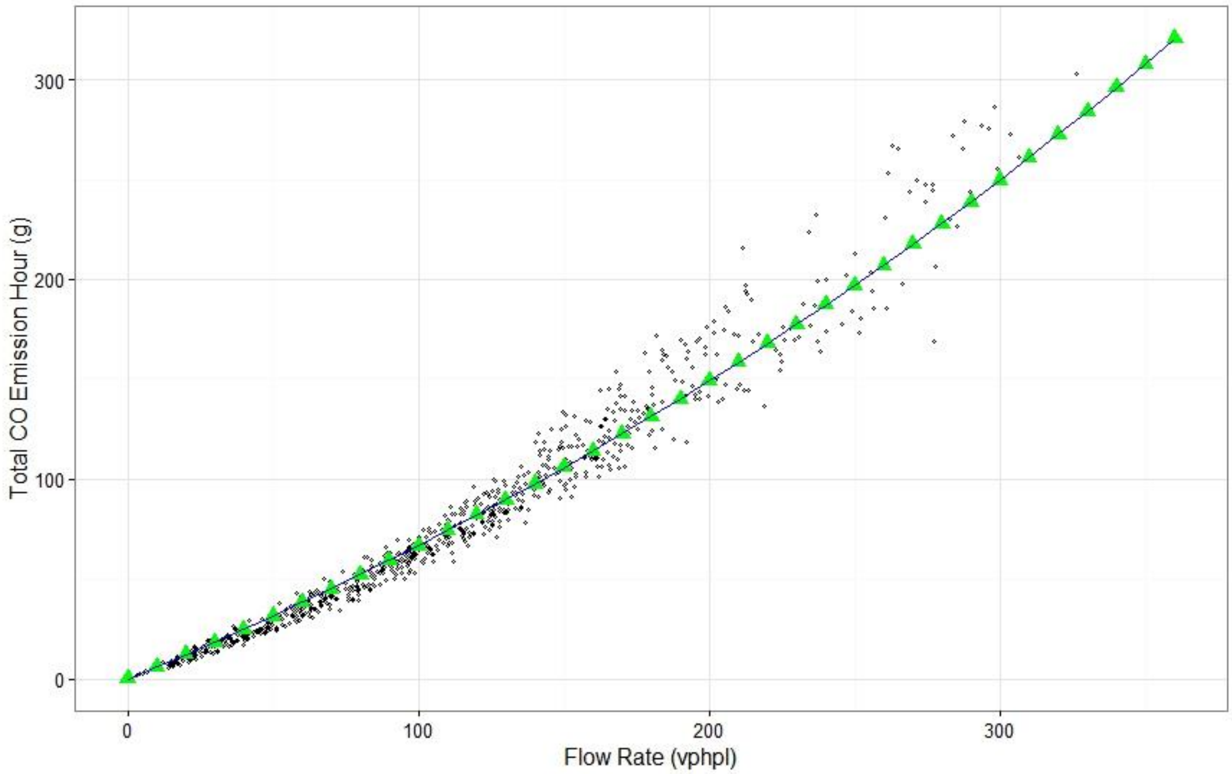

Figure 5.15 Hourly Total CO Emissions Validation

6 Conclusions and Future Work

6.1 Conclusions

This dissertation introduces a new and novel microscopic methodology for estimating vehicle emissions at signalized intersections. Radar based vehicle detections system, when placed at intersection approaches, is able to track vehicle operational characteristics at very high frequency, and provides an ideal data source for emission estimation. The advantages of this data source compared with previous ones are: it will be able to provide second-by-second vehicle operations data for the entire traffic flow, not just a few test vehicle data compared with, and it does not need calibration compared with microsimulation data since the radar data is real-world data. Such high-resolution data greatly assist the use operating mode distribution method for emission estimation.

A detailed procedure is proposed to convert the raw vehicle operations data collected by radar detectors to an operating mode distribution through a series of computations and by combining with emission factors extracted from MOVES, the emission computation can be automatically and continuously completed without having the run MOVES each time. This entire procedure is realized in the "Emission Computation Tool" for radar data using R programming language. Based on this tool, a full system framework for real-time estimation of vehicle emissions at signalized intersections is proposed. The system will be comprised of several different modules, including data collection, configurations, emission estimation, dispersion modeling, and data visualization and decision support module.

A case study is conducted to test the feasibility and validity of the proposed real-time emission estimation system. The test intersection is located in Appleton, WI. The results showed that data collected could be used in computing a variety of parameters, including the traffic volume, average speed, operating mode distribution and total emissions and emission rates for various pollutants. With emission rates, existing pollutant dispersion models such as AERMOD can be applied, yielding pollutant concentrations at various locations. These could be used for air quality conformity and hotspot analysis purposes, thus providing additional functionalities of the proposed system. Finally, the proposed system has been validated through three different perspectives to prove that the results match with real world conditions.

With the abundant raw data from the case study, an operating mode based macroscopic emission model is developed by using both empirical data from the case study as well as incorporating existing traffic flow dynamics model. This emission model is based on estimating total time spent in each operating mode directly from traffic variables and signal variables. Total time idling is modeled using kinematic wave theory and queuing theory, while other total time decelerating and cruising/acceleration are modeled using empirical data from case studies. The validation results showed that the model is able to achieve a high degree of accuracy, with an approximately 10 percent error rate.

Along with the successes with the proposed system, challenges were also identified. The major challenge is that the detection rate of radar detectors becomes lower as the distance from the center of intersection increases. A low detection rate can underestimate the vehicle volume on certain links. Secondly, vehicle length information collected by radar detectors is sometime inaccurate. As emission rates are vehicle class dependent, the absence of accurate vehicle length information can deteriorate the estimation result. Solution to the above issues can be simply switching to other radar detector product with more reliable detection, or adding a video detector into the system to collect more reliable vehicle classification data.

6.2 Future Work

6.2.1 Short Term Future Work

Based on the limitations of the currently proposed system, short term future work may include:

- Use more advanced radar detection devices, or use radar detection along with video camera for data collection to improve downstream coverage area, and better distinguish vehicle types, especially with the prevalence of alternative fueled vehicles.
- Explore the feasibility and validity of such system at other roadway types, including roundabouts, interchanges, or arterial/freeway segments.

6.2.2 Long Term Future Work

Long-term future research directions could focus on the following topics:

- Build a stronger emission model by collecting radar based vehicle detection data at intersections with different characteristics, for example, three leg vs. four leg, stop controlled vs. signalized, different approach speeds, etc.
- Apply an emission factor that is a continuous distribution to VSP changes, compared with the current operating mode method which categorizes with a range of VSP values.

References

1. Rising Pollution in the Developing Word. World Economic Forum. 2015.
2. Seven Million Premature Deaths Annually Linked to Air Pollution. World Health Organization. 2014.
3. National Air Quality and Emissions Trends Report, 2003 Special Studies Edition; U.S. Environmental Protection Agency. Air Quality Trends Analysis Group: Research Triangle Park, NC, 2003.
4. Fast Facts. U.S. Transportation Sector Greenhouse Gas Emissions 1990-2013. U.S. Environmental Protection Agency. 2015.
5. Pandian, S., Gokhale, S., Ghoshal, A.K. Evaluating effects of traffic and vehicle characteristics on vehicular emissions near traffic intersections. Transportation Research Part D, 14(3). 2009.
6. Air Now. United States Environmental Protection Agency (EPA). http://airnow.gov/index.cfm?action=aqibasics.aqi. Accessed July 2015.
7. Synthesis of State DOT and MPO Planning and Analysis Strategies to Reduce Greenhouse Gas Emissions. American Association of State Highway and Transportation Officials. 2012.
8. You, S., Lee G., Ritchie S., Saphores J., Sangkapichai M., and Ayala R. Air Pollution Impacts of Shifting San Pedro Bay Ports Freight from Truck to Rail in Southern California. University of California, Irvine. 2010.
9. Motor Vehicle Emission Simulator (MOVES) User Guide for MOVES2014. U.S. Environmental Protection Agency. 2014.

10. EMFAC2014 User Guide. California EPA Air Resources Board (ARB). 2014.
11. Scora, G., Barth, M., 2006. Comprehensive modal emissions model (CMEM), version 3.01 user's guide. University of California, Riverside Center for Environmental Research and Technology.
12. Transportation Conformity Guidance for Quantitative Hot-spot Analyses in PM2.5 and PM10 Nonattainment and Maintenance Areas. U.S. Environmental Protection Agency. 2015.
13. VISSIM User Manual. PTV Vision. 2011.
14. Quadstone Paramics. http://www.paramics-online.com/. Accessed Jan 2016.
15. O'Cinneide, D. and O'Mahoney, B. The Evaluation of Traffic Microsimulation Modeling. Urban Transport. 2005.
16. Seo T. Kusakabe T. and Asajura Y. Estimation of flow and density using probe vehicles with spacing measurement equipment. Transportation Research Part C: Emerging Technologies. 2015.
17. Hellinga B. and Fu L. Assessing Expected Accuracy of Probe Vehicle Travel Time Reports. ASCE Journal of Transportation Engineering 1999.
18. Lighthill, M. and G. Witham, On kinematic waves. II. A theory of traffic flow on long crowded roads. In Proceedings of the Royal Society of London Series A, Mathematical and Physical Sciences, 1955,pp. 317–345.
19. United States Environmental Protection Agency (EPA). Our Nation's Air Status and Trends Through 2010. 2012.
20. Abou-Senna H. Microscopic Assessment of Transportation Emissions on Limited Access Highways. Ph.D. Dissertation. University of Central Florida. 2012.

21. National Ambient Air Quality Standard (NAAQS). United States Environmental Protection Agency. http://www.epa.gov/air/criteria.html. Accessed June 2015.

22. Automobile Emissions: An Overview. United States Environmental Protection Agency (EPA). 1994.

23. Development of Emission Rates for Light-Duty Vehicles in the Motor Vehicle Emissions Simulator (MOVES2010). United States Environmental Protection Agency (EPA). 2011.

24. Idling Vehicle Emissions for Passenger Cars, Light-Duty Trucks, and Heavy Duty Trucks. United States Environmental Protection Agency (EPA). 2008.

25. Annual Energy Outlook 2015. United States Energy Information Administration (EIA). 2015.

26. Barth M. and Boriboonsomsin K. Traffic Congestion and Greenhouse Gases. Access Magazine. 2009.

27. Unal, A., Rouphail, N., Frey, C. Effect of Arterial Signalization and Level of Service on Measured Vehicle Emissions. *In Transportation Research Record: Journal of the Transportation Research Board, No. 1842,* Transportation Research Board of the National Academies, Washington, D.C., 2003.

28. Yu, L., Jia, S. and Shi, Q. Research on Transportation-Related Emissions: Current Status and Future Directions. Journal of Air & Waste Management Association. 2009. 59:183-195.

29. Atmospheric dispersion modeling. Wikipedia. Accessed October 2016.

30. Turner, D.B. Workbook of atmospheric dispersion estimates: an introduction to dispersion modeling. 1994.

31. U.S. EPA. AERMOD: Description of Model Formulation. U.S. Environmental Protection Agency. 2004.

32. Scire. A., Strimaitis D. and Yamartinos R. A User's Guide to CALPUFF Dispersion Model. 2000.

33. Benson P. CALINE3 – A Versatile Dispersion Model for Predicting Air Pollutant Levels Near Highways and Arterial Streets. 1979.

34. User's Guide to CAL3QHC Version 2.0: A Modeling Methodology for Predicting Pollutant Concentrations Near Roadway Intersections. U.S. Environmental Protection Agency. 1995.

35. Portable emissions measurement system (PEMS). Wikipedia. https://en.wikipedia.org/wiki/Portable_emissions_measurement_system. Accessed July 2015.

36. A. H. S. Lai and N. H. C. Yung, Vehicle-type identification through automated virtual loop assignment and block-based direction-biased motion estimation. *IEEE Transactions on Intelligent Transportation Systems,* Vol. 1, No. 2, June 2000.

37. V. Kastrinaki, M. Zervakis, and K. Kalaitzakis, A survey of video processing techniques for traffic applications. *Image and Vision Computing*, Vol. 21, No. 4, April 2003.

38. Morris B., Tran C., Scora G., Trivedi M. and Barth M. Real-Time Video-Based Traffic Measurement and Visualization System for Energy/Emissions. *IEEE Transactions on Intelligent Transportation Systems*, Vol. 13, No. 4, December 2012.

39. Hallmark S., Fomunung I., Guensler R., Bachman W. Assessing impacts of improved signal timing as a transportation control measure using an activity-specific modeling approach. In Transportation Research Record: Journal of the Transportation Research

Board, No. 1738, Transportation Research Board of the National Academies, Washington, D.C., 2000, pp. 49-55.

40. Hallmark, Shauna L., Randall Guensler, and Ignatius Fomunung. "Characterizing on-Road Variables That Affect Passenger Vehicle Modal Operation." Transportation Research: Part D: Transport and Environment 7, No. 2. 2002.

41. Jackson E., Aultman-Hall. Analysis of Real-World Lead Vehicle Operation for Modal Emissions and Traffic Simulation Models. In Transportation Research Record: Journal of the Transportation Research Board, No. 2158, Transportation Research Board of the National Academies, Washington, D.C., 2010, pp. 44-53.

42. Jackson, E. D., Y. Qu, B. Holmen, and L. Aultman-Hall. Driver and Road Type Effects on Light-Duty Gas and Particulate Emissions. In Transportation Research Record: Journal of the Transportation Research Board, No. 1987, Transportation Research Board of the National Academies, Washington, D.C., 2006, pp. 118–127.

43. Zhang K., Batterman S. and Dion F. Vehicle Emissions in Congestion: Comparison of Work Zone, Rush Hour and Free-flow Conditions. Atmospheric Environment, 45. 2011. 1929-1939.

44. Int Panis, L., C. Beckx, S. Broekx, I. De Vlieger, L. Schrooten, B. Degraeuwe, and L. Pelkmans. PM, NO_x and CO_2 Emission Reductions from Speed Management Policies in Europe. Transport Policy 18, No. 1. 2011.

45. Int Panis, L., C. Beckx, S. Broekx, and Ronghui Liu. Modelling Instantaneous Traffic Emission and the Influence of Traffic Speed Limits. Science of the Total Environment 371, No. 1-3. 2006.

46. De Vlieger, I., D. De Keukeleere, and J. G. Kretzschmar. Environmental Effects of Driving Behavior and Congestion Related to Passenger Cars. Atmospheric Environment 34, no. 27. 2000.

47. Samuel, S., L. Austin, and D. Morrey. Automotive Test Drive Cycles for Emission Measurement and Real-World Emission Levels—a Review. Proceedings of the Institution of Mechanical Engineers. Part D, Journal of Automobile Engineering. 2002.

48. Chen K, and Yu L. "Microscopic Traffic-Emission Simulation and Case Study for Evaluation of Traffic Control Strategies." *Journal of Transportation Systems Engineering and Information Technology* 7, No. 1. 2007.

49. Sun Z., Hao P., Ban J. and Yang D. Trajectory-based vehicle energy/emissions estimation for signalized arterials using mobile sensing data. *Transportation Research Part D.* 2015.

50. Yao, Z., Wei, H., Li, Z.., Liu, H. and Yang J. Developing Operating Mode Distribution Inputs for MOVES using Computer Vision-based Vehicle Data Collector. *In Transportation Research Record: Journal of the Transportation Research Board, No. 2340*:49-58, 2013.

51. Wei H., Liu H., Lu M. and Coifman B. Traffic Data for Integrated Project-Level PM2.5 Conformity Analysis. University of Cincinnati. 2014.

52. Tao F., Shi Q., Yu L. Evaluation of Effectiveness of Coordinated Signal Control in Reducing Vehicle Emissions During Peak Hours Versus Nonpeak Hours. In Transportation Research Record: Journal of the Transportation Research Board, No. 2233, Transportation Research Board of the National Academies, Washington, D.C., 2011, pp. 45-52.

53. Den Braven K., Abdel-Rahim A., Henrickson K., and Battles A. Modeling Vehicle Fuel Consumption and Emissions at Signalized Intersection Approaches: Integrating Field-Collected Data into Microscopic Simulation. National Institute for Advanced Transportation Technology. University of Idaho. 2012.

54. Nesamani, K. S., Lianyu Chu, Michael G. McNally, and R. Jayakrishnan. Estimation of Vehicular Emissions by Capturing Traffic Variations. *Atmospheric Environment* 41, no. 14 (2007): 2996-3008.

55. Shabihkhani R. and Gonzalez E. Analytical Model for Vehicle Emissions at a Signalized Intersection: Integrating Traffic and Microscopic Emissions Models. Transportation Research Board Annual Meeting. 2013.

56. Chen X., Hadi M., Xiao Y. and Elefteriadou L. Vehicle Emission Models based on Macroscopic Performance Measures Derived Utilizing the MOVES Operating Mode Distribution Method. In Transportation Research Board 95th Annual Meeting Compendium of Papers. 2016.

57. Salamati K, Rouphail N, Frey C., Liu B. and Schroeder B. Simplified Method for Comparing Emissions in Roundabouts and at Signalized Intersections. *In Transportation Research Record: Journal of the Transportation Research Board, No. 2517*:48-60, 2015.

58. A Summary of Vehicle Detection and Surveillance Technologies used in Intelligent Transportation Systems. *The Vehicle Detector Clearinghouse.* 2000.

59. R Core Team. R: A language and environment for statistical computing. R Foundation for Statistical Computing, Vienna, Austria. 2013.

60. Jimenez, J. Understanding and Quantifying Motor Vehicle Emissions with Vehicle Specific Power and TILDAS Remote Sensing. Ph.D. dissertation. Massachusetts Institute of Technology, 1999.

61. Frey, H.C., N.M. Rouphail and H. Zhai, Speed- and Facility-Specific Emission Estimates for On-Road Light-Duty Vehicles on the Basis of Real-World Speed Profiles, *Transportation Research Record: Journal of the Transportation Research Board,* No. 1987:128-137, 2006.

62. Chang W, Cheng J. et al. Shiny: Web Application Framework for R. 2015.

63. Beychok M. Fundamentals of Stack Gas Dispersion. Fourth Edition. 2005.

64. Roadrunner. *Wisconsin Department of Transportation.* 2013. https://trust.dot.state.wi.us/roadrunner/

65. Intersector Motion and Presence Sensor Cut Sheet. MsSedco. 2015.

66. Santiago-Chaparro K., Chitturi M., Bill A. and Noyce D.A. Real-time Performance Measures form Radar Based Vehicle Detection Systems. In 19th ITS World Congress. Vienna, Austria. 2012.

67. Geographic Names Information System (GNIS). United States Geological Survey (USGS). Accessed September 2016.